

A functional analysis of a signaling center of the insect head



Georg Oberhofer

born in Innichen (Italy)

Department of Developmental Biology

Georg-August-University Göttingen

A thesis submitted for the degree of

Philosophiæ Doctor (Ph.D.)

December, 2013

Member of the Thesis Committee (Reviewer): Prof. Dr. Gregor Bucher
Department of Developmental Biology, University Göttingen

Member of the Thesis Committee (Reviewer): Prof. Dr. Andreas Wodarz
Department of Anatomy and Cell Biology, Universitätsmedizin Göttingen

Member of the Thesis Committee: Prof. Dr. Steven Johnsen
Department of Tumor Biology, Universitätsklinikum Hamburg-Eppendorf

Day of the defense:

Signature from head of PhD committee:

Declaration

I herewith declare that I have produced this thesis without the prohibited assistance of third parties and without making use of aids other than those specified; notions taken over directly or indirectly from other sources have been identified as such. This thesis has not previously been presented in identical or similar form to any other German or foreign examination board.

Göttingen, 31 December 2013

Abstract

Most of our knowledge on embryonic development comes from the fruit fly *Drosophila melanogaster*. An elaborate genetic model explains the segmentation process in the trunk. However, the anterior head region is patterned in a different way, and many details are not well understood so far. This work analyzes the genetic regulations that govern anterior head patterning in the the red flour beetle *Tribolium castaneum*.

Especially, functional analysis with RNAi against crucial components of the Wnt and hedgehog signaling pathways is used to reveal the genetic interactions of these. In addition, the combination of reverse genetics with next generation sequencing is applied to identify downstream genetic components of these signaling pathways and to discriminate between anterior and posterior targets in the early germ band.

With this work I propose a new model for the patterning of the antennal segment in *Tribolium* based on the cross regulation of head-gap genes, gap-genes and segment polarity genes. The RNAseq approach successfully identified target genes of the Wnt and hedgehog pathways, as confirmed via in situ hybridization, showing the great potential of this method. Finally, this study reveals an unexpected essential role of *Tc-senseless* in hindgut establishment.

Meiner Großmutter
Anna Bodner

Acknowledgements

First of all I'd like to thank my supervisor Dr. Gregor Bucher. Thank you for the opportunity to work in this environment. Your open door policy was much appreciated, and helped a lot to keep my work focused and on track. Thank you for your faith in me when we started all this new and risky projects. Finally, thank you for your kind words, when they were needed the most.

I want to thank the members of my thesis committee, Dr. Andreas Wodarz and Dr. Steve Johnsen. You were a great help in steering the project in the right direction.

A big thank you goes to Claudia Hinnners, who put in a lot of effort in the daily lab work and thank you for bringing order into the chaos or for your never ending want of trying.

I'd like to thank Dr. Ernst Wimmer for asking the right questions during progress reports and personal meetings. You always made me rethink my point of view, which was a great benefit for my project and myself.

Thanks to Dr. Gabriela Salinas-Riester and the members of the TAL Göttingen for the NGS work.

I want to thank Dr. Tim Beissbarth for introducing me to the world of R and helping with statistical analysis of my data.

Special thanks to Stefan Dippel, Dr. Nico Posnien, Dr. Bernhard Schmid and Jonas Schwirz for the endless discussions and the tons of input resulting from

them.

Thanks to Dr. Daniela Grossmann for helping out with injections and chocolate. Also, thanks to Kathrin Kanbach for prepping all those embryos and Elke Küster for providing me with fresh beetles.

Thanks to all my bachelor and master students (and Hiwi's), Nina Heckmann, Verena Nick, Christoph Schomburg, Anna Stief and Tobias Vollmer. You were a great help! Here is hoping you learned something, too.

I would like to thank all my lab members, Dr. Sebastian Kittelmann, Peter Kitzmann, Dr. Nikolaus Koniszewski, Janna Siemanowski, Julia Ulrich and Yong Gang. It was always fun to work in this atmosphere, even when it wasn't.

I am very grateful to the secretary staff, Birgit Rossi, Selen Pfändner and as of late Inga Schild and Bettina Hucke, for pulling me out when I was drowning in German bureaucracy. You are total angels!

Thanks to all the members of our department. It was great working with all of you for the last four years.

A big thank you goes to the open source software community. Without your endless effort in developing all these powerful software tools, this work would have never been accomplished.

Finally, I'd like to thank my mother Annemarie Oberhofer, who made all this possible. Thank you for your endless mental and financial support. You are the best!

Contents

List of Figures	xvii
List of Tables	xix
1 Introduction	1
1.1 Head Patterning	2
1.1.1 Head patterning in <i>Tribolium</i>	3
1.1.2 Potential signaling centers in the <i>Tribolium</i> germ rudiment	5
1.2 Unraveling genetic networks with RNAseq	6
2 Aims of the project	7
3 Materials & Methods	9
3.1 Strains	9
3.2 Molecular Cloning	9
3.3 Stainings	10
3.3.1 Fixation	10
3.3.2 NBT-BCIP stainings with alkaline phosphatase	10
3.3.3 Double fluorescent in situ hybridization with tyramide signal amplification	11
3.3.4 NBT/BCIP-TSA double in situ stainings	14
3.3.5 Immunohistochemistry	14
3.3.6 Generation of a <i>Tc-Armadillo1</i> antibody	14
3.3.7 Mounting	14
3.3.8 Microscopy and Imaging	14
3.4 Heatshock mediated misexpression	15

CONTENTS

3.5	RNAi-RNAseq	15
3.5.1	RNAi	15
3.5.2	RNA isolation	16
3.5.3	RNA sequencing	16
3.5.4	RNAseq analysis	16
3.5.5	Annotation of RNAseq results	17
4	Results	19
4.1	Establishment of parasegment boundaries in the head	19
4.1.1	Hedgehog pathway effects	20
4.1.2	<i>Tc-knirps</i> is needed for the establishment of the antennal parasegment boundary	21
4.1.3	The role of <i>Tc-empty spiracles</i> in the stripe splitting process	24
4.2	Heatshock mediated misexpression of <i>empty spiracles</i>	25
4.3	Differences in anterior and posterior interactions of the Wnt- and hedgehog Pathways	28
4.4	RNAi-RNAseq reveals differences in anterior and posterior target gene sets of the Wnt and hedgehog pathways	30
4.4.1	Quality control	30
4.4.2	In situ hybridization of candidate gene sets	34
4.4.3	Expression profiles of anterior expressed genes	41
4.5	RNAi screen of selected candidates	43
4.6	A novel role for <i>Tc-senseless</i> in hindgut development in <i>Tribolium</i>	46
4.6.1	<i>Tc-senseless</i> is required for hindgut development in <i>Tribolium</i>	47
5	Discussion	51
5.1	Dynamic expression patterns in the establishment of the ocular and antennal parasegment boundaries	51
5.1.1	Genetic model for the patterning of the antennal segment .	52
5.1.2	Outlook stripe splitting project	54
5.2	RNAseq after RNAi reveals differences in anterior and posterior target gene sets	56
5.2.1	Segment polarity interactions in head and growth zone . .	56
5.2.2	The ocular parasegment boundary as anterior signaling center	58

CONTENTS

5.2.3	Posterior target genes	59
5.2.4	Outlook RNAseq	60
References		61
A Clones and Primer		77
B RNAseq		81
B.1	Candidate Genes	81
B.2	Gene ontology enrichment	88
B.3	<i>Tc-senseless</i> phylogenetic tree	95
C Scripts		97
C.1	R	97
C.1.1	DESeq Analysis	97
C.1.2	Miscellaneous	100
C.2	Console	106
C.2.1	Mapping and counting RNAseq reads	106
C.2.2	BLAST	106
Curriculum Vitae		109
List of Publications		111

CONTENTS

List of Figures

1.1	Segmentation in the insect head	4
4.1	Segment polarity expression in the head	20
4.2	Double in situ stainings of <i>Tc-hedgehog</i> and <i>Tc-wingless</i> in (A) <i>Tc-cubitus interruptus</i> ^{RNAi} and (B) <i>Tc-smoothened</i> ^{RNAi}	21
4.3	Double in situ stainings of <i>Tc-hedgehog</i> and <i>Tc-wingless</i> in <i>Tc-kni</i> ^{RNAi}	22
4.4	Double in situ stainings of <i>Tc-knirps</i> and <i>Tc-wingless</i>	23
4.5	Double fluorescent in situ stainings	24
4.6	Double in situ stainings of <i>Tc-wingless</i> and <i>Tc-hedgehog</i> in <i>Tc-empty spiracles</i> ^{RNAi}	25
4.7	Hatch rates of heatshocked transgenic (#111) and wild type (VW) embryos	26
4.8	Phenotypes of <i>empty spiracles</i> overexpression	27
4.9	Complementary interactions of Wnt- and hedgehog signaling in the head and growth zone	29
4.10	Subtractive RNAseq after RNAi	31
4.11	Quality controls of RNAseq experiment	33
4.12	MA-plots of RNAseq treatments	33
4.13	Wnt candidates in situ stainings	38
4.14	Posterior hedgehog candidates	40
4.15	Fold change values of potential anterior target genes	41
4.16	Fold change values of target genes with anterior and posterior expression domains	43
4.17	Phenotype classes of RNAi screen	45

LIST OF FIGURES

4.18	au2.g7984 dsRNA cuticle phenotype	45
4.19	Expression of <i>Tc-senseless</i>	46
4.20	<i>Tc-senseless</i> ^{RNAi}	48
5.1	Genetic model to establish the antennal parasegment boundary in <i>Tribolium</i>	55
5.2	Segment polarity interactions in head and growth zone	57
B.1	<i>Tc-senseless</i> phylogenetic tree	95

List of Tables

3.1	TSA conjugate synthesis	11
A.1	Primer to clone genes and for dsRNA templates	77
A.2	Primer for clones obtained from colleagues	78
A.3	Primer for the RNAseq in situ screen candidates	78
A.4	Primer for non overlapping fragments of RNAseq in situ screen candidates	80
B.1	Posterior Wnt targets	81
B.2	Anterior Wnt targets	84
B.3	Posterior hedgehog targets	84
B.4	Anterior hedgehog targets	88
B.5	Biological Process	89
B.6	Cellular Component	92
B.7	Molecular Function	93

LIST OF TABLES

1

Introduction

Embryonic segmentation is a process well studied in the fruit fly *Drosophila melanogaster*. It starts at the syncytial blastoderm stage where the nuclei are not yet separated by cell walls. The fly employs the long germ mode of development [Liu and Kaufman, 2005] wherein all segments are patterned at this stage by the well known genetic cascade involving maternal, gap and pair-rule genes. Therefore, diffusion of transcription factors between nuclei is important during *Drosophila* patterning [Johnston and Nüsslein-Volhard, 1992]. After cellularization, signaling pathways are required to transmit external signals into the cells. During segmentation, the Wnt and hedgehog signaling pathways contribute to the setting up and the maintenance of the parasegment boundaries [Nüsslein-Volhard and Wieschaus, 1980]. Eventually, the Hox- genes give the segments their identity [McGinnis and Krumlauf, 1992].

Most insects, however, perform pattern formation mostly in a fully cellularized environment. For instance, abdominal segments are formed sequentially from a posterior elongation and differentiation zone (growth zone) [Tautz et al., 1994]. The red flour beetle *Tribolium castaneum* has become a major model for this short germ mode of embryogenesis and many differences to *Drosophila* have been found. The anterior morphogen bicoid is lacking [Stauber et al., 1999, Brown et al., 2001]. Instead, repression of canonical Wnt signaling at the anterior is essential for axis formation [Fu et al., 2012] and *Tc-caudal* translational repression is performed by *Tc-mex3* and *Tc-zen* [Schoppmeier et al., 2009].

In the trunk, the gap gene orthologs do not directly position the pair rule stripes

1. INTRODUCTION

[Bucher and Klingler, 2004, Cerny et al., 2005]. Instead, a pair rule gene circuit is at the core of an oscillating segmentation clock [Choe et al., 2006, El-Sherif et al., 2012, Sarrazin et al., 2012]. The terminal gap genes *Tc-huckebein* and the torso pathway do not appear to play a role in *Tribolium* head development [Schoppmeier and Schroeder, 2005, Kittelmann et al., 2013] while transcription factors from vertebrate neural plate patterning are involved [Posnien et al., 2011]. Several signaling pathways contribute to *Tribolium* growth zone patterning: Torso signaling is required for the establishment of the growth zone [Schoppmeier and Schroeder, 2005] and Wnt signaling components are needed for patterning of the growth zone and the segments [Bolognesi et al., 2008, Beermann et al., 2011] while FGF signaling is required for mesoderm formation during posterior elongation [Sharma et al., 2013]. *Tc-hedgehog* is expressed in the growth zone throughout segmentation without being required for elongation or segment specification but for segment maintenance [Farzana and Brown, 2008].

1.1 Head Patterning

The head is subdivided in a procephalic and gnathocephalic region (figure 1.1). The gnathocephalic part is patterned by the classic genetic cascade as explained above [Pankratz and Jäckle, 1990]. Patterning of the anterior head region must be different for some obvious reasons. Pair rule genes are not expressed there [Bucher and Wimmer, 2005] and the anterior most Hox gene (*labial*) is expressed in the intercalary segment [Abzhanov and Kaufman, 1999, Posnien and Bucher, 2010].

In *Drosophila* the terminal system (*torso*) and the *bicoid* morphogen gradient are the key factors to pattern anterior structures. It activates the so called head-gap genes *orthodenticle*, *empty spiracles*, *buttonhead* and *sloppy paired* which are involved in the patterning of the anterior head [Finkelstein and Perrimon, 1990, Cohen and Jürgens, 1990, Grossniklaus et al., 1992]. They are expressed in overlapping domains and loss of function mutations lead to the deletion of adjacent segments. The idea was that these genes define segment borders as well as their identity [Cohen and Jürgens, 1991] but this hypothesis could not be verified by

ectopic expression of those genes [Gallitano-Mendel and Finkelstein, 1998, Wimmer et al., 1997].

Instead it was found that a second-order regulator, *collier*, acts between the head gap genes and the segment polarity genes, as do the pair-rule genes in the trunk [Crozatier et al., 1996, 1999]. For the intercalary segment it was shown that *collier* directly activates *hedgehog* by binding to a specific cis-regulatory element in the promoter region of *hedgehog* [Ntini and Wimmer, 2011a,b].

In summary the head gap genes, along with the terminal gap genes *tailless* and *huckebein*, regulate the expression of the segment polarity genes in the head [Mohler, 1995], although the underlying genetic network remains unclear. Further, the interactions of the segment polarity genes in the head are not the same as in the trunk region [Gallitano-Mendel and Finkelstein, 1997].

In spiders a wave of *hedgehog* expression is required for the metamerization of the anterior head [Pechmann et al., 2009]. *Hedgehog* is co-expressed with *orthodenticle* in a generative zone from which additional segments emerge via the traveling and splitting of the *hedgehog* expression domain [Kanayama et al., 2011]. However, the proposed auto-regulatory feedback loop of these genes does not include the input of other head-gap genes.

1.1.1 Head patterning in *Tribolium*

In *Tribolium* the functions of the head gap genes differ. In *Tc-orthodenticle*^{RNAi} the complete head is lost [Schröder, 2003], due to an early function in dorso-ventral patterning [Kotkamp et al., 2010]. A later function of *Tc-orthodenticle* specifically affects parts of the procephalic head, whereas *Tc-empty spiracles*^{RNAi} leads to misoriented antennae and loss of eyes. *Tc-buttonhead*^{RNAi} has no effect on head formation [Schinko et al., 2008].

The classic gap gene *knirps* is not involved in head patterning in *Drosophila* whereas in *Tribolium*, it is needed for the establishment of the antennal and mandibular segments [Cerny et al., 2008]. Recently it was shown that *Tc-knirps* receives input from the pair rule gene *even skipped* being another difference to the *Drosophila* model wherein the gap genes act upstream of the pair-rule genes [Peel et al., 2013]. *Tc-sloppy paired* is expressed in narrow stripes compared to the

1. INTRODUCTION

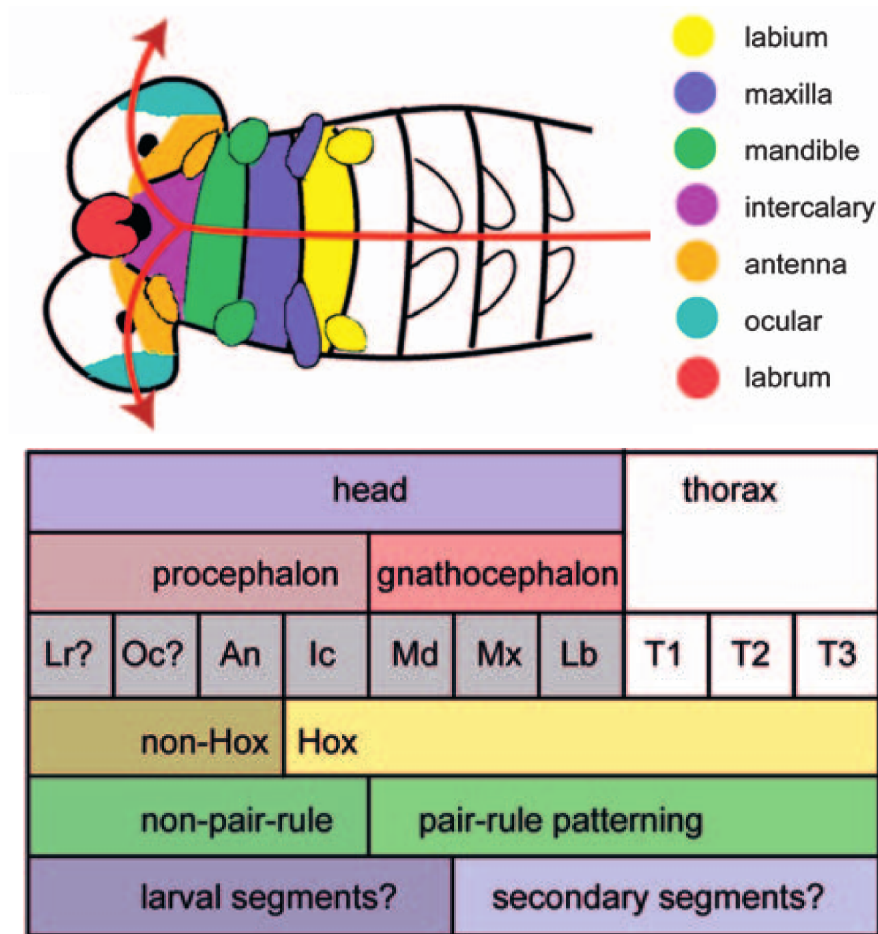


Figure 1.1: Segmentation in the insect head - Anterior head (procephalic): labrum, ocular, antenna, intercalary. Posterior head (gnathocephalic): mandible, maxilla, labium. No pair-rule genes and hox genes (from intercalary onwards) are expressed in the anterior head. Figure taken from [Bucher and Wimmer, 2005]

gap gene-like expression in *Drosophila* and *Tc-sloppy paired*^{RNAi} shows additional defects in the abdomen [Choe and Brown, 2007].

With the lack of pair rule input the classic trunk segmentation model is not working [Posnien et al., 2010] and it remains unclear how parasegment boundaries are established in the head.

1.1.2 Potential signaling centers in the *Tribolium* germ rudiment

At the germ rudiment stage the signaling ligands *Tc-wingless* and *Tc-hedgehog* are expressed in adjacent domains in the head. This is the first postblastodermal stage and directly precedes posterior elongation and antennal segment formation suggesting that crucial signaling events are taking place.

The expression domains of orthologous head patterning genes in the anterior region show a high similarity between insects and vertebrates [Wurst and Bally-Cuif, 2001, Urbach, 2007]. More recently the list of conserved head patterning genes and their similar expression domains compared to vertebrates was expanded in *Tribolium* and it was shown that several of these head specific genes are expressed in stripes parallel or overlapping the ocular parasegment boundary [Posnien et al., 2011]. Therefore, it is assumed that the ocular parasegment boundary corresponds to the vertebrate mid-hind-brain boundary.

The other expression domain of *Tc-wingless* and *Tc-hedgehog* is in the growth zone. RNAi against crucial components of the Wnt pathway interferes with posterior elongation [Bolognesi et al., 2008, 2009] whereas disruption of the hedgehog pathway does not have an effect on the elongation process. However, later during development parasegment boundaries are not stable without a functioning hedgehog pathway and the germ band collapses during retraction [Farzana and Brown, 2008].

Taken together, the head and growth zone expression domains of these pathways are likely to be a part of anterior and posterior signaling centers.

1. INTRODUCTION

1.2 Unraveling genetic networks with RNAseq

The interactions of the Wnt and hedgehog pathway seem to be conserved in trunk segmentation between *Drosophila* and *Tribolium* [Oppenheimer et al., 1999]. However, the interactions of the pathways in the anterior head region and in the growth zone had not been well studied so far. Their respective target gene sets were not known and specifically, it had remained elusive in how far the target gene sets of these two pathways differ within and between these putative head and growth zone signaling centers.

In RNAseq a sample RNA is reverse transcribed and the resulting cDNA is used in massively parallel sequencing to yield millions of short reads in one single run. After mapping these reads back to a reference genome (transcriptome) the expression levels of all the transcribed genes in the sample are obtained [Wilhelm et al., 2008, Nagalakshmi et al., 2008, Mortazavi et al., 2008, Sultan et al., 2008].

In this work, I used this method to identify the target genes of the Wnt and hedgehog pathways, by comparing RNAi samples, where the pathways had been disrupted, to wild type embryos. The chosen developmental stage was the germ rudiment stage, where the trunk parasegment boundaries are not yet developed. This allows to examine the interactions and functions of the segment polarity signaling pathways independently from their function in the trunk.

2

Aims of the project

The main aim of this study is to analyze the underlying genetic network of the early expression of the segment polarity genes *Tc-wingless* and *Tc-hedgehog* at the ocular parasegment boundary and in the growth zone. This includes

- The identification of upstream regulators
- A description of the interactions of the two pathways
- The identification of downstream target gene sets in order to compare them between head and growth zone

The first part is achieved by a candidate gene approach. Candidates are selected according to their expression pattern and time point and knocked down via RNAi. To study the interactions of the pathways their function is disrupted with RNAi. In both approaches the effect on the expression pattern of *Tc-wingless* and *Tc-hedgehog* is examined.

By a combination of RNAi against key components of the two pathways with RNAseq, downstream target genes can be identified genome wide. The resulting candidates are further examined in an in situ screen to verify their correct expression pattern. Finally, genes showing the predicted expression pattern are analyzed in more detail.

2. AIMS OF THE PROJECT

3

Materials & Methods

3.1 Strains

Tribolium San Bernardino wild type strain was used for all experiments if not stated differently. Beetles were maintained at standard conditions (32°C on full grain flour supplemented with 5% dry yeast) [Sokoloff, 1974]. Transgenic beetle line # 111 used in heatshock experiments¹ was generated with piggyback transgenesis in *vermillion white* and contained the *Tc-empty spiracles* open reading frame under the control of an endogenous heatshock promoter.

Black males were used for RNAi experiments with candidate genes from the RNAseq experiment. For egg collections beetles were maintained at 32°C on white flour supplemented with 5% dry yeast.

3.2 Molecular Cloning

All genes used in this thesis were cloned using standard techniques. Genes were amplified from cDNA² with Phusion™ or advantageTaq™ and cloned into pJET1.2 or pCRII vector, respectively. Primers were designed using Primer3 software [Untergasser et al., 2012]. A complete list of all primers used in this thesis can

¹Transgenic beetle line was generated by Johannes Schinko as detailed in [Schinko et al., 2012]

²cDNA synthesis by Sebastian Kittelmann and Jonas Schwirz with the SMART PCR cDNA kit (ClonTech)

3. MATERIALS & METHODS

be found in the appendix (section A). The obtained sequences were verified using blastall [Altschul et al., 1997] in bioperl [Stajich et al., 2002] with the Tc-au2 gene set as the reference¹.

3.3 Stainings

In Situ probes were synthesized with the DIG (Digoxigenin), FLU (Fluorescein) and BIO (Biotin) labeling kits from Roche using T7 or SP6 polymerases according to the manufacturers instructions.

3.3.1 Fixation

Embryos were dechorionated 2 times for 3 minutes in 50% commercial bleach in small sieves (mesh size 180 μ m). Fixation was performed as described previously [Schinko et al., 2009]. The recipe for the fixation buffer was modified after [Sandmann et al., 2006]: 1 mM EDTA, 0.5 mM EGTA, 100 mM NaCl, 2.5% formaldehyde, 50 mM HEPES, pH 8.

3.3.2 NBT-BCIP stainings with alkaline phosphatase

In situ hybridization was performed as described previously [Schinko et al., 2009] with minor changes: 2% Roche blocking reagent was added to the HybeA buffer. PBT was substituted with maleic acid buffer (MABT) as the standard washing buffer². 2% Roche blocking reagent in MABT was used as the standard blocking buffer in all following steps.

¹Gene set based on Tcas3.0 [Tribolium Genome Sequencing Consortium et al., 2008], re-annotated by Mario Stanke with augustus software [Stanke and Waack, 2003], unpublished; hosted on bioinf.uni-greifswald.de

²see page 12 for the recipe

3.3.3 Double fluorescent in situ hybridization with tyramide signal amplification

This protocol is an adaption of the [Lauter et al., 2011] zebrafish in situ protocol to the NBT-BCIP protocol described above. Detection is based on tyramide signal amplification (TSA).

Synthesis of fluorescent tyramide conjugates

4 Å molecular sieves (Fluka) are activated twice for two minutes in a microwave. 3 ml DMF (dimethylformamide) are dried twice over the activated molecular sieves. 10 mg tyramine HCl are dissolved in 990 µl dry DMF containing 10 µl triethylamine. Fluorescent dyes are modified to contain NHS-ester groups (Pierce, Dylight-NHS conjugates). 1 mg NHS-conjugate is dissolved in 100 µl dry DMF. The complete NHS solution and the tyramine solution are mixed at a 1.1:1 molar ratio (see table 3.1). The mixture is incubated in the dark for two hours and diluted to 1 ml with ethanol afterwards.

Table 3.1: TSA conjugate synthesis

Dye	Mr(Dye)[g/mol]	n(Dye)[µmol]	n(Tyramin)[µmol]	V(Tyramin)[µl]
Dylight 405	793	1.261	1.146	19.9
Dylight 488	1011	0.989	0.899	15.6
Dylight 550	1040	0.962	0.874	15.2
Dylight 633	1066	0.938	0.853	14.8

Buffers

- HybeA, 100 ml for 350 stainings:
100 ml HybeB, 0.1 ml heparin [50 mg/ml], 0.5 ml yeast RNA [20 mg/ml] and 2 ml sonicated salmon sperm DNA [20 mg/ml] are boiled for 10 min and cooled on ice for 3 min.
Add 2 g dextran sulfate, 2 g Roche blocking reagent and 1 ml Denhardtts solution. Heat to 65°C until everything is dissolved (ca. 30 min). Store at -20°C.

3. MATERIALS & METHODS

- Denhardt's solution: 20 mg Ficoll, 20 mg Polyvinylpyrrolidone and 20 mg BSA in 1 ml H₂O
- 5 x MABT stock: 500 mM maleic acid, pH to 7.5 with NaOH, 750 mM NaCl, 0.5% Tween 20
- Blocking buffer : 1 x MABT, 2% Roche blocking reagent. Store at 4°C.
- Borate buffer: 100 mM boric acid, pH to 8.5 with NaOH, 0.1% Tween 20
- TSA staining buffer, prepare freshly before use (100 µl/staining): borate buffer with 2% dextran sulfate, 450 µg/ml 4-iodophenol, 0.003% H₂O₂ and 0.4 µl tyramide conjugate. Protect from light if a fluorescent tyramide is used.
- Inactivation buffer: 100 mM glycine, pH to 2 with HCl, 0.1% Tween 20

Procedure The protocol starts at the pre-hybridization step. All previous steps are identical to [Schinko et al., 2009].

- Replace HybeB with 250 µl HybeA and prehybridize for 1 h at 60°C.
- Dilute your probes to the desired concentration in 30 µl HybeA. Heat to 90°C for 2 min and place on ice for 5 min. Preheat the probes to 60°C.
- Remove HybeA, add the probes and incubate over night at 60°C.
- Increase the temperature to 65°C.
- Wash three times for 10 min with HybeB. Wash once with a 1:1 mixture of HybeB: MABT. Wash three times for 10 min with MABT.
- Switch to room temperature and wash three times for 10 min with MABT.
- Block for 1 h in blocking buffer.

3.3 Stainings

- Prepare a 1:2000 dilution¹ of your HRP/POD conjugated antibody of choice in 1 ml blocking buffer.
- Incubate with the antibody for at least 1 h.
- Wash four times for 10 min with MABT. Wash over night at 4°C in blocking buffer.
- Wash four times for 10 min with MABT. Wash two times for 5 min with borate buffer.
- Prepare the TSA staining buffer during the borate washes. Stain for 30 to 60 min without agitation.
- Wash three times with MABT.

Continue with the inactivation step for another round of detection or skip to the final washing steps.

- Incubate for 15 min with inactivation buffer.
- Wash three times for 10 min with MABT.
- Block for 1 h in blocking buffer.
- Repeat antibody addition, washes and staining reaction for your second target as described above.

Final washes: Wash three times for 10 min with MABT. Wash over night at 4°C with MABT. Replace MABT, add 0.015% sodium azide as a preservative and store at 4°C.

¹Tested for Roche anti-Dig-POD, Roche anti-Fluo-POD and Jackson streptavidin-HRP; supplier suggestions of 1:200 or more resulted in background

3. MATERIALS & METHODS

3.3.4 NBT/BCIP-TSA double in situ stainings

The alkaline phosphatase driven NBT/BCIP reaction was combined with the horseradish peroxidase mediated TSA reaction. Therefore, both antibodies could be added at the same time in the in situ staining without the need of an inactivation step. This method reduced the time to carry out a double in situ staining to that of a single staining. In double in situ stainings using the same enzyme, the harsh inactivation step often reduces the signal of the second staining, which is another advantage of the here described approach.

3.3.5 Immunohistochemistry

Immunostainings were carried out with the same protocol as the in situ hybridizations. The hybridization steps were omitted.

3.3.6 Generation of a *Tc-Armadillo1* antibody

A 15 amino acid peptide of the C-terminus¹ of *Tc-Armadillo1* was conjugated to KLH and injected in two rabbits. Peptide synthesis and immunization of rabbits was carried out by Eurogentec.

The obtained rabbit serum was used at a 1:10000 dilution in immunostainings [Panfilio et al., 2013].

3.3.7 Mounting

Embryos from in situ hybridizations and immuno stainings were mounted in 100% glycerol. Cuticles of first instar larvae were mounted in a 1:1 mixture of lactic acid and Hoyer's medium [Anderson, 1954] and incubated for two days at 65°C.

3.3.8 Microscopy and Imaging

Cuticles were imaged on a Zeiss LSM780 using a 550 nm LASER. The resulting stacks were loaded into Amira 5.32. 4 steps of Blind deconvolution and gaussian

¹Sequence: PQDNNQVAAWYDTDL

3.4 Heatshock mediated misexpression

smoothing were applied. Intensity levels were set to range from 5-200.

TSA double fluorescent in situ stainings were also imaged on a Zeiss LSM780 using 488 nm and 550 nm lasers. The stacks were imported in Amira v5.3.2 and 3D models were reconstructed with the voltex module.

NBT/BCIP single and NBT/BCIP - TSA double stainings were imaged on a ZEISS Axioplan2 using ImagePro v6.2 software. All images were assembled in Photoshop CS2. The levels for fluorescent in situ stainings were adjusted to increase intensity. NBT/BCIP stainings were not modified. All figures were imported in Inkscape for labeling and formatting.

3.4 Heatshock mediated misexpression

The transgenic beetle line #111 was used to study overexpression of *Tc-empty spiracles*. Heatshock experiments were carried out as described previously [Schinko et al., 2012]. 0-24 hour old embryos were heatshocked for ten minutes at 48°C. In the case of multiple heatshocks they were applied every two hours.

3.5 RNAi-RNAseq

3.5.1 RNAi

DsRNA was synthesized as described previously [Fu et al., 2012]. Lithium precipitation was used for templates longer than 400bp and phenol/chloroform extraction followed by isopropanol precipitation for shorter ones. DsRNA was injected in female pupae (RNAseq) or adults (downstream candidates). With this parental RNAi technique the phenotype is passed on to the offspring[Bucher et al., 2002]. All genes used in the RNAi-RNAseq procedure were published previously with no off target effects reported [Bolognesi et al., 2009, Beermann et al., 2011, Farzana and Brown, 2008, Bolognesi et al., 2008, Kotkamp et al., 2010, Schoppmeier and Schroeder, 2005].

3. MATERIALS & METHODS

3.5.2 RNA isolation

RNA of 10-11h old RNAi and wildtype embryos was extracted using Trizol (Ambion) according to the manufacturers protocol, followed by DNase digestion with turbo DNase (Ambion) and phenol/chloroform (Ambion, pH=6.9) extraction.

3.5.3 RNA sequencing

Library preparation for RNA-Seq was performed using the TruSeq RNA Sample Preparation Kit (Illumina, Cat.No:RS-122-2002) starting from 400 ng of total RNA. Accurate quantitation of cDNA libraries was performed by using the QuantiFluor dsDNA System (Promega). The size range of final cDNA libraries was determined applying the DNA 1000 chip on the Bioanalyzer 2100 from Agilent (280 bp). cDNA libraries were amplified and sequenced by using the cBot and HiSeq2000 from Illumina (Single Read; 1x50 bp and 1x100bp). Sequence images were transformed with Illumina software BaseCaller to bcl files, which were demultiplexed to fastq files with CASAVA v1.8.2. Quality check was done via fastqc (v. 0.10.0, Babraham Bioinformatics). All treatments were sequenced in biological triplicates.

Library preparation, quality control, sequencing and demultiplexing was carried out by the Transkriptom Analyse Labor Göttingen.

3.5.4 RNAseq analysis

The obtained fastq formatted Illumina reads were mapped to the *Tribolium* au2 gene set using bowtie2 (version 2.1.0) [Langmead and Salzberg, 2012] with the these settings: -q -D 20 -R 3 -N 1 -L 20 -i S,1,0.50. Reads were counted with samtools [Li et al., 2009] and combined in a counts table. Statistical analysis of the data and differentially expressed gene calling was performed in R [Team, 2013] using the DESeq (version1.12.0) [Anders and Huber, 2010] package from bioconductor [Gentleman et al., 2004]. Genes were considered to be differentially expressed if log2 fold change was $\geq |1|$ and an adjusted p value < 0.1 . Intersects and Venn diagrams were build with the Overlapper.R function from the Bioconductor manuals by Thomas Girke [Girke]. Heatmaps were plotted with gplots

[Bolker et al., 2013] and RColorBrewer [Neuwirth, 2011], barplots with ggplot2 [Wickham, 2009].

3.5.5 Annotation of RNAseq results

The au2 gene set was BLASTed against the gene set from Flybase [Gelbart et al., 1997] using BLAST [Altschul et al., 1997] implemented in bioperl [Stajich et al., 2002] and a custom perl script¹. Reciprocal best BLAST scores were reported as orthologs. Hits with an $E - value < 10^{-5}$ are considered homologs. The resulting list of au2 gene IDs with their corresponding Fbpp ID was merged to the Drosophila GO annotations downloaded from Flybase (GOC Validation Date: 01/25/2013) in R.

¹Perl script written by Mario Stanke and downloaded from bioinf.uni-greifswald.de. The script was modified to allow for multi threaded BLAST search.

3. MATERIALS & METHODS

4

Results

4.1 Establishment of parasegment boundaries in the head

The ocular parasegment boundary is the first to be established in the *Tribolium* embryo. To learn more about its initiation, the differences in segment polarity expression patterns were investigated in wild type and different RNAi knock down situations.

Double fluorescent in situ hybridizations (FISH) was used to get the expression topologies of *Tc-wingless* and *Tc-hedgehog* in the head. After the ocular parasegment boundary was established, the *Tc-hedgehog* domain became broader, extended backwards and splitted up. This process gave rise to the antennal *Tc-hedgehog* domain. Later the antennal *Tc-wingless* expression arised de novo adjacent to *Tc-hedgehog* (figure 4.1).

I tried to understand the underlying genetic mechanisms by looking at candidate genes that modify the stripe splitting. In this section the term head was used in a simplified way, including the antennal and ocular parasegment boundaries only. The complete process was described with these terms:

1. Establishment at the ocular domain
2. Stripe broadening and backwards extension
3. Stripe splitting

4. RESULTS

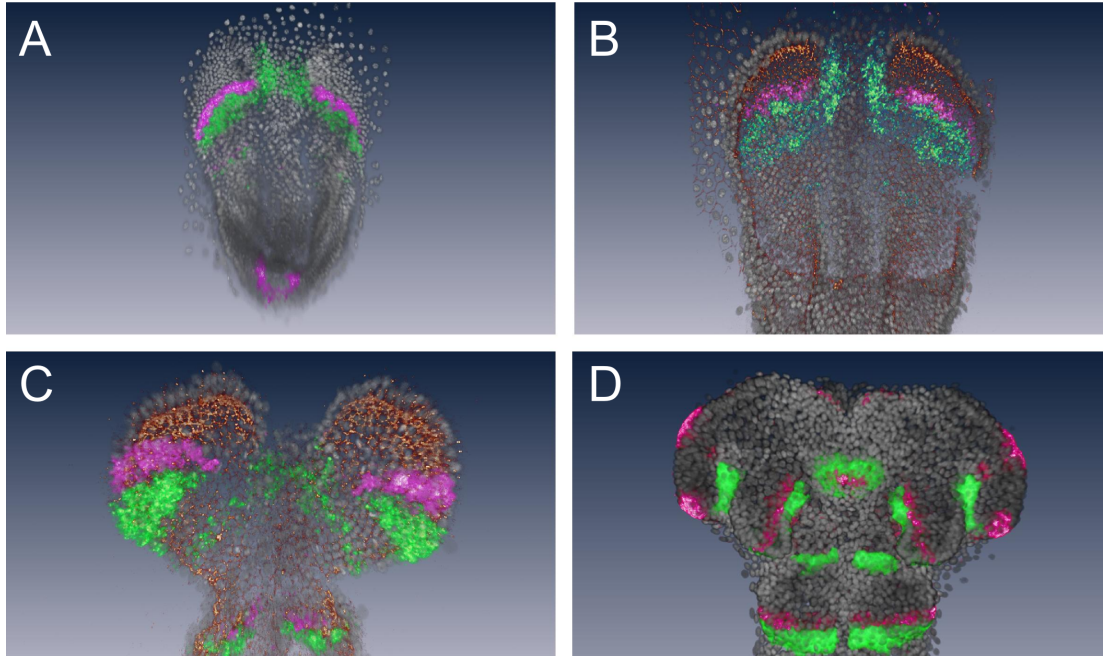


Figure 4.1: Segment polarity expression in the head - FISH stainings at different developmental timepoints (*A* to *C* dorsal views, *D* ventral view, anterior to the top) of *Tc-wingless* (magenta) and *Tc-hedgehog* (green) showing the dynamic expression pattern of *Tc-hedgehog*. Nuclei were colored in gray, Tc-Armadillo1 antibody staining in brown. (*A*) Initial expression of *Tc-hedgehog* and *Tc-wingless* at the ocular parasegment. (*B*) The ocular *Tc-hedgehog* domain becomes broader, extends backwards and starts to split up. (*C*) Split process was completed and antennal *Tc-hedgehog* was established. (*D*) Antennal *Tc-wingless* arises de novo (ventral view)

4.1.1 Hedgehog pathway effects

To check for auto regulation of *Tc-hedgehog* expression in the head I disrupted the hedgehog pathway via *Tc-cubitus interruptus*^{RNAi} and *Tc-smoothened*^{RNAi}. In the absence of hedgehog signaling *cubitus interruptus* was cleaved to its repressive form [Aza-Blanc et al., 1997]. In *Tc-smoothened*^{RNAi} hedgehog targets were always repressed, whereas *Tc-cubitus interruptus*^{RNAi} additionally derepressed hedgehog targets in cells without hedgehog signaling.

In both treatments the *Tc-wingless* expression domains were fading in the trunk

4.1 Establishment of parasegment boundaries in the head

indicating the important role of the hedgehog pathway in stabilizing parasegment boundaries. Ocular *Tc-wingless* seems unaffected while the expression in the growth zone was lost in *Tc-cubitus interruptus*^{RNAi}. In *Tc-smoothened*^{RNAi} it was the other way round (figure 4.2). In addition in *Tc-smoothened*^{RNAi} the broad anterior *Tc-hedgehog* domain indicates that the stripe splitting failed (see also figure 4.9).

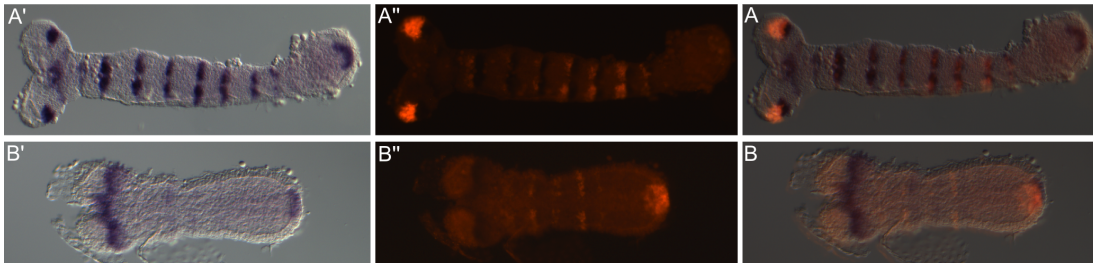


Figure 4.2: Double in situ stainings of *Tc-hedgehog* and *Tc-wingless* in (A) *Tc-cubitus interruptus*^{RNAi} and (B) *Tc-smoothened*^{RNAi} - *Tc-hedgehog* in blue (NBT/BCIP) and *Tc-wingless* in red (TSA-Dylight550). (A) *Tc-cubitus interruptus*^{RNAi}; The antennal and ocular *Tc-hedgehog* domains were unaffected. Ocular *Tc-wingless* was unaffected, but antennal *Tc-wingless* was lost along with most trunk and the growth zone domains. (B) *Tc-smoothened*^{RNAi}; The anterior *Tc-hedgehog* domain was broadened, trunk domains were lost but the growth zone was unaffected. *Tc-wingless* expression was lost in the head, reduced or fading in the trunk but unaffected in the growth zone.

In summary the hedgehog pathway was required for the stripe splitting process, but not for the establishment of *Tc-hedgehog* expression in the head. The trunk parasegment boundaries were fading without hedgehog signaling. Growth zone expression of the segment polarity genes was unaffected only in *Tc-smoothened*^{RNAi}, but strikingly, *Tc-wingless* expression was lost in *Tc-cubitus interruptus*^{RNAi} without affecting elongation.

4.1.2 *Tc-knirps* is needed for the establishment of the antennal parasegment boundary

From previously published data it was clear that *Tc-knirps* plays a major role in establishing the antenna anlagen. Antennal expression of *Tc-hedgehog* and *Tc-*

4. RESULTS

wingless was lost in *Tc-knirps*^{RNAi} (see Figure 4.3 and [Cerny et al., 2008, Peel et al., 2013]). This makes *Tc-knirps* a good candidate for the activation of *Tc-hedgehog* during the backwards extension of the expression domain. The ocular parasegment boundary was not affected by *Tc-knirps*^{RNAi}, whereas the dynamic *Tc-hedgehog* expression, leading to the formation of the antennal parasegment boundary, was abolished.

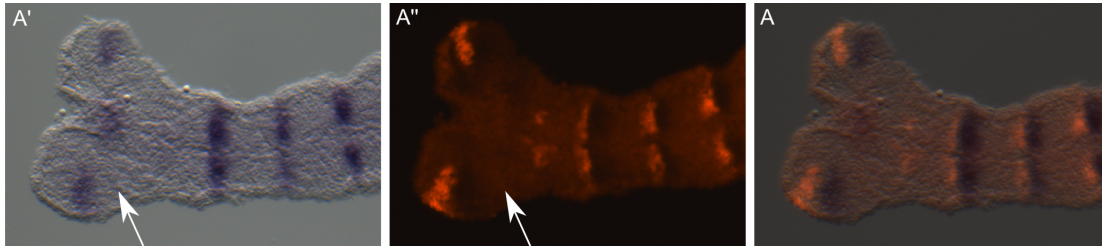


Figure 4.3: Double in situ stainings of *Tc-hedgehog* and *Tc-wingless* in *Tc-kni*^{RNAi} - (A') *Tc-hedgehog* (NBT/BCIP) expression, antennal expression missing (arrow). (A'') *tc-wingless* (TSA-Dylight550) expression, antennal expression missing (arrow). (A) Overlay

For *Tc-knirps* to be the upstream activator of *Tc-hedgehog* during its movement from the ocular to the antennal domain, it should show similar expression dynamics. Double in situ stainings of *Tc-wingless* and *Tc-knirps* showed adjacent expression domains in very early germ bands before the serosa window had formed. As the serosa window began to close, the two expression domains became separated from each other. At later timepoints, as shown by the smaller serosa window, the gap between the domains increased further (see figure 4.4).

In summary, *Tc-knirps* function was essential for *Tc-hedgehog* expression at the antennal parasegment boundary and its early expression domain showed the same backwards extension.

4.1 Establishment of parasegment boundaries in the head

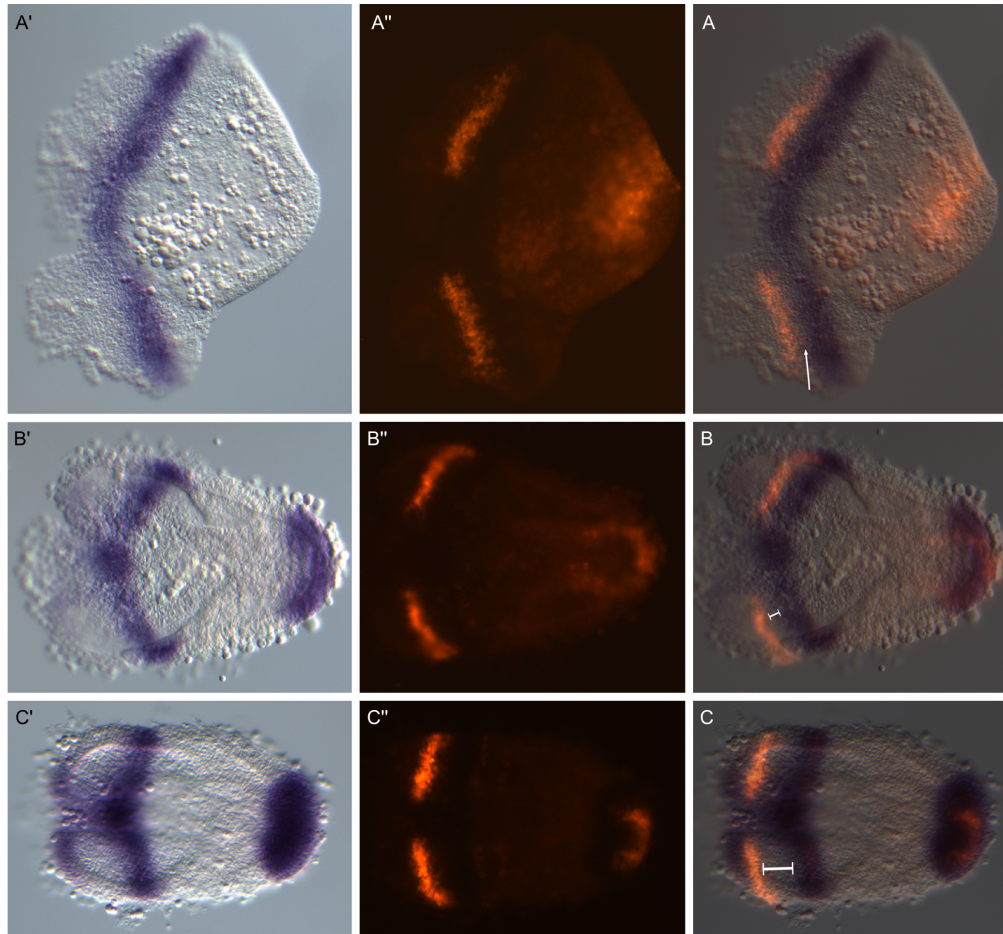


Figure 4.4: Double in situ stainings of *Tc-knirps* and *Tc-wingless* - *Tc-knirps* in blue (NBT/BCIP) (A'-C'), *Tc-wingless* in red (TSA-Dylight550) (A''-C'') in early germbands. Panels were sorted from youngest (A) to oldest (C) as marked by the size of the serosa window. (A) No serosa window, adjacent expression domains (arrow in A). (B) Slightly older germ band with formed serosa window. Gap between *Tc-wingless* and *Tc-kni* domains increased. (C) Gap increased further

4. RESULTS

4.1.3 The role of *Tc-empty spiracles* in the stripe splitting process

In wild type embryos, *Tc-empty spiracles* was expressed exactly between the ocular and antennal *Tc-wingless* domains. In *Tc-empty spiracles*^{RNAi} the antenna of first instar larva were misoriented and the eyes were absent [Schinko et al., 2008]. The backwards extension and splitting of *Tc-hedgehog* occurred in this field. After the broadening, the *Tc-hedgehog* domain has moved beyond the *Tc-empty spiracles* field, and the antennal *Tc-wingless* domain arised de novo (see figure 4.5).

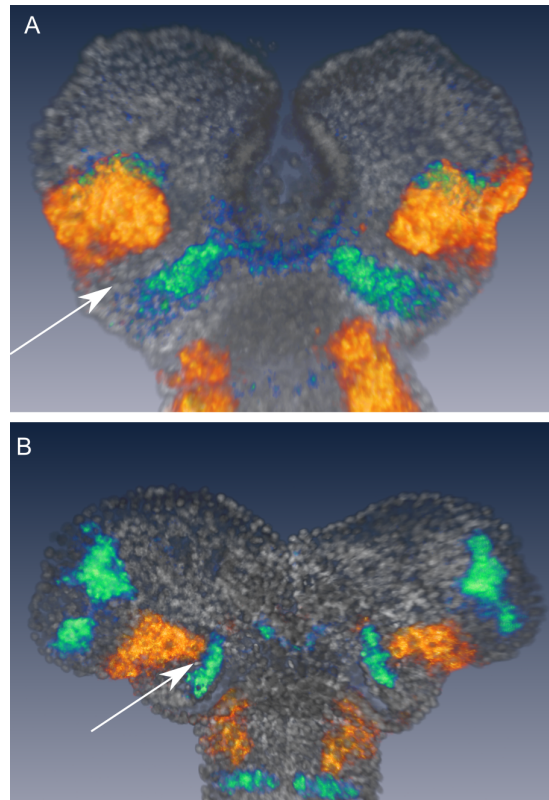


Figure 4.5: Double fluorescent in situ stainings - (A) *Tc-empty spiracles* in orange (TSA-Dylight550) and *Tc-hedgehog* in green (TSA-Dylight488). The arrow marks the gap between antennal *Tc-hedgehog* expression and the *Tc-empty spiracles* domain, where the new *Tc-wingless* domain arised. (B) *Tc-empty spiracles* in orange (TSA-Dylight550) and *Tc-wingless* in green (TSA-Dylight488). The arrow marks the adjacent expression domains of *Tc-empty spiracles* and *Tc-wingless*.

4.2 Heatshock mediated misexpression of *empty spiracles*

In *Tc-empty-spiracles^{RNAi}*, the initial ocular *Tc-hedgehog* expression (figure 4.6 A) and the backwards extension were unaffected. Due to the loss of the repressive effect of *Tc-empty spiracles* on *Tc-wingless*, all cells between the ocular and antennal segment became *Tc-wingless* positive and ocular *Tc-hedgehog* was lost. As a consequence the ocular parasegment boundary was lost which explains the phenotype described in [Schinko et al., 2008].

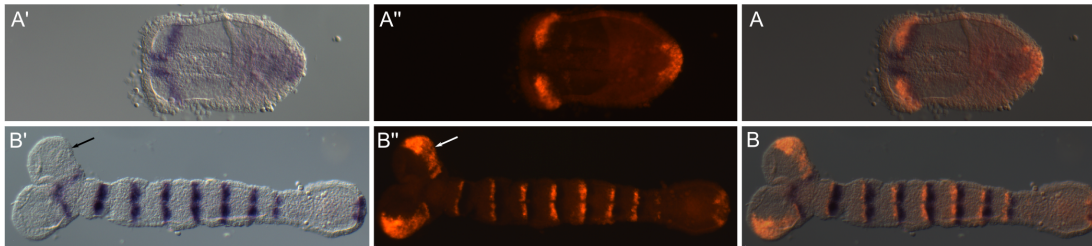


Figure 4.6: Double in situ stainings of *Tc-wingless* and *Tc-hedgehog* in *Tc-empty spiracles^{RNAi}* - (Panel A) Early *Tc-empty spiracles^{RNAi}* embryos. (*A'*, *A''*) The ocular parasegment was established. *Tc-wingless* began to expand towards posterior (compare to the narrow wild type *Tc-wingless* domain in 4.1 A). (Panel B) In elongating germ bands ocular *Tc-hedgehog* was missing (arrow in *B'*) whereas *Tc-wingless* expanded all the way from the ocular domain to the antennal *Tc-hedgehog* expression border (arrow in *B'*). (*B*) overlay

In conclusion, *Tc-empty spiracles* had no effect on the backwards moving of *Tc-hedgehog*, but played an important role in hindering *Tc-wingless* to do the same, which led to the loss of the ocular *Tc-hedgehog* domain.

4.2 Heatshock mediated misexpression of *empty spiracles*

To confirm the repressive effect of *Tc-empty spiracles* on *Tc-wingless*, I analyzed a transgenic beetle line, where *Tc-empty spiracles* was driven ubiquitously via heatshock¹.

In a pretest the experimental conditions were optimized. The transgenic line

¹The transgenic line was generated by Johannes Schinko as described in [Schinko et al., 2012], but with the *Tc-empty spiracles* open reading frame instead of *Tc-orthodenticle1*

4. RESULTS

(#111) and the background strain (vermillion white, VW) were kept at 32°C and subjected to a different amount of heatshocks at 48°C. Heatshocks were applied for ten minutes followed by a regeneration time of two hours at 32°C. The maximum amount of heatshocks tested was four. Each experiment was repeated four times with new embryos. Figure 4.7 shows box plots of hatch rates for the transgenic line and the control (injection strain of the transgenic line). Hatch rates were decreasing with increasing number of heat shocks and approached zero for four heatshocks. However, in the the wild type strain the hatch rate started to decrease significantly with three or more heatshocks, too. Therefore, two heatshocks was considered as the best trade off between high effects of the heatshock in the transgenic line compared to low effects in the control.

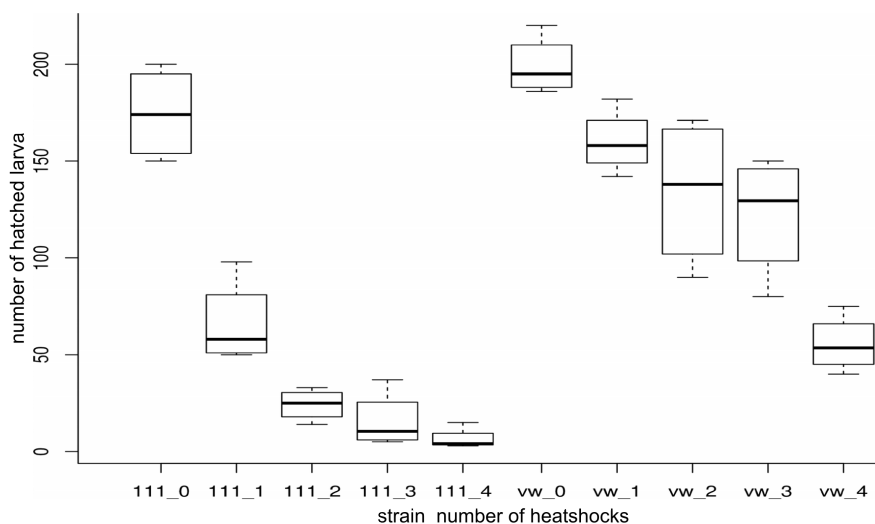


Figure 4.7: Hatch rates of heatshocked transgenic (#111) and wild type (VW) embryos - Y-axis shows the absolute numbers of hatched larva. X-axis shows the type of embryo (#111 or VW) followed by the amount of consecutive heat shocks (0-4)

Initial phenotype analysis showed some dramatic effects of *Tc-empty spiracles* overexpression. Segmentation was disrupted and bristles were misoriented in the whole larva. Interestingly, a small number developed ectopic antennae in the head (figure 4.8 A-C). Double in situ stainings of *Tc-hedgehog* and *Tc-wingless* as segmental markers were performed. *Tc-hedgehog* was expressed in a single broad domain in the head lobes, but was depleted in the rest of the germ band. Ocular

4.2 Heatshock mediated misexpression of *empty spiracles*

Tc-wingless was reduced and spotty. The trunk *Tc-wingless* expression domains were not able to build stable segmental boundaries and collapsed, whereas the expression domain in the growth zone seemed unaffected (figure 4.8 *D*).

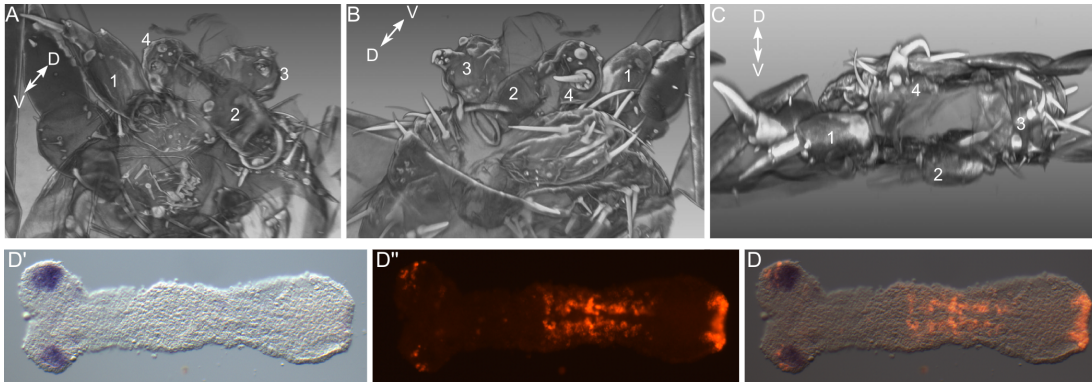


Figure 4.8: Phenotypes of *empty spiracles* overexpression - (A-C) 3D reconstruction of cuticle phenotypes with D \leftrightarrow V indicating the dorsal-ventral axis. (D) In situ staining of elongating germ band. (A) Ventral view of a cuticle 3D model. Head shows 4 antennae, labeled 1-4. Antenna 1 and 2 look rather normal. Antenna 3 and 4 were smaller and located in the labrum. (B) Dorsal view showing the antennae on the labrum (3, 4). (C) View from the anterior (D') *Tc-hedgehog* staining (NBT/BCIP). Only a single broad *Tc-hedgehog* domain remains in the head lobes. (D'') *Tc-wingless* staining (TSA-Dylight550). Some remnants of ocular *Tc-wingless* expression remain, whereas trunk stripes have collapsed. The growth zone was not affected. (D) Overlay

Taken together, *Tc-empty spiracles* leads to the loss¹ of anterior *Tc-wingless* domains in line with the expansion of *Tc-wingless* in the knock down situation. The ocular *Tc-hedgehog* domain expanded backwards, but failed to split up. Additionally, the overexpression led to the development of ectopic antennae. From the position of these antennae it seems that the labrum was transformed. However, this novel role of *Tc-empty spiracles* needs to be confirmed in further studies.

¹reduction in the ocular domain

4. RESULTS

4.3 Differences in anterior and posterior interactions of the Wnt- and hedgehog Pathways

In the trunk the mutual activation of the segment polarity genes *wingless* and *hedgehog* led to the stabilization of parasegment boundaries. However, these interactions were different in the anterior head region in *Drosophila* [Gallitano-Mendel and Finkelstein, 1997]. Therefore, I checked the cross-regulation of these genes in *Tribolium* and included the posterior growth zone in the analysis, an embryonic structure not present in *Drosophila*.

Tc-wingless and *Tc-hedgehog* regulation was examined in the head and growth zone regions of early (10-11 h old) and elongating (12-15 h old) germ bands in wild type and RNAi knock down embryos. RNAi embryos included:

- *Tc-arrow*^{RNAi} disrupting the canonical Wnt pathway (figure 4.9 *B*₁₋₄).
- *Tc-hedgehog*^{RNAi} disrupting the hedgehog pathway for *Tc-wingless* stainings (figure 4.9 *C*_{1,2}).
- *Tc-smoothened*^{RNAi} disrupting the hedgehog pathway for *Tc-hedgehog* stainings (figure 4.9 *C*_{3,4}).

Strikingly, the interactions were complementary: hedgehog signaling acts upstream of *Tc-wingless* expression in the head (figure 4.9 *C*_{1,2}) but Wnt signaling controls *Tc-hedgehog* expression in the growth zone (figure 4.9 *B*_{3,4}). Autoregulation was apparent only for the Wnt pathway in the growth zone, as indicated by the loss of *Tc-wingless* in *Tc-arrow*^{RNAi} but not in *Tc-hedgehog*^{RNAi} (figure 4.9 *B*_{1,2}). Wnt signaling was also needed to maintain ocular but not antennal *Tc-hedgehog* (figure 4.9 *B*₃). I do not find an indication for mutual activation like in the trunk parasegment boundaries of *Drosophila*. In *Tc-smoothened*^{RNAi} antennal and ocular *Tc-hedgehog* expression were fused (figure 4.9 *C*_{3,4}). The trunk *Tc-hedgehog* domains were reduced and were fading completely in stronger RNAi's (compare trunk stripes in *A*₄ with *C*₄, also shown in figure 4.2 *B'*).

4.3 Differences in anterior and posterior interactions of the Wnt- and hedgehog Pathways

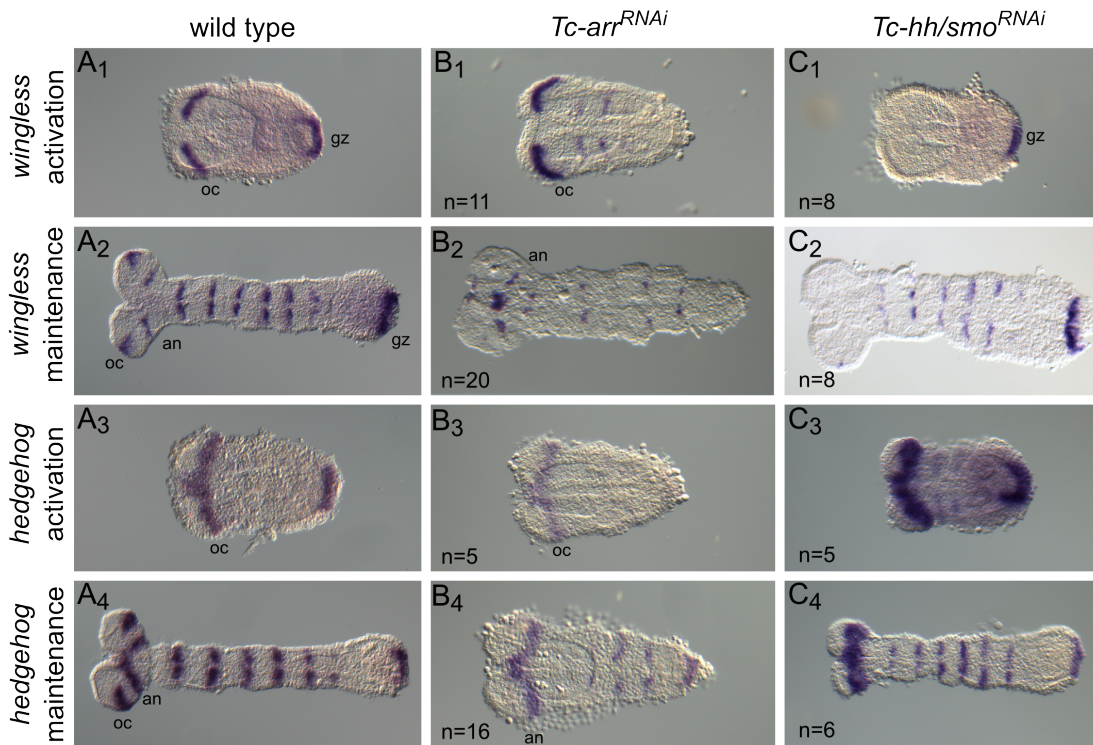


Figure 4.9: Complementary interactions of Wnt- and hedgehog signaling in the head and growth zone - Expression of *Tc-wingless* (rows 1 and 2) and *Tc-hedgehog* (rows 3 and 4) in wildtype ($A_1 - A_4$) and RNAi treated embryos with interrupted Wnt ($B_1 - B_4$) or hedgehog pathway ($C_1 - C_4$) in germ rudiments (row 1 and 3) and elongating germ bands (row 2 and 4) with anterior oriented to the left. ($B_1 - B_4$) Wnt pathway disrupted: Both *Tc-wingless* and *Tc-hedgehog* expression were abolished in *Tc-arrow*^{RNAi} embryos in the growth zone. ($C_1 - C_4$) Hedgehog pathway disrupted: ($C_1 - C_2$) *Tc-wingless* expression was missing in the head of *Tc-hedgehog*^{RNAi} embryos. ($C_3 - C_4$) Ocular and antennal *Tc-hedgehog* expression domains were fused in *Tc-smoothened*^{RNAi}. Trunk expression domains were reduced.

4. RESULTS

4.4 RNAi-RNAseq reveals differences in anterior and posterior target gene sets of the Wnt and hedgehog pathways

To identify target gene sets of the Wnt and hedgehog signaling pathways, I knocked down pathway components and identified the genes down-regulated in germ rudiments (10-11h, figure 4.9 A_1) by comparing their transcript expression levels to wild type controls. The hedgehog pathway was disrupted by *Tc-hedgehog*^{RNAi}, canonical Wnt signaling was suppressed by *Tc-arrow*^{RNAi}. In order to reduce the resulting large candidate gene set for the Wnt pathway, I added *Tc-frizzled1/2*^{RNAi} and *Tc-wntless*^{RNAi} treatments. In addition I included treatments where either the head (*Tc-orthodenticle*^{RNAi}) or the growth zone (*Tc-torso*^{RNAi}) *Tc-wingless* and *Tc-hedgehog* domains were depleted (figure 4.10 $C-F$) (shown for *Tc-wingless* in [Schinko et al., 2008, Schoppmeier and Schroeder, 2005]). This allowed identifying head versus growth zone specific target genes. For example, those *Tc-hedgehog* target genes, which were in addition down-regulated in *Tc-torso*^{RNAi} but not in *Tc-orthodenticle*^{RNAi} were considered exclusive posterior targets of hedgehog signaling (figure 4.10).

4.4.1 Quality control

Three biological replicates were sequenced per treatment. A cluster analysis revealed that all treatments clustered together with the exception of *Tc-hedgehog*^{RNAi}. The *Tc-hedgehog* libraries were not sequenced on the same day, which resulted in a clustering of sequencing days instead of treatments (figure 4.11 A). Cuticle analysis of siblings of the sequenced animals confirmed the high penetrance of the RNAi treatments (see figure 4.11 B for details). The RNAi knockdowns resulted in a transcript reduction of the targeted genes by 80-90%, except for *Tc-frizzled2* with 40% reduction (figure 4.11 C).

In the RNAseq analysis a gene was considered downregulated if the transcript number was reduced by two and the adjusted p-value was < 0.1 (figure 4.12). By building intersects of the downregulated genes I identified potential anterior and posterior target genes of the two pathways (figure 4.10).

4.4 RNAi-RNAseq reveals differences in anterior and posterior target gene sets of the Wnt and hedgehog pathways

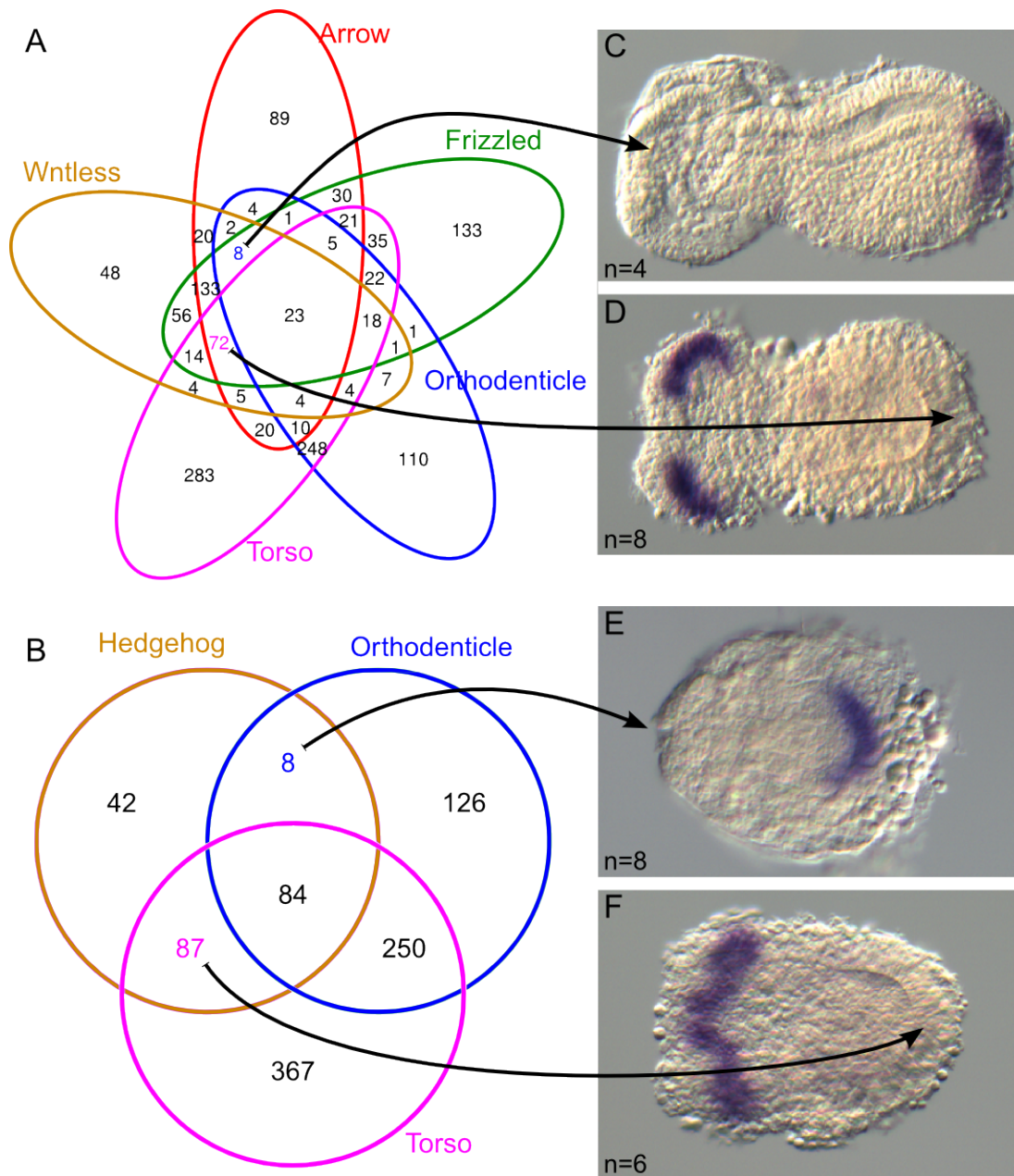
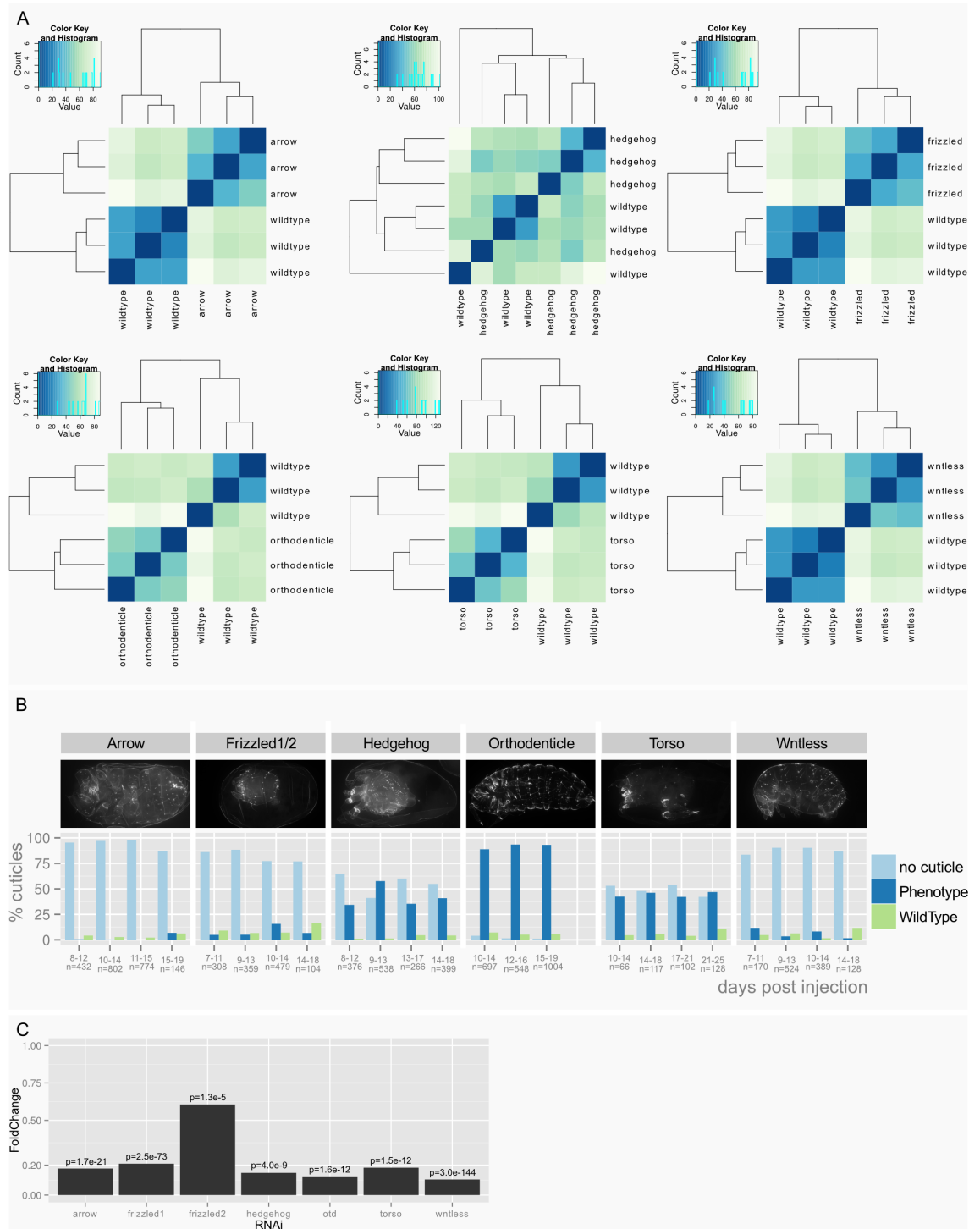


Figure 4.10: Subtractive RNAseq after RNAi - (A, B) Venn diagrams show the number of downregulated genes in the different treatments and their intersects. (C, D) *Tc-wingless* staining; (E, F) *Tc-hedgehog* staining. In order to distinguish between anterior and posterior target gene sets, the head and growth zone expression domains were depleted by an independent treatment: In *Tc-orthodenticle*^{RNAi}, the head domains were missing (C, E) while in *Tc-torso*^{RNAi} the growth zone domains were absent (D, F). Blue numbers indicate the head specific target gene sets and red numbers the growth zone specific gene sets (see black arrows).

4. RESULTS



4.4 RNAi-RNAseq reveals differences in anterior and posterior target gene sets of the Wnt and hedgehog pathways

Figure 4.11 (preceding page): Quality controls of RNAseq experiment

- (A) Cluster analysis of RNAseq treatments. All three replicates of the different treatments clustered together with the exception of the *Tc-hedgehog* treatment. The sequencing libraries of *Tc-hedgehog* were not prepared and sequenced in the same run resulting in a clustering of the sequencing runs instead of the treatment replicates. Analysis was performed with DESeq, heatmaps were plotted with gplots and RcolorBrewer. (B) Quantitative cuticular phenotype analysis of RNAseq treatments: As an additional control egg collections from the same dsRNA injections were set apart and the cuticular phenotypes of all treatments were analyzed quantitatively showing the high penetrance of those. The cuticle analysis was repeated on subsequent days showing the persistence of the RNAi effect. (C) The RNAi treatments resulted in a transcript reduction of 80 to 90% for the single knock downs. In the double RNAi *Tc-frizzled1* was reduced by 80% and *Tc-frizzled2* by 40%. Barplots show fold changes of transcript levels compared to the wild type with Benjamini Hochberg adjusted p-values (false discovery rate)

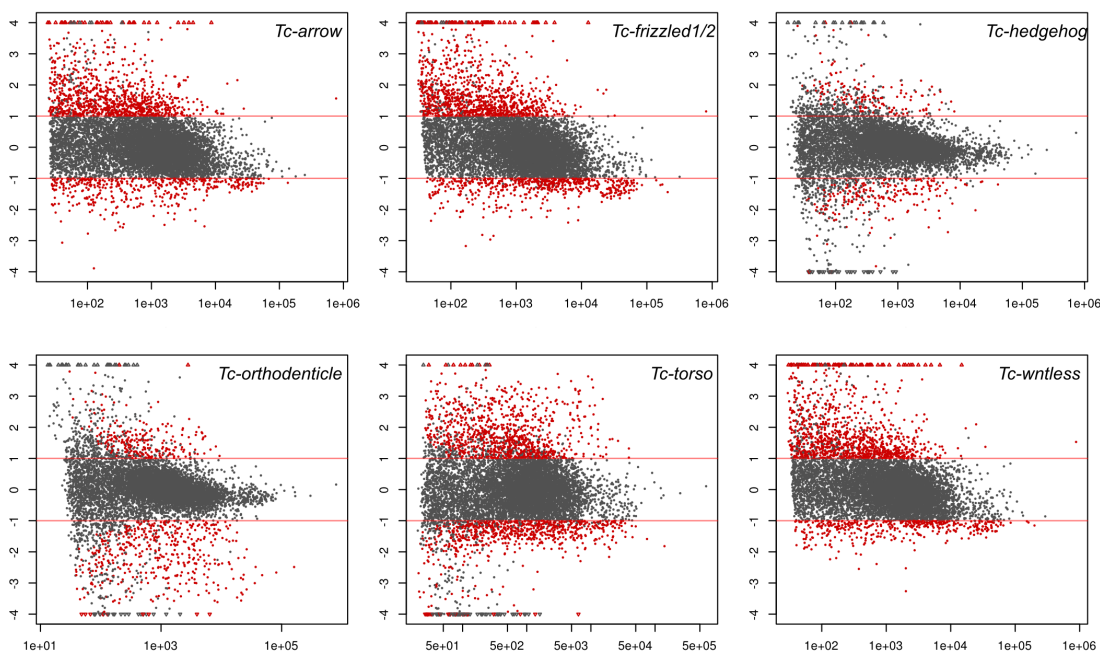


Figure 4.12: MA-plots of RNAseq treatments - Y-axis: log2 fold change values. X-axis: mean normalized counts of treatment and wild type samples for all genes. Significant differentially expressed genes (false discovery rate < 0.1) are shown in red.

4. RESULTS

4.4.2 In situ hybridization of candidate gene sets

In order to validate the candidate gene sets obtained from the RNAseq experiment I performed in situ hybridization for all transcription factors and signaling molecules and all genes without ortholog in *Drosophila*. Genes with low expression levels (below a normalized count of 200 in wild type) were excluded.

4.4.2.1 Posterior Wnt targets

The gene set contained 72 candidates (see figure 4.10). 22 of them were ribosomal genes. An additional seven genes (*Tc-brachyenteron*, *Tc-caudal*, *Tc-twist*, *Tc-even skipped*, *Tc-odd skipped*, *Tc-hairy*, *Tc-ladybird*) were already known to be expressed in the growth zone in *Tribolium*. From the remaining 43 genes I selected 23 candidates for evaluation in the situ screen with the criteria described above. I obtained clones for 21 of them. These included seven genes with a *Drosophila* ortho- or homolog known to be involved in signaling or to be transcription factors. Six of these candidates showed specific posterior expression in the early germ band rudiment. From the remaining 14 genes without *Drosophila* homolog ten showed posterior expression. Three genes with highly similar sequences related to a retro transposon gave ubiquitous staining and one gene did not stain at all.

In summary the gene set contained

- 22 ribosomal genes
- 7 published genes showing posterior expression
- 21 selected candidates
 - 7 with *Dm* homolog
 - * 6 showed posterior expression
 - 14 without *Dm* homolog
 - * 10 showed posterior expression

4.4 RNAi-RNAseq reveals differences in anterior and posterior target gene sets of the Wnt and hedgehog pathways

Of the 28 genes (including previously published genes) 23 showed posterior expression (82%). See figure 4.13 for stainings and further details.

Several genes, not previously known to be active in the growth zone, were involved in signaling pathways: *Tc-cAMP dependent PK1* (Hedgehog), *elbowB* (Notch), *ETS-domain lacking* and *Misexpression suppressor of ras3* (Ras) [Baker et al., 2001, Bucher and Klingler, 2005, Huang and Rubin, 2000, Luque and Miln, 2007, Wang and Holmgren, 2000]. In line with the role of canonical Wnt signaling in the growth zone [Bolognesi et al., 2009, Beermann et al., 2011], important posterior patterning genes were included: *Tc-caudal* [Schulz et al., 1998, Copf et al., 2004] and the pair rule genes *Tc-hairy*, *Tc-even skipped* and *Tc-odd skipped* [Sommer and Tautz, 1993, Choe et al., 2006] in addition to the mesodermal genes *Tc-twist* [Sommer and Tautz, 1994] and *Tc-ladybird* [Cande et al., 2009, Jagla et al., 1997]. Unexpectedly for this early embryonic stage, I found two genes with a known function in *Drosophila* hind gut formation: *Tc-brachyenteron* and *Tc-dichaete* [Berns et al., 2008, Snchez-Soriano and Russell, 2000, Singer et al., 1996] and identified *Tc-senseless* as a novel player in gut development (see section 4.6 on page 46). GO enrichment analysis using the *Drosophila* annotations included processes like “gene expression” and “hindgut morphogenesis”. The complete table including all enriched GO terms can be found in the appendix on page 88.

4.4.2.2 Anterior Wnt candidates

This set contained eight genes. One was *Tc-eyeless* which was known to be expressed at the anterior. I selected six more for the in situ screen and obtained clones for five. Three had a *Drosophila* homolog. *Tc-notum* was expressed at the anterior in the germ band. *Tc-adenosine2* was expressed in the extra embryonic region at the anterior. *Tc-amylase distal* showed no expression. Of the unknown genes one was expressed in the anterior extra embryonic region and one in the anterior region of the germ band.

In total, I looked at six genes (one published, three with *Dm* homologs and two unknown). Three were localized in the anterior germ band and two in the anterior extra embryonic region. Taken together five of six genes were expressed in the anterior region of the embryo (83%). See figure 4.13 for stainings and further

4. RESULTS

details.

Apart from *Tc-notum* (a negative Wnt regulator Giraldez et al. [2002]) and *Tc-eyeless* [Yang et al., 2009, Posnien et al., 2011], not many target genes for the putative head signaling center were found.

4.4.2.3 Posterior hedgehog candidates

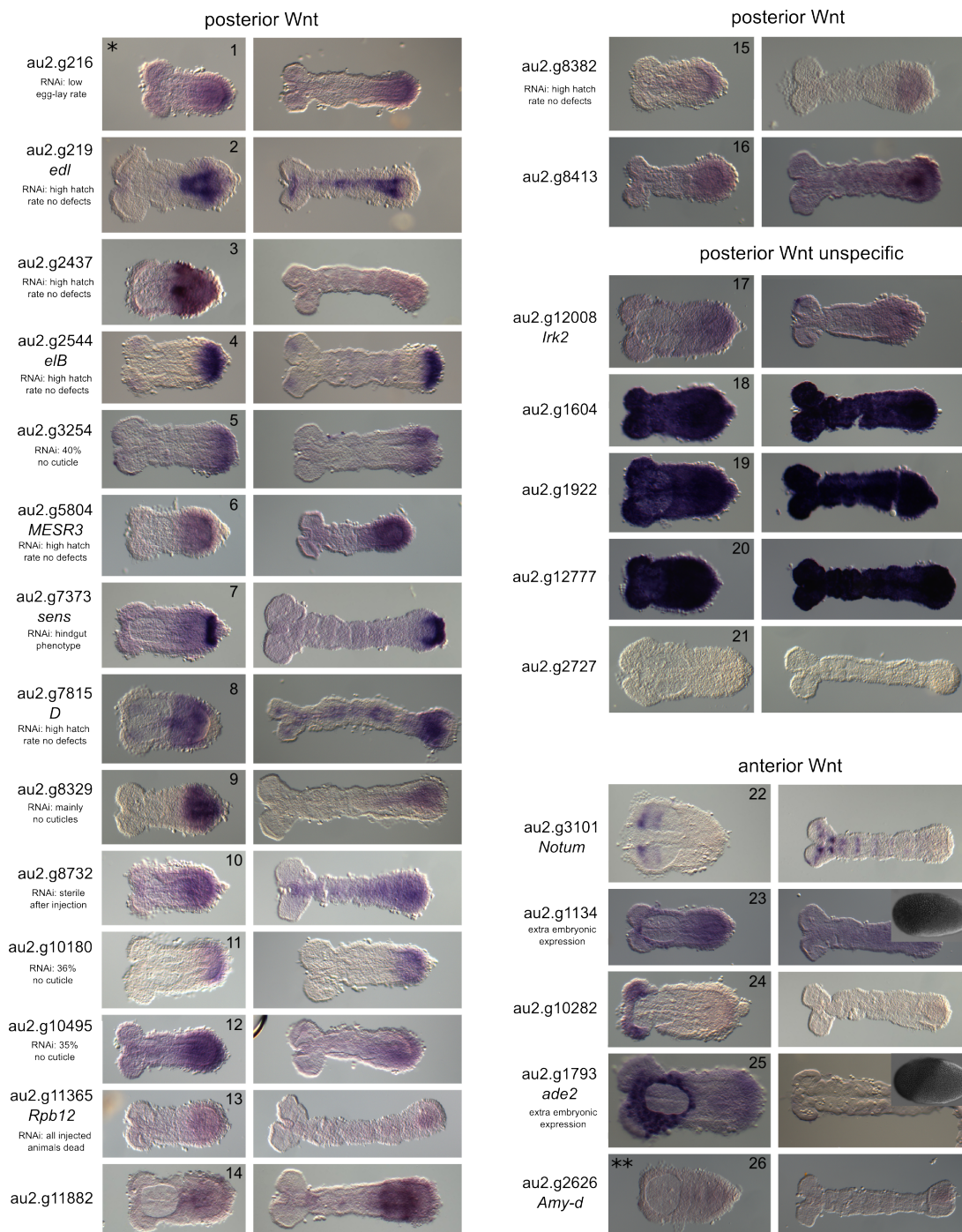
This gene set comprised 87 genes. Twelve genes with a *Drosophila* homolog and 15 without were selected for the in situ screen. I found that in the group of *Drosophila* homologs nine genes showed posterior expression compared to eight in the group without a *Drosophila* homolog. In total 17 of 27 candidates showed posterior expression in the in situ stainings (63%). See figure 4.14 for stainings and further details.

In line with the overall correct germ band elongation in *Tc-hedgehog*^{RNAi} embryos ([Farzana and Brown, 2008] and figure 4.9 C₂), I did not find segmentation genes apart from *Tc-sloppy paired*, which is a secondary pair rule gene in *Tribolium* [Choe and Brown, 2007]. I found four ortho/homologs of *Drosophila* genes involved in signaling across cell membranes: *roadkill* (hedgehog), *cln3* (Notch, JNK), *CG10960* (Jak/Stat) and *spatzle* (Toll) [Kent et al., 2006, Morisato and Anderson, 1994, Müller et al., 2005, Tuxworth et al., 2009]. Furthermore, I found eight ortho/homologs known to act as peptidases or peptidase inhibitors (*CG5618*, *CG5639*, *CG32473*, *Jonah65Aiii*, *Puromycin sensitive peptidase*, *calpainB*, *Serpin42Da*, *fat spondin*) [Gelbart et al., 1997, Jekely and Friedrich, 1999]. GO term analysis using the *Drosophila* annotations as reference did not reveal any significantly enriched terms.

4.4.2.4 Anterior hedgehog candidates

This set contained eight genes. Three had a homologous gene in *Drosophila*. I selected seven for the in situ screen with only one (au2.g954) showing anterior expression at a later stage (14%).

4.4 RNAi-RNAseq reveals differences in anterior and posterior target gene sets of the Wnt and hedgehog pathways

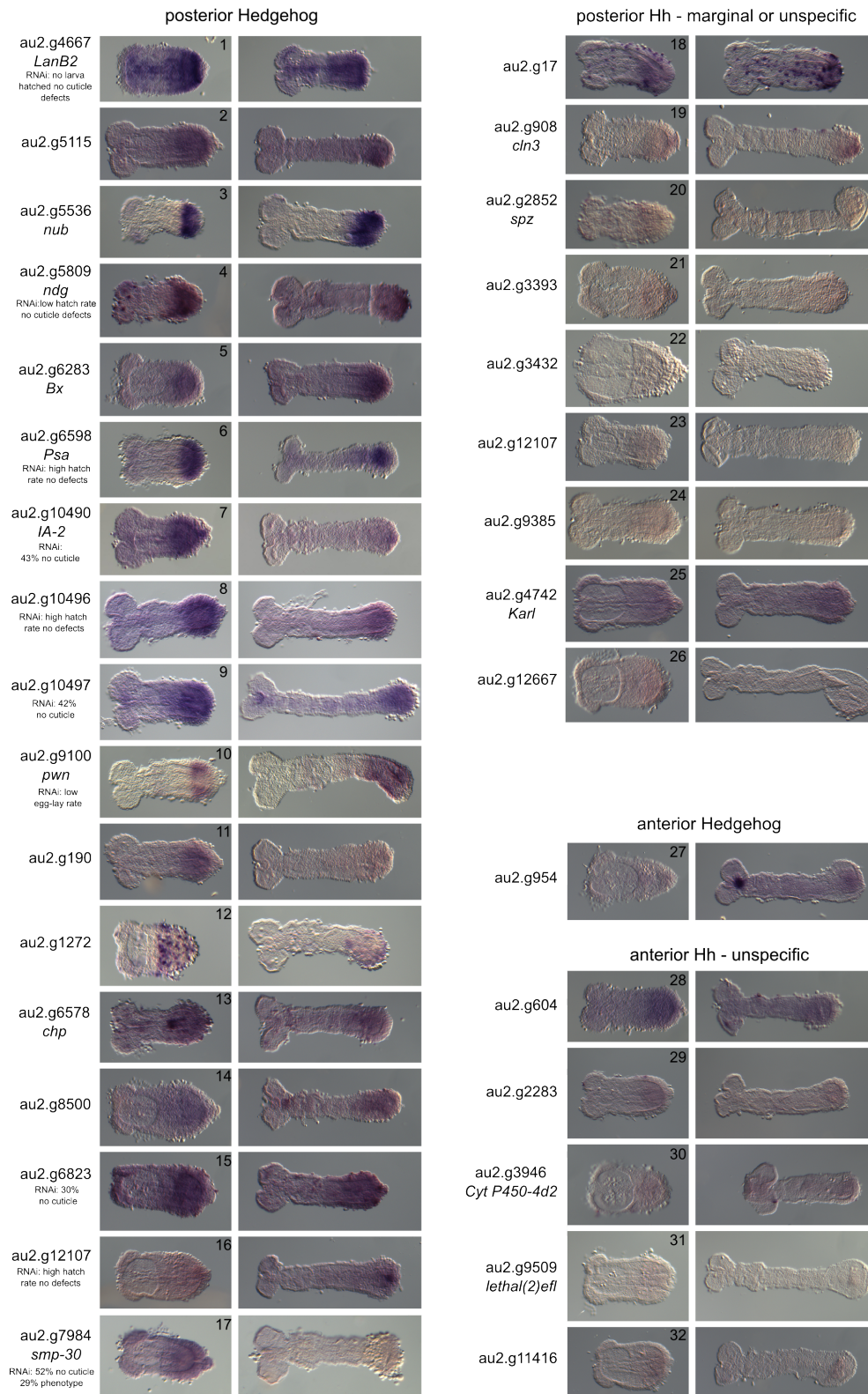


4. RESULTS

Figure 4.13 (preceding page): Posterior Wnt Candidates: - 23 candidate genes were selected for evaluation in the situ screen. I obtained clones for 21 of them. Those included seven genes with a *Drosophila* ortho- or homolog known to be involved in signaling and transcription factors. Six of these candidates showed specific posterior expression in the early germ band rudiment (2, 4, 6, 7, 8, 13). In addition 14 genes with no *Drosophila* homolog were added to the candidates for the in situ screen. 10 showed posterior expression (1, 3, 5, 9, 10, 11, 12, 14, 15, 16). Three genes with highly similar sequences related to a retro transposon gave ubiquitous staining (18, 19, 20) and one gene did not stain at all (21). Gene au2.g216 (*) was an overlapping candidate from both the Wnt and hedgehog gene sets.

Anterior Wnt candidates: This gene set contains 8 genes. I selected six for the in situ screen and obtained clones for five. *Tc-notum* (22) and au2.g10282 (24) were expressed exclusively in the head at this early stage. *Tc-adenosine2* (25) and au2.g1134 (23) were expressed in the extra embryonic region at the anterior. *Tc-amylase distal* showed no expression (26). *Tc-eyeless* was known to be expressed in the head. Tc-amylase distal (**) was an overlapping candidate from both the Wnt and hedgehog gene sets

4.4 RNAi-RNAseq reveals differences in anterior and posterior target gene sets of the Wnt and hedgehog pathways



4. RESULTS

Figure 4.14 (preceding page): Posterior hedgehog candidates: - 27 genes were selected for the in situ screen including twelve with a homologous gene in *Drosophila* and 15 without. Among the genes with a homolog nine showed posterior expression (1, 3, 4, 5, 6, 7, 10, 13, 17). In the group of unknown genes eight were expressed in posterior regions (2, 8, 9, 11, 12, 14, 15, 16).

Anterior hedgehog candidates: Eight genes were in the gene set. Seven genes were stained, with only one (27) showing anterior expression (14%). One gene was a candidate in the anterior Wnt set and can be found there (figure 4.13).

4.4 RNAi-RNAseq reveals differences in anterior and posterior target gene sets of the Wnt and hedgehog pathways

4.4.3 Expression profiles of anterior expressed genes

In a study previously conducted in our lab, the orthologs of vertebrate head patterning genes were analyzed¹. Many of these genes were expressed at the ocular parasegment boundary at the germ rudiment stage. Surprisingly, only *Tc-eyeless* was among the downregulated genes in the anterior candidate sets (intersect of *Tc-orthodenticle*). Therefore, I checked how these potential anterior genes were regulated in the different RNAseq treatments. The selected genes included:

1. **Genes with an exclusive anterior expression domain:** *Tc-cubitus interruptus*, *Tc-empty spiracles*, *Tc-eyeless*, *Tc-goosecoid*, *Tc-lim1*, *Tc-orthodenticle*, *Tc-sloppy paired* and *Tc-twin of eyeless*.
2. **Genes with an anterior and posterior expression domain:** *Tc-hedgehog*, *Tc-tailless* and *Tc-wingless*.

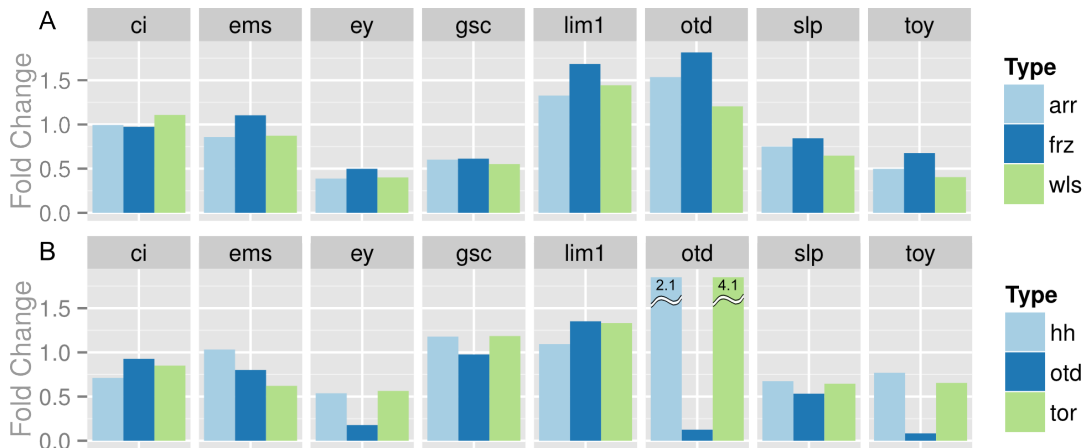


Figure 4.15: Fold change values of potential anterior target genes - (A) Wnt treatments, *Tc-arrow*^{RNAi}, *Tc-frizzled*^{RNAi} and *Tc-wntless*^{RNAi}. (B) *Tc-hedgehog*^{RNAi}, *Tc-orthodenticle*^{RNAi} and *Tc-torso*^{RNAi}

¹PhD thesis Nico Posnien: Function and Evolution of highly conserved head genes in the red flour beetle *Tribolium castaneum*, Table 5.1 on page 82 and [Posnien et al., 2011]

4. RESULTS

The candidate genes showed very similar expression profiles in the Wnt treatments, i.e. *Tc-arrow*^{RNAi}, *Tc-frizzled1/2*^{RNAi} and *Tc-wntless*^{RNAi} (figure 4.15 A). The expression levels of *Tc-cubitus interruptus* and *Tc-empty spiracles* were not affected. *Tc-eyeless* was highly reduced. *Goosecoid* was reduced by 40% and did therefore not pass the threshold of 50%. *Tc-lim1* and *Tc-orthodenticle* were upregulated. *Tc-sloppy paired* was only slightly downregulated. *Tc-twin of eyeless* was downregulated by more than 50% in *Tc-arrow*^{RNAi} and *Tc-wntless*^{RNAi} but not in *Tc-frizzled1/2*^{RNAi}.

In *Tc-hedgehog*^{RNAi} only *Tc-eyeless* was downregulated by 50%. *Tc-cubitus interruptus*, *Tc-sloppy paired* and *Tc-twin of eyeless* were downregulated between 66% and 75%. *Tc-empty spiracles*, *Tc-goosecoid* and *Tc-lim1* were unaffected, whereas *Tc-orthodenticle* was upregulated by more than 100% (figure 4.15 B, light blue bars).

In *Tc-orthodenticle*^{RNAi}, *Tc-eyeless* and *Tc-twin of eyeless* were downregulated by over 75%. *Tc-sloppy paired* was downregulated by 50%, whereas the rest was unaffected (figure 4.15 B, dark blue bars). In *Tc-torso*^{RNAi} four genes (*Tc-empty spiracles*, *Tc-eyeless*, *Tc-sloppy paired* and *Tc-twin of eyeless*) were downregulated by over 40% indicating that *Tc-torso* played an unexpected role in anterior patterning, which was also reflected by the over 4-fold increase in *Tc-orthodenticle* transcript levels (4.15 B, green bars).

The second group of candidate genes contained those with an anterior and posterior domain in the germ rudiment, i.e. *Tc-hedgehog*, *Tc-tailless* and *Tc-wingless* (figure 4.16). *Tc-hedgehog* was reduced by 40% in the Wnt treatments, corresponding to the loss of the posterior domain. In *Tc-orthodenticle*^{RNAi} it was reduced by 60% (loss of the anterior domains) and in *Tc-torso*^{RNAi} it was reduced by 50%.

Tc-tailless was downregulated in all treatments with the exception of *Tc-hedgehog*^{RNAi}. Therefore I could not assign it to the anterior or posterior gene set. *Tc-wingless* was downregulated between 70% and 50% in all treatments, again reflecting the loss of the anterior or posterior domain.

4.5 RNAi screen of selected candidates

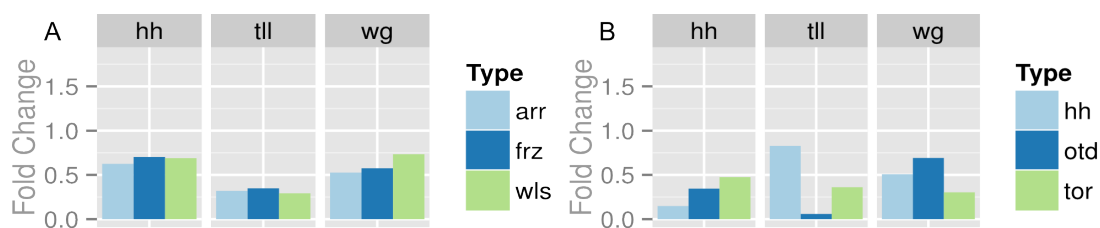


Figure 4.16: Fold change values of target genes with anterior and posterior expression domains - (A) Wnt treatments, *Tc-arrow*^{RNAi}, *Tc-frizzled*^{RNAi} and *Tc-wntless*^{RNAi}. (B) *Tc-hedgehog*^{RNAi}, *Tc-orthodenticle*^{RNAi} and *Tc-torso*^{RNAi}

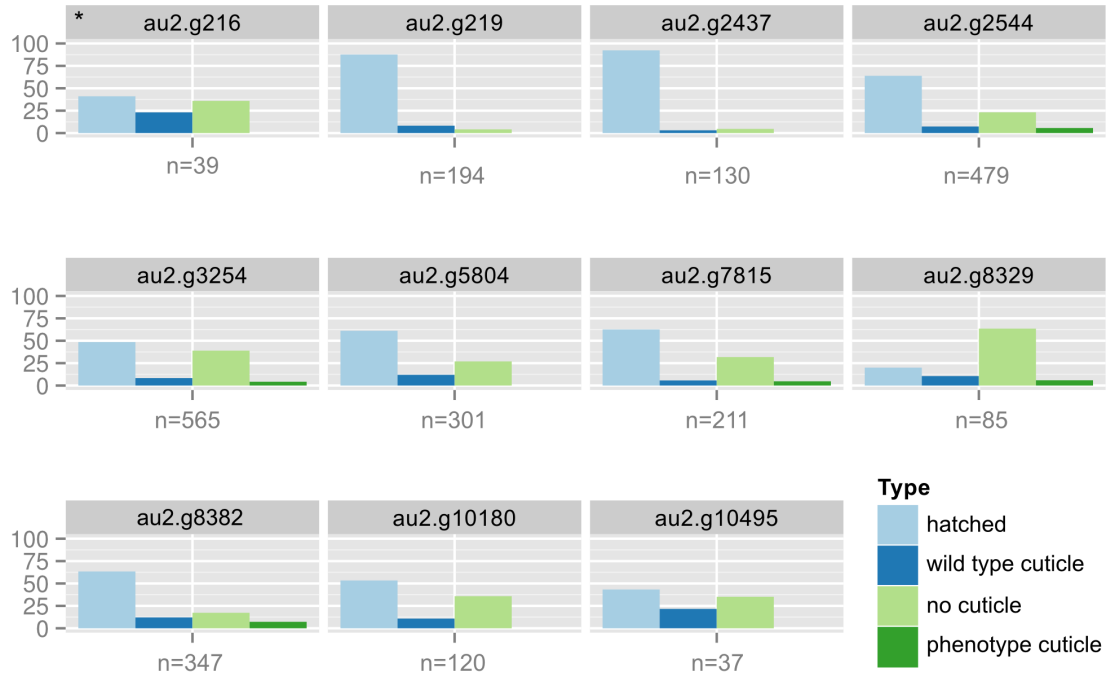
4.5 RNAi screen of selected candidates

As many posterior segmentation and hind gut formation genes were comprised in the posterior gene sets, I searched for novel posterior patterning genes by knocking down selected genes specifically expressed in the growth zone, including 13 from the posterior Wnt targets, 10 from the posterior hedgehog targets and one gene found in both sets (figures 4.13 and 4.14 for stainings, figure 4.17 for quantification of cuticle phenotypes).

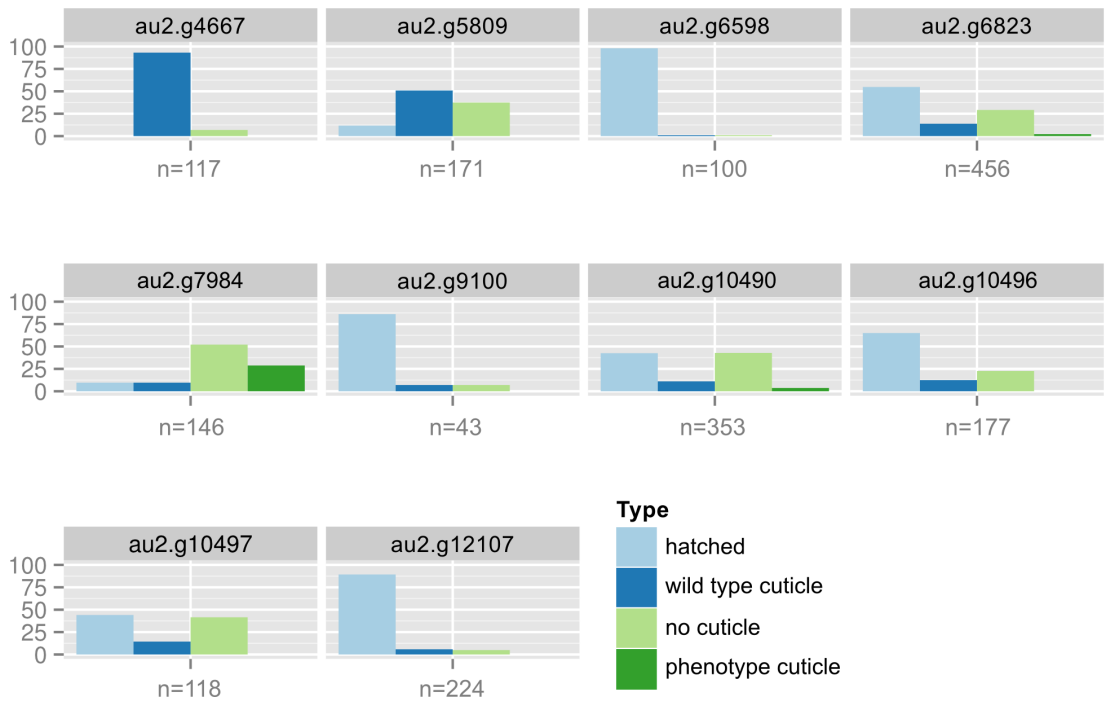
Eight genes led to significant empty egg phenotypes (>30%, au2.g3254, au2.g6823, au2.g7815/ *Dichaete*, au2.g8329, au2.g10180, au2.g10490/ *IA-2*, au2.g10495, au2.g10497). Three genes led to low egg-lay rate or sterility (au2.g216, au2.g8732, au2.g9100/ *pwn*). Two RNAi's resulted in a very low hatch rate but without cuticle defects (au2.g4667/ *LanB2*, au2.g5809/ *ndg*), in one injection all animals died (au2.g11365/ *Rpb12*) and one gene (au2.g7984/ *smp-30*) led to severe cuticle defects. Posterior segments were missing and the bristle pattern was disturbed in the entire larva (figure 4.18).

4. RESULTS

A



B



4.5 RNAi screen of selected candidates

Figure 4.17 (preceding page): Phenotype classes of RNAi screen: - Barplots showing percentages of phenotype categories, i.e hatched, wild type cuticle (not hatched, no defects), no cuticle (empty egg) and phenotype cuticles. (A) Posterior Wnt candidates: 14 dsRNA injections were performed. One injection killed all animals (au2.g11365/Rpb12) and one injection led to sterility (au2.g8732). The phenotype of au2.g7373/sens is described in detail in figure 4.20. The remaining eleven genes were shown. Gene au2.g216 (*also candidate in hedgehog set) resulted in a low egg-lay rate. Genes au2.g3254, au2.g7815, au2.g8329, au2.g10180 and au2.g10495 showed a high percentage (>30%) of empty eggs (no cuticle produced). Only a very small percentage of cuticles showed severe but unspecific defects in various treatments (dark green bars) which were not considered to be significant. (B) Posterior hedgehog candidates: Ten dsRNA injections were performed. One additional gene was included in the Wnt and hedgehog sets (au2.g216, shown above). au2.g9100/pwn led to a reduced egg-lay rate. The genes au2.g6823, au2.g10490/IA-2 and au2.g10497 resulted in increased empty eggs as described above. The two candidates au2.g4667/LanB2 and au2.g5809/ndg resulted in very low hatch rates but no cuticular defects could be detected. au2.g7984/smp-30 resulted in 50% empty eggs and 29% the phenotype shown in figure 4.18.

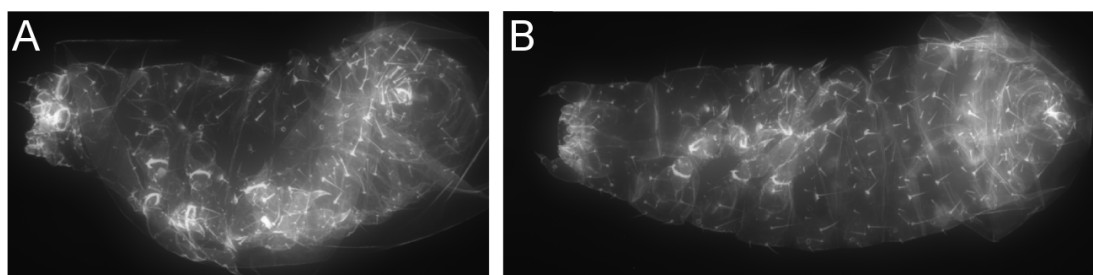


Figure 4.18: au2.g7984 dsRNA cuticle phenotype - (A) Lateral and (B) ventral views of RNAi cuticles showing the loss of posterior segments and misoriented bristles

4. RESULTS

4.6 A novel role for *Tc-senseless* in hindgut development in *Tribolium*

Senseless, a Zn finger transcription factor, was first described in *Drosophila* where it plays a major role in peripheral nervous system development [Nolo et al., 2000]. Furthermore, it was shown that *senseless* was a target gene of *wingless* in the context of wing sensory organ development [Jafar-Nejad et al., 2006].

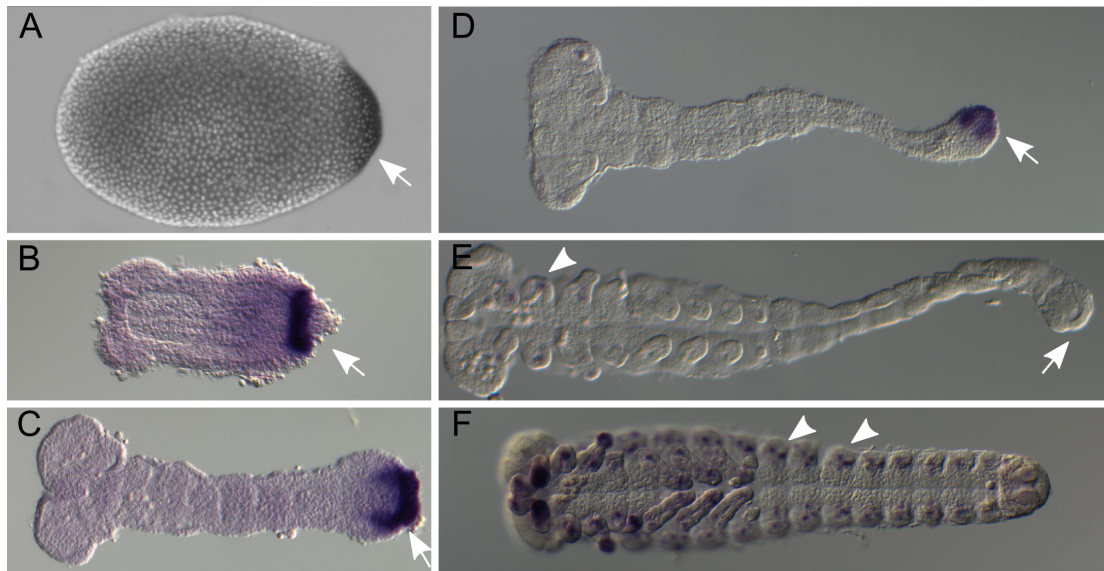


Figure 4.19: Expression of *Tc-senseless* - Developmental time series from undifferentiated blastoderms (A) to retracting germbands (F). Arrows mark growth zone expression, arrow heads mark lateral expression in the peripheral nervous system. Expression of *Tc-senseless* starts at the posterior pole in undifferentiated blastoderms (A) and was maintained in the growthzone throughout elongation (arrows in B-D). During germ band retraction the posterior expression was lost (arrow in E) and arised de novo in putative PNS precursors (arrow heads in E, F). Pictures B and C are the same as in figure 4.13 #7

In our RNAseq experiment *Tc-senseless* was a candidate in the posterior Wnt target gene set and was confirmed to be expressed in early germ rudiments at the posterior end (figure 4.13, gene au2.g7373). *Tc-senseless* expression started in blastoderms at the posterior pole. In early and elongating germ bands it was

4.6 A novel role for *Tc-senseless* in hindgut development in *Tribolium*

expressed in the growth zone. Later, during germ band retraction, expression was lost in the growth zone and started to arise in lateral spots, which likely corresponded to the expression in the peripheral nervous system known from *Drosophila* [Nolo et al., 2000] (see figure 4.19).

4.6.1 *Tc-senseless* is required for hindgut development in *Tribolium*

The first instar external larval cuticles did not show defects after adult RNAi but the hind gut cuticle was missing or highly reduced (figure 4.20 *B, C*). To exclude RNAi off-target effects, two non overlapping fragments of *Tc-senseless* dsRNA, were injected, with both reproducing the phenotype. 60% lacked the complete hindgut and 15% showed reduced hindgut structures with dsRNA fragment 1. The penetrance was slightly weaker for fragment 2 with only 50% missing the hindgut but over 20% having reduced hindgut structures (figure 4.20 *D*).

The hindgut becomes visible only much later during development. Therefore, I wondered whether *T-senseless* was required early (figure 4.19 *A, B*) or at later elongating stages (figure 4.19 *C*). To confirm that the gut phenotype was due to the early expression in the growth zone, staggered embryonic RNAi¹ was performed. *Tc-senseless* dsRNA was injected in 4-7 hour (early blastoderm) and in 14-15 hour (elongating germ band) embryos. About 60% of the early injected eggs did not develop a cuticle in *Tc-senseless*^{eRNAi} compared to 50% in the injection buffer control. Another 10% of injected eggs showed severe cuticular defects, both in *Tc-senseless*^{eRNAi} and the injection buffer control. In the later time point injections the percentages of empty (no cuticle) and severely defected cuticles were slightly lower but again comparable between *Tc-senseless*^{eRNAi} and injection buffer controls. As shown previously, this makes it likely that these effects were due to the injection treatment and not the RNAi [Grossmann et al., 2009].

¹embryonic injections were carried out by Daniela Grossmann

4. RESULTS

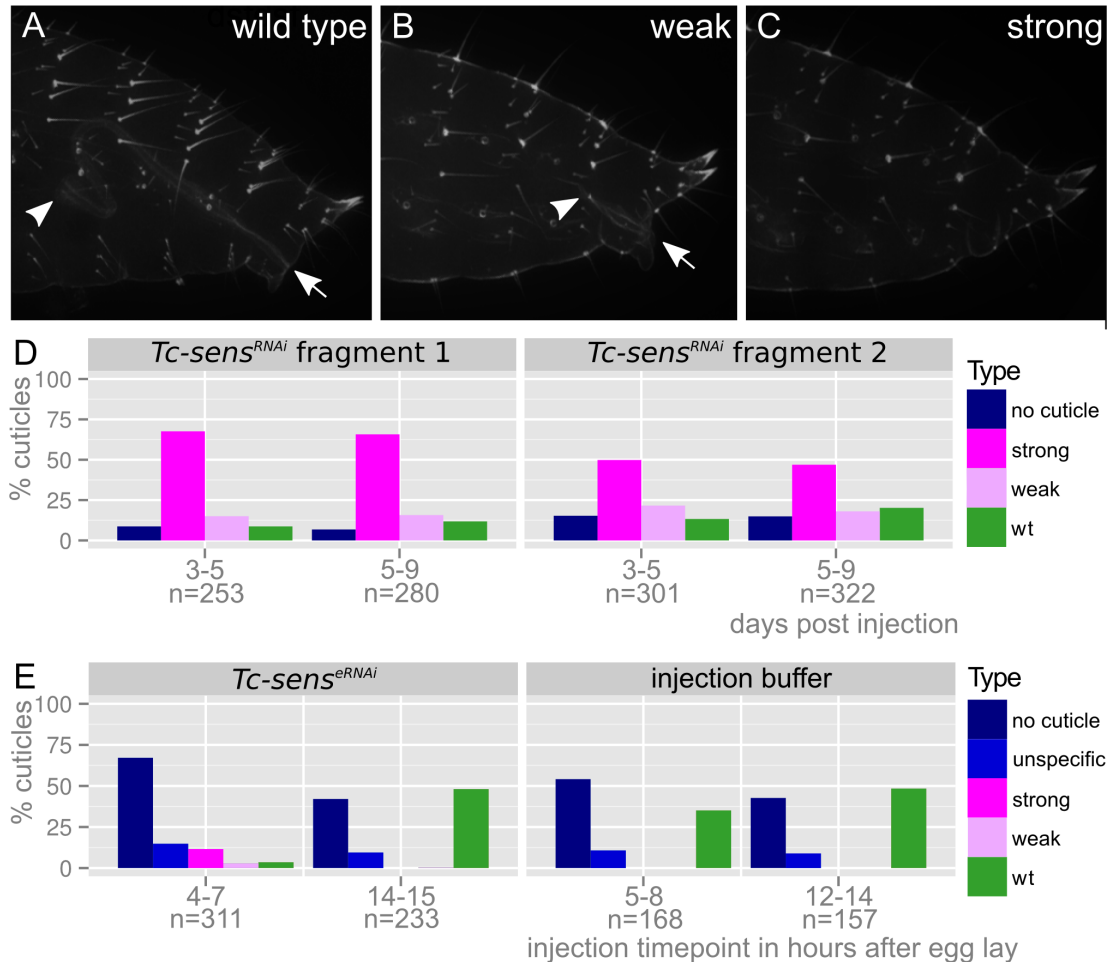


Figure 4.20: *Tc-senseless*^{RNAi} - (A-C) LSM images: arrow and arrowhead mark extremes of the hind gut. (D) Phenotype penetrance in non overlapping dsRNA fragments. (E) Staggered embryonic RNAi. (A) Wild type hind gut, extending in length over four segments. Weak phenotypes (B) show a shortened hindgut (compare arrows with wild type in A) while strong phenotypes lack the hindgut altogether (C). (D) Cuticles showing the phenotype on different days post dsRNA injection in adults. au2.g7373_F1 and au2.g7373_F2 were non overlapping dsRNA fragments of *Tc-senseless* with both reproducing the phenotype. (E) In staggered embryonic RNAi the phenotype could only be reproduced in early injected eggs (4-7 hour old). Later injection (14-15 h) did not show the hindgut phenotype, indicating an early essential function of *Tc-senseless* in the growth zone.

4.6 A novel role for *Tc-senseless* in hindgut development in *Tribolium*

Only injections in early blastoderm stages (4-7h, figure 4.19 *A*) interfered with gut formation (11.6% strong phenotype, 3.6% weak phenotype), while injection in elongating embryos (14-15h, similar to stage in figure 4.19 *C*) did not elicit the gut phenotype (no strong phenotype detected, 0.4% or one cuticle showed the weak phenotype). Hence, *Tc-senseless* was required early in the growth zone for hind gut development.

4. RESULTS

5

Discussion

5.1 Dynamic expression patterns in the establishment of the ocular and antennal parasegment boundaries

Using high resolution fluorescent in situ hybridization I observed a dynamic expression pattern of *Tc-hedgehog* in the head. Expression starts at the ocular parasegment boundary, extends backwards to split up and gives rise to the antennal domain. Only later, during development *Tc-wingless* arises at the antennal boundary to probably stabilize the parasegmental border. I analyzed two candidate genes (*knirps* and *empty spiracles*) known to interfere with antennal development and studied the effects of these candidates on the segment polarity genes *wingless* and *hedgehog*.

Based on the following observations I propose a genetic model that could explain this segmentation process:

***Tc-orthodenticle* activates *Tc-hedgehog* at the ocular parasegment boundary.** In *Tc-orthodenticle*^{RNAi} ocular *Tc-hedgehog* is lost (figure 4.10). In *Tc-hedgehog*^{RNAi} ocular *Tc-wingless* is lost, but in *Tc-arrow*^{RNAi} *Tc-hedgehog* is unaffected initially and fades only later (figure 4.9). This puts *Tc-hedgehog* between *Tc-orthodenticle* and *Tc-wingless* in the activation cascade.

5. DISCUSSION

***Tc-knirps* activates *Tc-hedgehog* posterior of the ocular parasegment boundary.** In *Tc-knirps*^{RNAi} antennal *Tc-hedgehog* never arises, whereas ocular *Tc-hedgehog* is unaffected ([Cerny et al., 2008, Peel et al., 2013] and figure 4.3).

***Tc-empty spiracles* represses *Tc-wingless*.** *Tc-empty spiracles* is expressed between the ocular and antennal *Tc-wingless* domains and *Tc-empty spiracles*^{RNAi} leads to ectopic *Tc-wingless* expression in this region ([Schinko et al., 2008] and figure 4.6).

Convergent extension is the driving force in separating ocular and antennal *Tc-hedgehog*. This was shown in spiders where a similar patterning process occurs [Kanayama et al., 2011]. In *Tribolium*, the early germ rudiment becomes longer and narrower during development hinting at a similar process (figure 4.4). In addition, immunohistochemistry stainings for the cell division marker Phosphohistone-H3 (PH3) showed no significant amount of cell division during this stages¹.

A negative self-regulatory loop splits the *Tc-hedgehog* domain. In *Tc-smoothened*^{RNAi} and *Tc-cubitus interruptus*^{RNAi} the anterior *Tc-hedgehog* domain is broadened but fails to split (figure 4.2 *B* and 4.9 *C*₃, *C*₄).

5.1.1 Genetic model for the patterning of the antennal segment

Here I propose a new model for *Tribolium* anterior head patterning, adding some key genes and interactions, starting with the initial activation of *hedgehog* via *orthodenticle* at the ocular parasegment boundary.

1. Establishment of the ocular parasegment boundary

Tc-hedgehog has an anterior expression domain in the blastoderm, whereas *Tc-wingless* is expressed only in the growth zone before germ band formation [Farzana and Brown, 2008, Bolognesi et al., 2008]. Together with the loss of ocular

¹data not shown and PhD thesis Sebastian Kittelmann, page 39-40, although n was only 2

5.1 Dynamic expression patterns in the establishment of the ocular and antennal parasegment boundaries

Tc-wingless in *Tc-hedgehog*^{RNAi} (figure 4.9 C₁) the establishment of the ocular parasegment can be summarized in two steps:

1. *Tc-orthodenticle* activates *Tc-hedgehog*
2. *Tc-hedgehog* activates *Tc-wingless*

Now the parasegment boundary is stabilized via the cross-regulatory interactions as in the trunk, indicated by the loss of ocular *Tc-hedgehog* in *Tc-arrow*^{RNAi} later during development (figure 4.9 B₄).

2. Backwards expansion of *Tc-hedgehog*

In *Tc-knirps*^{RNAi} ocular *Tc-hedgehog* is unaffected, while the antennal domain does not develop ([Cerny et al., 2008] and figure 4.3). Therefore I assume that *Tc-knirps* activates *Tc-hedgehog* in all cells posterior to the ocular domain. Double in situ stainings with *Tc-knirps* and *Tc-wingless* show that they are expressed adjacently before the backwards expansion of *Tc-hedgehog* starts. As the *hedgehog* domain extends backwards, the gap between *Tc-wingless* and *Tc-knirps* increases (figure 4.4). Convergent extension is probably the driving force that increases this gap. Cell tracking in in vivo imaging could show that this is the case.

Tc-hedgehog cannot activate *Tc-wingless* anterior to it because of the repressing function of *Tc-empty spiracles* on *Tc-wingless*. In *Tc-empty spiracles*^{RNAi} all cells become *Tc-wingless* positive in the antennal segment. Once the moving *Tc-hedgehog* domain is beyond the *Tc-empty spiracles* domain it succeeds in activating *Tc-wingless* and by doing so the antennal parasegment boundary is established and stabilized. In support of this mechanism in *Tc-hedgehog*^{RNAi} antennal *Tc-wingless* is lost (figure 4.9 C₂).

3. Splitting of *Tc-hedgehog*

In *Tc-smoothened*^{RNAi} the *Tc-hedgehog* domain moves backwards but stays attached to the ocular domain. The result is a single broad *Tc-hedgehog* domain that fails to split up (figure 4.9 C₃, C₄). This leads to the assumption that a functional hedgehog pathway is essential for the *Tc-hedgehog* domain splitting. However, in *Tc-cubitus interruptus*^{RNAi} the splitting process is unaffected. Because of the dual role of *cubitus interruptus* as repressor and activator [Aza-Blanc

5. DISCUSSION

et al., 1997] the interpretation of these effects is difficult.

4. Stopping the backwards movement of *Tc-hedgehog*

No experimental data altering the position of antennal *Tc-hedgehog* has been obtained. However, one simple hypothesis could be that once *Tc-knirps* enters into the field where pair-rule genes are expressed, the activating properties of *Tc-knirps* on *Tc-hedgehog* are overridden by them. In RNAi embryos against different pair-rule genes antennal *Tc-engrailed* seems to be affected in some cases [Choe et al., 2006]. Antennal *Tc-engrailed* is expressed relatively late during development which would make *Tc-hedgehog* a better read out to test this assumptions. In addition in *Tc-even skipped*^{RNAi} the *Tc-knirps* domain is expanded into more posterior regions [Peel et al., 2013].

Previous findings showed that a similar process occurs during anterior segment patterning in spiders [Pechmann et al., 2009]. *Orthodenticle* is the key factor activating *hedgehog* in the anterior head. A model involving an autoregulatory signaling network was proposed. The key players involved were *hedgehog*, *cubitus interruptus*, *orthodenticle* and *odd-paired*. The model implies short- and long range morphogen activities of *hedgehog* and an unknown mechanism for the stripe splitting [Kanayama et al., 2011].

5.1.2 Outlook stripe splitting project

Some key experiments are still missing to complete this project. Those include:

- **In vivo imaging:** In spiders, the backwards movement of *hedgehog* is explained by the traveling of *hedgehog* expression across a field of cells in a wave-like manner. This would include that single cells have to turn the expression of *hedgehog* on and off. Another approach to describe the phenomenon would be that there is no dynamic expression of *hedgehog*. Instead the movement of *hedgehog* is due to the influx of lateral cells, i.e. convergent extension. A live imaging movie with a nuclear GFP¹ line could

¹GFP- green fluorescent protein

5.1 Dynamic expression patterns in the establishment of the ocular and antennal parasegment boundaries

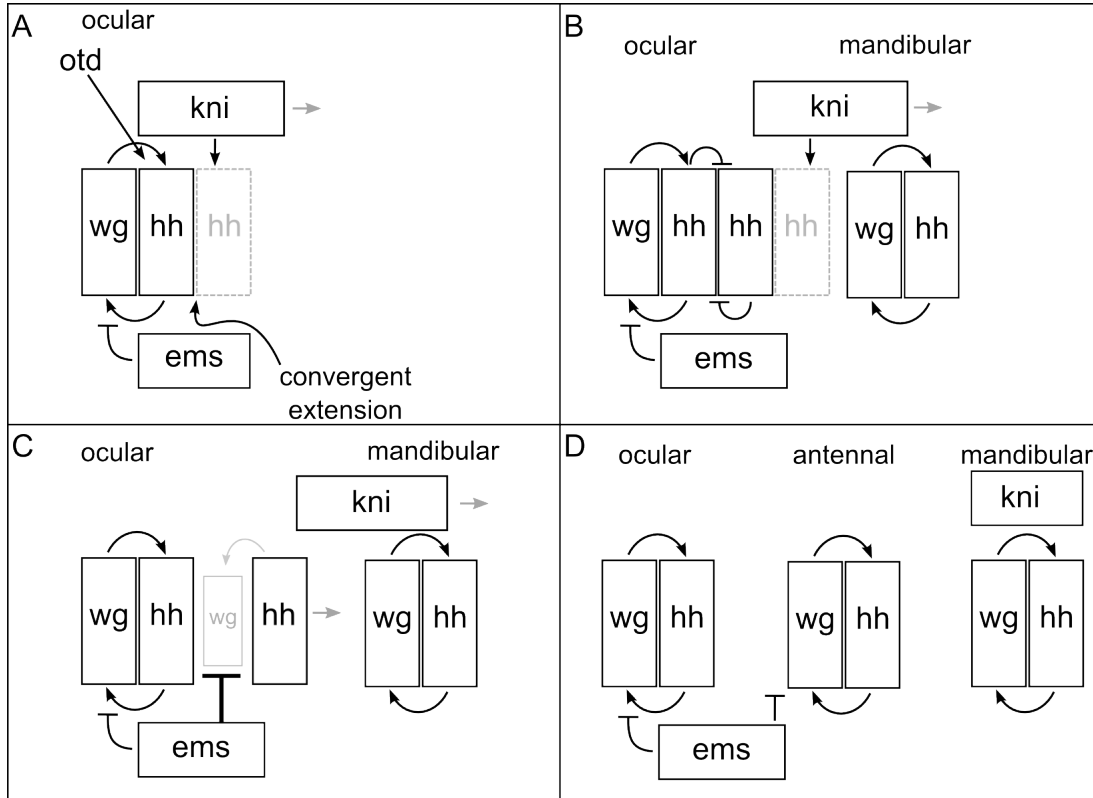


Figure 5.1: Genetic model to establish the antennal parasegment boundary in *Tribolium* - (A) *Tc-orthodenticle* activates ocular *Tc-hedgehog*. Ocular *Tc-hedgehog* activates *Tc-wingless*. Once established, both segment polarity pathways stabilize the boundary. *Tc-knirps*, initially expressed adjacent to *Tc-wingless*, is separated and pushed towards the posterior pole (convergent extension), activating *Tc-hedgehog* in the process. (B) The broadening *Tc-hedgehog* domain initiates a negative auto-regulatory loop of the hedgehog pathway, which leads to the stripe splitting. (C) During its backwards expansion and splitting, *Tc-hedgehog* cannot activate *Tc-wingless* due to the repressive effect of *Tc-empty spiracles* in this field. (D) Once *Tc-hedgehog* moves clear of the *Tc-empty spiracles* expression domain, it activates *Tc-wingless* and stabilizes the antennal segment. The activating function of *Tc-knirps* during backwards traveling has come to a halt at the mandibular segment. The pair-rule gene circuit is active there and governs patterning in classic mode.

5. DISCUSSION

be used to show that such processes occur in the early *Tribolium* germ rudiment.

- **In situ stainings:** To refine the expression topologies of the key genetic factors in the model, some double in situ stainings have to be done, including:
 - *Tc-hedgehog* - *Tc-knirps* to show co-expression of the two genes.
 - *Tc-empty spiracles* - *Tc-knirps* to show initial co-expression and later adjacent expression.
- **RNAi experiments:** Since it is unclear how the posterior (antennal) *Tc-hedgehog* domain comes to a halt, RNAi against some candidate genes could be used to modify the location of these boundary. Candidate genes include: pair rule genes and genes with an expression domain at the posterior border of antennal *Tc-hedgehog*, e.g. *Tc-labial*

5.2 RNAseq after RNAi reveals differences in anterior and posterior target gene sets

5.2.1 Segment polarity interactions in head and growth zone

This work identifies the first comprehensive target gene sets of the hedgehog and Wnt pathways in *Tribolium* embryogenesis using RNAseq. Further, I found a complementary cross regulation of Wnt and hedgehog pathways in head and trunk: hedgehog signaling acts upstream of *Tc-wingless* in the head but has no influence on posterior *Tc-wingless* expression (figure 4.9 C_1, C_2). In the growth zone Wnt signaling acts upstream of *Tc-hedgehog* and is also needed for *Tc-wingless* initiation while hedgehog signaling has no influence on *Tc-wingless* expression. Apparently, the canonical mutual activation between these pathways is restricted to the trunk parasegment boundaries not only in *Drosophila* [Gallitano-Mendel and Finkelstein, 1997] but also in *Tribolium* [Oppenheimer et al., 1999].

5.2 RNAseq after RNAi reveals differences in anterior and posterior target gene sets

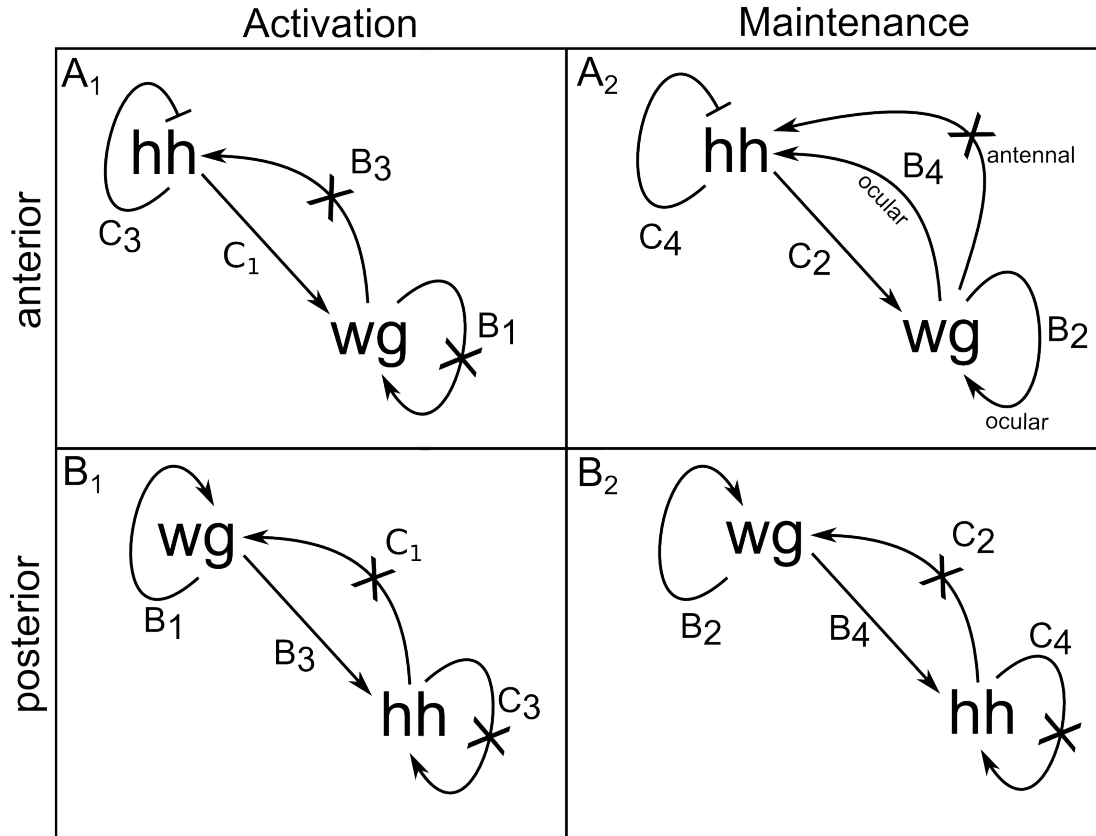


Figure 5.2: Segment polarity interactions in head and growth zone - (A_1, A_2) Anterior; (B_1, B_2) Posterior; arrows indicate activation, crossed arrows non activation, dotted arrows mark ambiguous interactions. Arrows are labeled with the in situ from which the respective interaction was deduced (see figure 4.9). (A_1) Anterior activation: Hedgehog pathway acts upstream of *Tc-wingless*. Hedgehog pathway represses *Tc-hedgehog* expression during backwards traveling. Wnt pathway has no effect on *Tc-wingless* and *Tc-hedgehog* expression. (A_2): Hedgehog pathway acts upstream of *Tc-wingless* expression at the ocular and antennal parasegment boundaries. Hedgehog pathway represses *Tc-hedgehog* expression during backwards traveling. Wnt pathway has no effect on antennal *Tc-hedgehog* but is needed for maintenance of ocular *Tc-hedgehog*. With a disrupted Wnt pathway ocular *Tc-wingless* is lost which could indicate autoregulation (dotted arrow). However, mutual activation between the two pathways is also possible and more likely. (B_1) Posterior activation: The Wnt pathway is needed for *Tc-wingless* (auto regulation) and *Tc-hedgehog* activation. The hedgehog pathway has no effect on *Tc-wingless* or *Tc-hedgehog* expression. (B_2) Posterior Maintenance: The interactions are the same as in posterior activation.

5. DISCUSSION

5.2.2 The ocular parasegment boundary as anterior signaling center

Based on the expression of their ligands, both Wnt and hedgehog signaling pathways were likely to play crucial roles in early head and growth zone patterning. Unexpectedly, I did not find many targets in the head (eight compared to 72/87 in the growth zone) domain, although this domain corresponds to the vertebrate mid-hind-brain boundary and several putative target genes start being expressed there [Posnien et al., 2011]. By looking at the expression levels in the single treatments I showed that most of these anterior target genes are indeed downregulated in *Tc-orthodenticle*^{RNAi}. In the Wnt and hedgehog treatments many of the anterior candidates were downregulated, however, they did not show in our intersects because the thresholds of reduction by half was not met in all treatments. *Tc-gooseoid*, a gene involved in stomatogastric nervous system development in the foregut in *Drosophila* [Hahn and Jäckle, 1996] was downregulated by only 40% in the Wnt and hedgehog treatments. *Tc-empty spiracles* was not affected by the treatments which is not surprising if it is considered a head-gap gene lying upstream of segment boundary formation [Cohen and Jürgens, 1990, Schinko et al., 2008]. *Tc-tailless* [Weigel et al., 1990, Schroder et al., 2000] was downregulated in all Wnt treatments, in *Tc-orthodenticle*^{RNAi} but also in *Tc-torso*^{RNAi}. Hence, it was not possible to distinguish between anterior and posterior in this case. *Tc-hedgehog* was downregulated by 40% in the Wnt treatments in correlation with the loss of *Tc-hedgehog* expression in the growth zone. In *Tc-orthodenticle*^{RNAi} it was reduced by 60% and in *Tc-torso*^{RNAi} by 50% corresponding to loss of the anterior or posterior domain. *Tc-orthodenticle* was upregulated in the Wnt and hedgehog treatments. Probably the ocular parasegment boundary can be interpreted as a barrier with repressive functions, constricting *Tc-orthodenticle* to the anterior most part of the head. *Tc-eyeless* and *Tc-twin of eyeless* [Yang et al., 2009] were both downregulated in the Wnt and hedgehog treatments making these two genes good downstream targets of the two pathways. *Tc-wingless* was reduced by almost 50% in *Tc-arrow*^{RNAi}, *Tc-frizzled*^{RNAi} and *Tc-hedgehog*^{RNAi} in line with the loss of the growth zone or ocular domain.

Another possible explanation for the low number of anterior targets could be the

5.2 RNAseq after RNAi reveals differences in anterior and posterior target gene sets

chosen developmental stage. Since the anterior head segments are not yet established, the segment polarity genes might still be involved with patterning and positioning processes (see section 4.1) and not in the activation of target genes. RNAseq at a later developmental stage could show if this is the case.

The large increase in *Tc-orthodenticle* transcripts in *Tc-torso*^{RNAi} (over 4-fold) showed that *Tc-torso* had an unexpected effect on anterior development. Due to this fact, some of the anterior target genes could be in the intersect of *Tc-orthodenticle* and *Tc-torso*. Hence, these genes were not found in the RNAseq approach.

One interesting hypothesis to test is that the ocular parsegment boundary represents a barrier with repressive properties instead of being a signaling center activating target genes.

5.2.3 Posterior target genes

A similar number of genes are regulated by hedgehog and Wnt signaling in the growth zone and the gene sets are quite different from each other. An intriguing feature of the hedgehog dataset is the large number of genes potentially involved in a proteolytic cascade including the Toll ligand *Tc-spatzle*. Based on this and on the fact that posterior segmentation is unaffected in *Tc-hedgehog*RNA^{RNAi} [Farzana and Brown, 2008] a role in ongoing non-ectodermal patterning in the growth zone could be hypothesized, where mesoderm and neuroectoderm probably need to be specified continuously [Handel et al., 2005].

The finding of several crucial posterior patterning genes in the growth zone Wnt set was not unexpected, given the conserved role of Wnt signaling in posterior patterning in bilaterians [Martin and Kimelman, 2009] and even pre-bilaterians [Petersen and Reddien, 2009]. However, the large number of ribosomal genes indicates that Wnt signaling does not only govern pattern formation but also ensures that the respective cells are metabolically prepared for growth. Recently it was shown that *pygo*, a transcriptional co-activator of *armadillo*/ β -*catenin* [Kramps et al., 2002], is involved in ribosome biogenesis in human cancer cell lines [Andrews et al., 2013]. Taken together, this could indicate that a link between the Wnt pathway and ribosome metabolism may be a more general feature.

5. DISCUSSION

Finally, I found several hindgut genes to be controlled by Wnt signaling [Lengyel and Iwaki, 2002], and identified *Tc-senseless* as novel gene involved in hindgut development. It is required early in the growth zone despite the fact that the hindgut develops only hours later. Apparently, there is molecular specification of posterior terminal cells before completion of abdominal segmentation. This function is different from the *Drosophila* ortholog *Dm-senseless*, which is not expressed in the hindgut but in sensory organ precursors and is required for their formation [Nolo et al., 2000]. Interestingly, the paralog *Dm-senseless-2* is expressed in the anterior midgut in *Drosophila* but a phenotype has not been described. Phylogenetic tree reconstruction showed that au2.g7373 is indeed the ortholog of *Dm-senseless* (see figure B.1). This could indicate that *Tc-senseless* fulfilled both functions in the last common ancestor. After a gene duplication the paralogs were used in different processes.

5.2.4 Outlook RNAseq

In summary the here described RNAseq after RNAi approach is robust and technically not too complex. It has great potential in the genetic deletion of certain tissues in embryos, which are not amenable to mechanical dissection because of their small size.

To check whether the ocular parasegment boundary has indeed a repressive function, RNAi against Wnt and hedgehog pathway components followed by in situ stainings of anterior candidate genes (e.g. *Tc-orthodenticle*), could clarify this hypothesis.

A functional analysis of the paralogs of *senseless* in *Drosophila* and *Tribolium* would help understanding the ancestral role of the gene.

References

- A. Abzhanov and T. C. Kaufman. Homeotic genes and the arthropod head: Expression patterns of the labial, proboscipedia, and deformed genes in crustaceans and insects. *Proceedings of the National Academy of Sciences of the United States of America*, 96(18):10224–10229, Aug. 1999. ISSN 0027-8424. URL <http://www.ncbi.nlm.nih.gov/pmc/articles/PMC17870/>. PMID: 10468590 PMCID: PMC17870. 2
- S. F. Altschul, T. L. Madden, A. A. Schäffer, J. Zhang, Z. Zhang, W. Miller, and D. J. Lipman. Gapped BLAST and PSI-BLAST: a new generation of protein database search programs. *Nucleic acids research*, 25(17):3389–3402, Sept. 1997. ISSN 0305-1048. PMID: 9254694. 10, 17
- S. Anders and W. Huber. Differential expression analysis for sequence count data. *Genome biology*, 11(10):R106, 2010. ISSN 1465-6914. doi: 10.1186/gb-2010-11-10-r106. PMID: 20979621. 16
- L. E. Anderson. Hoyer’s solution as a rapid permanent mounting medium for bryophytes. *The Bryologist*, 57(3):242, Sept. 1954. ISSN 00072745. doi: 10.2307/3240091. URL <http://www.jstor.org/discover/10.2307/3240091?uid=3737864&uid=2129&uid=2&uid=70&uid=4&sid=21102875966867>. 14
- P. G. P. Andrews, Z. He, Y. R. Tzenov, C. Popadiuk, and K. R. Kao. Evidence of a novel role for pygopus in rRNA transcription. *The Biochemical journal*, 453(1): 61–70, July 2013. ISSN 1470-8728. doi: 10.1042/BJ20121667. PMID: 23517060. 59
- P. Aza-Blanc, F. A. Ramirez-Weber, M. P. Laget, C. Schwartz, and T. B. Kornberg. Proteolysis that is inhibited by hedgehog targets cubitus interruptus protein to the nucleus and converts it to a repressor. *Cell*, 89(7):1043–1053, Jun 1997. 20, 53
- D. A. Baker, B. Mille-Baker, S. M. Wainwright, D. Ish-Horowicz, and N. J. Dibb. Mae mediates MAP kinase phosphorylation of ets transcription factors in drosophila.

REFERENCES

- Nature*, 411(6835):330–334, May 2001. ISSN 0028-0836. doi: 10.1038/35077122. URL <http://www.nature.com/nature/journal/v411/n6835/full/411330a0.html>. 35
- A. Beermann, R. Prühs, R. Lutz, and R. Schröder. A context-dependent combination of wnt receptors controls axis elongation and leg development in a short germ insect. *Development (Cambridge, England)*, 138(13):2793–2805, July 2011. ISSN 1477-9129. doi: 10.1242/dev.063644. PMID: 21652652. 2, 15, 35
- N. Berns, T. Kusch, R. Schröder, and R. Reuter. Expression, function and regulation of brachyenteron in the short germband insect *tribolium castaneum*. *Development genes and evolution*, 218(3-4):169–179, Apr. 2008. ISSN 0949-944X. doi: 10.1007/s00427-008-0210-7. PMID: 18392878. 35
- G. R. W. I. R. s. c. a. d. c. b. B. Bolker, L. Bonebakker, R. Gentleman, W. H. A. Liaw, T. Lumley, M. Maechler, A. Magnusson, S. Moeller, M. Schwartz, and B. Venables. *gplots: Various R programming tools for plotting data*. 2013. URL <http://CRAN.R-project.org/package=gplots>. R package version 2.11.0.1. 17
- R. Bolognesi, L. Farzana, T. D. Fischer, and S. J. Brown. Multiple wnt genes are required for segmentation in the short-germ embryo of *tribolium castaneum*. *Current biology: CB*, 18(20):1624–1629, Oct. 2008. ISSN 0960-9822. doi: 10.1016/j.cub.2008.09.057. PMID: 18926702. 2, 5, 15, 52
- R. Bolognesi, T. D. Fischer, and S. J. Brown. Loss of tc-arrow and canonical wnt signaling alters posterior morphology and pair-rule gene expression in the short-germ insect, *tribolium castaneum*. *Development genes and evolution*, 219(7):369–375, July 2009. ISSN 1432-041X. doi: 10.1007/s00427-009-0299-3. PMID: 19705150. 5, 15, 35
- S. Brown, J. Fellers, T. Shippy, R. Denell, M. Stauber, and U. Schmidt-Ott. A strategy for mapping bicoid on the phylogenetic tree. *Current biology: CB*, 11(2):R43–44, Jan. 2001. ISSN 0960-9822. PMID: 11231138. 1
- G. Bucher and M. Klingler. Divergent segmentation mechanism in the short germ insect *tribolium* revealed by giant expression and function. *Development (Cambridge, England)*, 131(8):1729–1740, Apr. 2004. ISSN 0950-1991. doi: 10.1242/dev.01073. PMID: 15084458. 2
- G. Bucher and M. Klingler. *Tribolium mae* expression suggests roles in terminal and midline patterning and in the specification of mesoderm. *Development*

REFERENCES

- genes and evolution*, 215(9):478–481, Sept. 2005. ISSN 0949-944X. doi: 10.1007/s00427-005-0004-0. PMID: 16025346. 35
- G. Bucher and E. Wimmer. Beetle a-head. *B.I.F. Futura*, 20:164–169, 2005. 2, 4
- G. Bucher, J. Scholten, and M. Klingler. Parental RNAi in tribolium (coleoptera). *Current biology: CB*, 12(3):R85–86, Feb. 2002. ISSN 0960-9822. PMID: 11839285. 15
- J. D. Cande, V. S. Chopra, and M. Levine. Evolving enhancer-promoter interactions within the tinman complex of the flour beetle, tribolium castaneum. *Development (Cambridge, England)*, 136(18):3153–3160, Sept. 2009. ISSN 1477-9129. doi: 10.1242/dev.038034. PMID: 19700619. 35
- S. Carbon, A. Ireland, C. J. Mungall, S. Shu, B. Marshall, and S. Lewis. AmiGO: online access to ontology and annotation data. *Bioinformatics*, 25(2):288–289, Jan. 2009. ISSN 1367-4803. doi: 10.1093/bioinformatics/btn615. URL <http://www.ncbi.nlm.nih.gov/pmc/articles/PMC2639003/>. PMID: 19033274 PMCID: PMC2639003. 88
- A. C. Cerny, G. Bucher, R. Schröder, and M. Klingler. Breakdown of abdominal patterning in the tribolium kruppel mutant jaws. *Development (Cambridge, England)*, 132(24):5353–5363, Dec. 2005. ISSN 0950-1991. doi: 10.1242/dev.02154. PMID: 16280347. 2
- A. C. Cerny, D. Grossmann, G. Bucher, and M. Klingler. The tribolium ortholog of knirps and knirps-related is crucial for head segmentation but plays a minor role during abdominal patterning. *Developmental biology*, 321(1):284–294, Sept. 2008. ISSN 1095-564X. doi: 10.1016/j.ydbio.2008.05.527. PMID: 18586236. 3, 22, 52, 53
- C. P. Choe and S. J. Brown. Evolutionary flexibility of pair-rule patterning revealed by functional analysis of secondary pair-rule genes, paired and sloppy-paired in the short-germ insect, tribolium castaneum. *Developmental Biology*, 302(1):281–294, Feb. 2007. ISSN 0012-1606. doi: 10.1016/j.ydbio.2006.09.037. URL <http://www.sciencedirect.com/science/article/pii/S0012160606012395>. 5, 36
- C. P. Choe, S. C. Miller, and S. J. Brown. A pair-rule gene circuit defines segments sequentially in the short-germ insect tribolium castaneum. *Proceedings of the National Academy of Sciences of the United States of America*, 103(17):6560–6564, Apr. 2006. ISSN 0027-8424. doi: 10.1073/pnas.0510440103. PMID: 16611732. 2, 35, 54

REFERENCES

- S. Cohen and G. Jürgens. Drosophila headlines. *Trends Genet*, 7(8):267–272, Aug 1991. 2
- S. M. Cohen and G. Jürgens. Mediation of drosophila head development by gap-like segmentation genes. *Nature*, 346(6283):482–485, Aug. 1990. ISSN 0028-0836. doi: 10.1038/346482a0. PMID: 1974035. 2, 58
- T. Copf, R. Schröder, and M. Averof. Ancestral role of caudal genes in axis elongation and segmentation. *Proceedings of the National Academy of Sciences of the United States of America*, 101(51):17711–17715, Dec. 2004. ISSN 0027-8424. doi: 10.1073/pnas.0407327102. PMID: 15598743. 35
- F. Corpet. Multiple sequence alignment with hierarchical clustering. *Nucleic acids research*, 16(22):10881–10890, Nov. 1988. ISSN 0305-1048. PMID: 2849754. 95
- M. Crozatier, D. Valle, L. Dubois, S. Ibnsouda, and A. Vincent. Collier, a novel regulator of drosophila head development, is expressed in a single mitotic domain. *Curr Biol*, 6(6):707–718, Jun 1996. 3
- M. Crozatier, D. Valle, L. Dubois, S. Ibnsouda, and A. Vincent. Head versus trunk patterning in the drosophila embryo; collier requirement for formation of the intercalary segment. *Development*, 126(19):4385–4394, Oct 1999. 3
- E. El-Sherif, M. Averof, and S. J. Brown. A segmentation clock operating in blastoderm and germband stages of tribolium development. *Development (Cambridge, England)*, 139(23):4341–4346, Dec. 2012. ISSN 1477-9129. doi: 10.1242/dev.085126. PMID: 23095886. 2
- L. Farzana and S. J. Brown. Hedgehog signaling pathway function conserved in tribolium segmentation. *Development genes and evolution*, 218(3-4):181–192, Apr. 2008. ISSN 0949-944X. doi: 10.1007/s00427-008-0207-2. PMID: 18392879. 2, 5, 15, 36, 52, 59
- R. Finkelstein and N. Perrimon. The orthodenticle gene is regulated by bicoid and torso and specifies drosophila head development. *Nature*, 346(6283):485–488, Aug 1990. doi: 10.1038/346485a0. URL <http://dx.doi.org/10.1038/346485a0>. 2
- J. Fu, N. Posnien, R. Bolognesi, T. D. Fischer, P. Rayl, G. Oberhofer, P. Kitzmann, S. J. Brown, and G. Bucher. Asymmetrically expressed axin required for anterior development in tribolium. *Proceedings of the National Academy of Sciences of the*

REFERENCES

- United States of America*, 109(20):7782–7786, May 2012. ISSN 1091-6490. doi: 10.1073/pnas.1116641109. PMID: 22552230. 1, 15
- A. Gallitano-Mendel and R. Finkelstein. Novel segment polarity gene interactions during embryonic head development in drosophila. *Dev Biol*, 192(2):599–613, Dec 1997. doi: 10.1006/dbio.1997.8753. URL <http://dx.doi.org/10.1006/dbio.1997.8753>. 3, 28, 56
- A. Gallitano-Mendel and R. Finkelstein. Ectopic orthodenticle expression alters segment polarity gene expression but not head segment identity in the drosophila embryo. *Dev Biol*, 199(1):125–137, Jul 1998. doi: 10.1006/dbio.1998.8917. URL <http://dx.doi.org/10.1006/dbio.1998.8917>. 3
- W. M. Gelbart, M. A. Crosby, B. Matthews, W. P. Rindone, J. Chillemi, S. R. Twombly, D. Emmert, M. Ashburner, R. A. Drysdale, E. Whitfield, G. H. Millburn, A. de Grey, T. Kaufman, K. Matthews, D. Gilbert, V. B. Strelets, and C. Tolstoshev. FlyBase: a drosophila database. the FlyBase consortium. *Nucleic Acids Research*, 25(1):63–66, 1997. URL <http://dblp.uni-trier.de/db/journals/nar/nar25.html#GelbartCMRCTEADWMGKMGST97>. 17, 36
- R. C. Gentleman, V. J. Carey, D. M. Bates, et al. Bioconductor: Open software development for computational biology and bioinformatics. *Genome Biology*, 5:R80, 2004. URL <http://genomebiology.com/2004/5/10/R80>. 16
- A. J. Giraldez, R. R. Copley, and S. M. Cohen. HSPG modification by the secreted enzyme notum shapes the wingless morphogen gradient. *Developmental cell*, 2(5): 667–676, May 2002. ISSN 1534-5807. PMID: 12015973. 36
- T. Girke. R & bioconductor - manuals. URL http://manuals.bioinformatics.ucr.edu/home/R_BioCondManual. 16
- D. Grossmann, J. Scholten, and N.-M. Prpic. Separable functions of wingless in distal and ventral patterning of the tribolium leg. *Development genes and evolution*, 219(9-10):469–479, Oct. 2009. ISSN 1432-041X. doi: 10.1007/s00427-009-0310-z. PMID: 20024581. 47
- U. Grossniklaus, R. K. Pearson, and W. J. Gehring. The drosophila sloppy paired locus encodes two proteins involved in segmentation that show homology to mammalian transcription factors. *Genes Dev*, 6(6):1030–1051, Jun 1992. 2

REFERENCES

- M. Hahn and H. Jäckle. Drosophila gooseoid participates in neural development but not in body axis formation. *The EMBO journal*, 15(12):3077–3084, June 1996. ISSN 0261-4189. PMID: 8670808. 58
- K. Handel, A. Basal, X. Fan, and S. Roth. Tribolium castaneum twist: gastrulation and mesoderm formation in a short-germ beetle. *Development genes and evolution*, 215(1):13–31, Jan. 2005. ISSN 0949-944X. doi: 10.1007/s00427-004-0446-9. PMID: 15645317. 59
- A. M. Huang and G. M. Rubin. A misexpression screen identifies genes that can modulate RAS1 pathway signaling in drosophila melanogaster. *Genetics*, 156(3): 1219–1230, Nov. 2000. ISSN 0016-6731, 1943-2631. URL <http://www.genetics.org/content/156/3/1219>. PMID: 11063696. 35
- H. Jafar-Nejad, A.-C. Tien, M. Acar, and H. J. Bellen. Senseless and daughterless confer neuronal identity to epithelial cells in the drosophila wing margin. *Development*, 133(9):1683–1692, May 2006. ISSN 0950-1991, 1477-9129. doi: 10.1242/dev.02338. URL <http://dev.biologists.org/content/133/9/1683>. PMID: 16554363. 46
- K. Jagla, T. Jagla, P. Heitzler, G. Dretzen, F. Bellard, and M. Bellard. ladybird, a tandem of homeobox genes that maintain late wingless expression in terminal and dorsal epidermis of the drosophila embryo. *Development*, 124(1):91–100, Jan. 1997. ISSN 0950-1991, 1477-9129. URL <http://dev.biologists.org/content/124/1/91>. PMID: 9006070. 35
- G. Jekely and P. Friedrich. Characterization of two recombinant Drosophila Calpains CALPA AND a NOVEL HOMOLOG, CALPB. *Journal of Biological Chemistry*, 274(34):23893–23900, Aug. 1999. ISSN 0021-9258, 1083-351X. doi: 10.1074/jbc.274.34.23893. URL <http://www.jbc.org/content/274/34/23893>. PMID: 10446155. 36
- D. S. Johnston and C. Nüsslein-Volhard. The origin of pattern and polarity in the drosophila embryo. *Cell*, 68(2):201–219, Jan 1992. 1
- M. Kanayama, Y. Akiyama-Oda, O. Nishimura, H. Tarui, K. Agata, and H. Oda. Travelling and splitting of a wave of hedgehog expression involved in spider-head segmentation. *Nature Communications*, 2:500, Oct. 2011. doi: 10.1038/ncomms1510. URL <http://www.nature.com/ncomms/journal/v2/n10/full/ncomms1510.html>. 3, 52, 54

REFERENCES

- D. Kent, E. W. Bush, and J. E. Hooper. Roadkill attenuates hedgehog responses through degradation of cubitus interruptus. *Development (Cambridge, England)*, 133(10):2001–2010, May 2006. ISSN 0950-1991. doi: 10.1242/dev.02370. PMID: 16651542. 36
- S. Kittelmann, J. Ulrich, N. Posnien, and G. Bucher. Changes in anterior head patterning underlie the evolution of long germ embryogenesis. *Developmental biology*, 374(1):174–184, Feb. 2013. ISSN 1095-564X. doi: 10.1016/j.ydbio.2012.11.026. PMID: 23201022. 2
- K. Kotkamp, M. Klingler, and M. Schoppmeier. Apparent role of tribolium orthodenticle in anteroposterior blastoderm patterning largely reflects novel functions in dorsoventral axis formation and cell survival. *Development (Cambridge, England)*, 137(11):1853–1862, June 2010. ISSN 1477-9129. doi: 10.1242/dev.047043. PMID: 20431120. 3, 15
- T. Kramps, O. Peter, E. Brunner, D. Nellen, B. Froesch, S. Chatterjee, M. Murone, S. Züllig, and K. Basler. Wnt/wingless signaling requires BCL9/legless-mediated recruitment of pygopus to the nuclear beta-catenin-TCF complex. *Cell*, 109(1):47–60, Apr. 2002. ISSN 0092-8674. PMID: 11955446. 59
- B. Langmead and S. L. Salzberg. Fast gapped-read alignment with bowtie 2. *Nature Methods*, 9(4):357–359, Apr. 2012. ISSN 1548-7091. doi: 10.1038/nmeth.1923. URL <http://www.nature.com/nmeth/journal/v9/n4/full/nmeth.1923.html>. 16
- G. Lauter, I. Söll, and G. Hauptmann. Multicolor fluorescent in situ hybridization to define abutting and overlapping gene expression in the embryonic zebrafish brain. *Neural Development*, 6(1):10, Apr. 2011. ISSN 1749-8104. doi: 10.1186/1749-8104-6-10. URL <http://www.neuraldevelopment.com/content/6/1/10/abstract>. PMID: 21466670. 11
- J. A. Lengyel and D. D. Iwaki. It takes guts: the drosophila hindgut as a model system for organogenesis. *Developmental biology*, 243(1):1–19, Mar. 2002. ISSN 0012-1606. doi: 10.1006/dbio.2002.0577. PMID: 11846473. 60
- H. Li, B. Handsaker, A. Wysoker, T. Fennell, J. Ruan, N. Homer, G. Marth, G. Abecasis, R. Durbin, and 1000 Genome Project Data Processing Subgroup. The sequence Alignment/Map format and SAMtools. *Bioinformatics (Oxford, England)*, 25(16):2078–2079, Aug. 2009. ISSN 1367-4811. doi: 10.1093/bioinformatics/btp352. PMID: 19505943. 16

REFERENCES

- P. Z. Liu and T. C. Kaufman. Short and long germ segmentation: unanswered questions in the evolution of a developmental mode. *Evolution & development*, 7(6):629–646, Dec. 2005. ISSN 1520-541X. doi: 10.1111/j.1525-142X.2005.05066.x. PMID: 16336416. 1
- C. M. Luque and M. Miln. Growth control in the proliferative region of the drosophila eyehead primordium: The elbow gene complex. *Developmental Biology*, 301(2): 327–339, Jan. 2007. ISSN 0012-1606. doi: 10.1016/j.ydbio.2006.07.050. URL <http://www.sciencedirect.com/science/article/pii/S0012160606011559>. 35
- B. L. Martin and D. Kimelman. Wnt signaling and the evolution of embryonic posterior development. *Current Biology*, 19(5):R215–R219, Mar. 2009. ISSN 0960-9822. doi: 10.1016/j.cub.2009.01.052. URL <http://www.sciencedirect.com/science/article/pii/S0960982209006241>. 59
- W. McGinnis and R. Krumlauf. Homeobox genes and axial patterning. *Cell*, 68(2): 283–302, Jan. 1992. ISSN 0092-8674. PMID: 1346368. 1
- J. Mohler. Spatial regulation of segment polarity gene expression in the anterior terminal region of the drosophila blastoderm embryo. *Mech Dev*, 50(2-3):151–161, Apr 1995. 3
- D. Morisato and K. V. Anderson. The spätzle gene encodes a component of the extracellular signaling pathway establishing the dorsal-ventral pattern of the drosophila embryo. *Cell*, 76(4):677–688, Feb. 1994. ISSN 0092-8674. PMID: 8124709. 36
- A. Mortazavi, B. A. Williams, K. McCue, L. Schaeffer, and B. Wold. Mapping and quantifying mammalian transcriptomes by RNA-Seq. *Nature methods*, 5(7):621–628, July 2008. ISSN 1548-7105. doi: 10.1038/nmeth.1226. PMID: 18516045. 6
- P. Müller, D. Kuttenukeuler, V. Gesellchen, M. P. Zeidler, and M. Boutros. Identification of JAK/STAT signalling components by genome-wide RNA interference. *Nature*, 436 (7052):871–875, Aug. 2005. ISSN 0028-0836. doi: 10.1038/nature03869. URL <http://www.nature.com/nature/journal/v436/n7052/full/nature03869.html>. 36
- U. Nagalakshmi, Z. Wang, K. Waern, C. Shou, D. Raha, M. Gerstein, and M. Snyder. The transcriptional landscape of the yeast genome defined by RNA sequencing. *Science (New York, N.Y.)*, 320(5881):1344–1349, June 2008. ISSN 1095-9203. doi: 10.1126/science.1158441. PMID: 18451266. 6

REFERENCES

- E. Neuwirth. *RColorBrewer: ColorBrewer palettes*. 2011. URL <http://CRAN.R-project.org/package=RColorBrewer>. R package version 1.0-5. 17
- R. Nolo, L. A. Abbott, and H. J. Bellen. Senseless, a zn finger transcription factor, is necessary and sufficient for sensory organ development in drosophila. *Cell*, 102(3): 349–362, Aug. 2000. ISSN 0092-8674. PMID: 10975525. 46, 47, 60
- E. Ntini and E. A. Wimmer. Second order regulator collier directly controls intercalary-specific segment polarity gene expression. *Developmental biology*, 360(2):403–414, Dec. 2011a. ISSN 1095-564X. doi: 10.1016/j.ydbio.2011.09.035. PMID: 22005665. 3
- E. Ntini and E. A. Wimmer. Unique establishment of procephalic head segments is supported by the identification of cis-regulatory elements driving segment-specific segment polarity gene expression in drosophila. *Development genes and evolution*, 221(1):1–16, May 2011b. ISSN 1432-041X. doi: 10.1007/s00427-011-0354-8. PMID: 21399984. 3
- C. Nüsslein-Volhard and E. Wieschaus. Mutations affecting segment number and polarity in drosophila. *Nature*, 287(5785):795–801, Oct. 1980. ISSN 0028-0836. PMID: 6776413. 1
- D. I. Oppenheimer, A. M. MacNicol, and N. H. Patel. Functional conservation of the wingless-engrailed interaction as shown by a widely applicable baculovirus misexpression system. *Current biology: CB*, 9(22):1288–1296, Nov. 1999. ISSN 0960-9822. PMID: 10574758. 6, 56
- K. A. Panfilio, G. Oberhofer, and S. Roth. High plasticity in epithelial morphogenesis during insect dorsal closure. *Biology open*, 2(11):1108–1118, 2013. ISSN 2046-6390. doi: 10.1242/bio.20136072. PMID: 24244847. 14
- M. J. Pankratz and H. Jäckle. Making stripes in the drosophila embryo. *Trends in genetics: TIG*, 6(9):287–292, Sept. 1990. ISSN 0168-9525. PMID: 2238086. 2
- M. Pechmann, A. P. McGregor, E. E. Schwager, N. M. Feitosa, and W. G. M. Damen. Dynamic gene expression is required for anterior regionalization in a spider. *Proceedings of the National Academy of Sciences of the United States of America*, 106(5):1468–1472, Feb. 2009. ISSN 1091-6490. doi: 10.1073/pnas.0811150106. PMID: 19147844. 3, 54

REFERENCES

- A. D. Peel, J. Schanda, D. Grossmann, F. Ruge, G. Oberhofer, A. F. Gilles, J. B. Schinko, M. Klingler, and G. Bucher. Tc-knirps plays different roles in the specification of antennal and mandibular parasegment boundaries and is regulated by a pair-rule gene in the beetle *tribolium castaneum*. *BMC developmental biology*, 13: 25, 2013. ISSN 1471-213X. doi: 10.1186/1471-213X-13-25. PMID: 23777260. 3, 22, 52, 54
- C. P. Petersen and P. W. Reddien. Wnt signaling and the polarity of the primary body axis. *Cell*, 139(6):1056–1068, Dec. 2009. ISSN 1097-4172. doi: 10.1016/j.cell.2009.11.035. PMID: 20005801. 59
- N. Posnien and G. Bucher. Formation of the insect head involves lateral contribution of the intercalary segment, which depends on tc-labial function. *Developmental biology*, 338(1):107–116, Feb. 2010. ISSN 1095-564X. doi: 10.1016/j.ydbio.2009.11.010. PMID: 19913530. 2
- N. Posnien, J. B. Schinko, S. Kittelmann, and G. Bucher. Genetics, development and composition of the insect head—a beetle’s view. *Arthropod structure & development*, 39(6):399–410, Nov. 2010. ISSN 1873-5495. doi: 10.1016/j.asd.2010.08.002. PMID: 20800703. 5
- N. Posnien, N. D. B. Koniszewski, H. J. Hein, and G. Bucher. Candidate gene screen in the red flour beetle *tribolium* reveals six3 as ancient regulator of anterior median head and central complex development. *PLoS genetics*, 7(12):e1002416, Dec. 2011. ISSN 1553-7404. doi: 10.1371/journal.pgen.1002416. PMID: 22216011. 2, 5, 36, 41, 58
- T. Sandmann, J. S. Jakobsen, and E. E. M. Furlong. ChIP-on-chip protocol for genome-wide analysis of transcription factor binding in *drosophila melanogaster* embryos. *Nature protocols*, 1(6):2839–2855, 2006. ISSN 1750-2799. doi: 10.1038/nprot.2006.383. PMID: 17406543. 10
- A. F. Sarrazin, A. D. Peel, and M. Averof. A segmentation clock with two-segment periodicity in insects. *Science (New York, N.Y.)*, 336(6079):338–341, Apr. 2012. ISSN 1095-9203. doi: 10.1126/science.1218256. PMID: 22403177. 2
- J. Schinko, N. Posnien, S. Kittelmann, N. Koniszewski, and G. Bucher. Single and double whole-mount in situ hybridization in red flour beetle (*tribolium*) embryos. *Cold Spring Harbor protocols*, 2009(8):pdb.prot5258, Aug. 2009. ISSN 1559-6095. doi: 10.1101/pdb.prot5258. PMID: 20147234. 10, 12

REFERENCES

- J. B. Schinko, N. Kreuzer, N. Offen, N. Posnien, E. A. Wimmer, and G. Bucher. Divergent functions of orthodenticle, empty spiracles and buttonhead in early head patterning of the beetle *tribolium castaneum* (coleoptera). *Developmental biology*, 317(2):600–613, May 2008. ISSN 1095-564X. doi: 10.1016/j.ydbio.2008.03.005. PMID: 18407258. 3, 24, 25, 30, 52, 58
- J. B. Schinko, K. Hillebrand, and G. Bucher. Heat shock-mediated misexpression of genes in the beetle *tribolium castaneum*. *Development Genes and Evolution*, 222(5):287–298, Sept. 2012. ISSN 0949-944X, 1432-041X. doi: 10.1007/s00427-012-0412-x. URL <http://link.springer.com/article/10.1007/s00427-012-0412-x>. 9, 15, 25
- M. Schoppmeier and R. Schroeder. Maternal torso signaling controls body axis elongation in a short germ insect. *Current biology: CB*, 15(23):2131–2136, Dec. 2005. ISSN 0960-9822. doi: 10.1016/j.cub.2005.10.036. PMID: 16332539. 2, 15, 30
- M. Schoppmeier, S. Fischer, C. Schmitt-Engel, U. Löhr, and M. Klingler. An ancient anterior patterning system promotes caudal repression and head formation in ecdysozoa. *Current biology: CB*, 19(21):1811–1815, Nov. 2009. ISSN 1879-0445. doi: 10.1016/j.cub.2009.09.026. PMID: 19818622. 1
- R. Schröder. The genes orthodenticle and hunchback substitute for bicoid in the beetle *tribolium*. *Nature*, 422(6932):621–625, Apr. 2003. ISSN 0028-0836. doi: 10.1038/nature01536. PMID: 12687002. 3
- R. Schroder, C. Eckert, C. Wolff, and D. Tautz. Conserved and divergent aspects of terminal patterning in the beetle *tribolium castaneum*. *Proceedings of the National Academy of Sciences of the United States of America*, 97(12):6591–6596, June 2000. ISSN 0027-8424. doi: 10.1073/pnas.100005497. PMID: 10823887. 58
- C. Schulz, R. Schröder, B. Hausdorf, C. Wolff, and D. Tautz. A caudal homologue in the short germ band beetle *tribolium* shows similarities to both, the *drosophila* and the vertebrate caudal expression patterns. *Development genes and evolution*, 208(5):283–289, July 1998. ISSN 0949-944X. PMID: 9683744. 35
- R. Sharma, A. Beermann, and R. Schröder. FGF signalling controls anterior extraembryonic and embryonic fate in the beetle *tribolium*. *Developmental biology*, 381(1):121–133, Sept. 2013. ISSN 1095-564X. doi: 10.1016/j.ydbio.2013.05.031. PMID: 23769707. 2

REFERENCES

- J. B. Singer, R. Harbecke, T. Kusch, R. Reuter, and J. A. Lengyel. Drosophila brachyenteron regulates gene activity and morphogenesis in the gut. *Development (Cambridge, England)*, 122(12):3707–3718, Dec. 1996. ISSN 0950-1991. PMID: 9012492. 35
- A. Sokoloff. *The biology of Tribolium: with special emphasis on genetic aspects*. Clarendon Press, 1974. 9
- R. J. Sommer and D. Tautz. Involvement of an orthologue of the drosophila pair-rule gene hairy in segment formation of the short germ-band embryo of tribolium (coleoptera). *Nature*, 361(6411):448–450, Feb. 1993. ISSN 0028-0836. doi: 10.1038/361448a0. PMID: 8429884. 35
- R. J. Sommer and D. Tautz. Expression patterns of twist and snail in tribolium (coleoptera) suggest a homologous formation of mesoderm in long and short germ band insects. *Developmental genetics*, 15(1):32–37, 1994. ISSN 0192-253X. doi: 10.1002/dvg.1020150105. PMID: 8187348. 35
- J. E. Stajich, D. Block, K. Boulez, S. E. Brenner, S. A. Chervitz, C. Dagdigian, G. Fullen, J. G. R. Gilbert, I. Korf, H. Lapp, H. Lehv slaiho, C. Matsalla, C. J. Mungall, B. I. Osborne, M. R. Pocock, P. Schattner, M. Senger, L. D. Stein, E. Stupka, M. D. Wilkinson, and E. Birney. The bioperl toolkit: Perl modules for the life sciences. *Genome research*, 12(10):1611–1618, Oct. 2002. ISSN 1088-9051. doi: 10.1101/gr.361602. PMID: 12368254. 10, 17
- M. Stanke and S. Waack. Gene prediction with a hidden markov model and a new intron submodel. *Bioinformatics*, 19(suppl 2):ii215–ii225, Sept. 2003. ISSN 1367-4803, 1460-2059. doi: 10.1093/bioinformatics/btg1080. URL http://bioinformatics.oxfordjournals.org/content/19/suppl_2/ii215. PMID: 14534192. 10
- M. Stauber, H. J ckle, and U. Schmidt-Ott. The anterior determinant bicoid of drosophila is a derived hox class 3 gene. *Proceedings of the National Academy of Sciences of the United States of America*, 96(7):3786–3789, Mar. 1999. ISSN 0027-8424. PMID: 10097115. 1
- M. Sultan, M. H. Schulz, H. Richard, A. Magen, A. Klingenhoff, M. Scherf, M. Seifert, T. Borodina, A. Soldatov, D. Parkhomchuk, D. Schmidt, S. O’Keeffe, S. Haas, M. Vingron, H. Lehrach, and M.-L. Yaspo. A global view of gene activity and alternative splicing by deep sequencing of the human transcriptome. *Science (New York, N.Y.)*, 321(5891):956–960, Aug. 2008. ISSN 1095-9203. doi: 10.1126/science.1160342. PMID: 18599741. 6

REFERENCES

- N. Snchez-Soriano and S. Russell. Regulatory mutations of the drosophila *sox* gene *dichaete* reveal new functions in embryonic brain and hindgut development. *Developmental Biology*, 220(2):307–321, Apr. 2000. ISSN 0012-1606. doi: 10.1006/dbio.2000.9648. URL <http://www.sciencedirect.com/science/article/pii/S0012160600996489>. 35
- D. Tautz, M. Friedrich, and R. Schröder. Insect embryogenesis what is ancestral and what is derived? *Development*, 1994(Supplement):193–199, Jan. 1994. ISSN 0950-1991, 1477-9129. URL <http://dev.biologists.org/content/1994/Supplement/193>. 1
- R. C. Team. *R: A Language and Environment for Statistical Computing*. Vienna, Austria, 2013. URL <http://www.R-project.org/>. 16
- Tribolium Genome Sequencing Consortium, S. Richards, R. A. Gibbs, G. M. Weinstock, S. J. Brown, R. Denell, R. W. Beeman, R. Gibbs, R. W. Beeman, S. J. Brown, G. Bucher, M. Friedrich, C. J. P. Grimmelikhuijzen, M. Klingler, M. Lorenzen, S. Richards, S. Roth, R. Schröder, D. Tautz, E. M. Zdobnov, D. Muzny, R. A. Gibbs, G. M. Weinstock, T. Attaway, S. Bell, C. J. Buhay, M. N. Chandrabose, D. Chavez, K. P. Clerk-Blankenburg, A. Cree, M. Dao, C. Davis, J. Chacko, H. Dinh, S. Dugan-Rocha, G. Fowler, T. T. Garner, J. Garnes, A. Gnirke, A. Hawes, J. Hernandez, S. Hines, M. Holder, J. Hume, S. N. Jhangiani, V. Joshi, Z. M. Khan, L. Jackson, C. Kovar, A. Kowis, S. Lee, L. R. Lewis, J. Margolis, M. Morgan, L. V. Nazareth, N. Nguyen, G. Okwuonu, D. Parker, S. Richards, S.-J. Ruiz, J. Santibanez, J. Savard, S. E. Scherer, B. Schneider, E. Sodergren, D. Tautz, S. Vattahil, D. Villasana, C. S. White, R. Wright, Y. Park, R. W. Beeman, J. Lord, B. Oppert, M. Lorenzen, S. Brown, L. Wang, J. Savard, D. Tautz, S. Richards, G. Weinstock, R. A. Gibbs, Y. Liu, K. Worley, G. Weinstock, C. G. Elsik, J. T. Reese, E. Elhaik, G. Landan, D. Graur, P. Arensburger, P. Atkinson, R. W. Beeman, J. Beidler, S. J. Brown, J. P. Demuth, D. W. Drury, Y.-Z. Du, H. Fujiwara, M. Lorenzen, V. Maselli, M. Osanai, Y. Park, H. M. Robertson, Z. Tu, J.-j. Wang, S. Wang, S. Richards, H. Song, L. Zhang, E. Sodergren, D. Werner, M. Stanke, B. Morgenstern, V. Solovyev, P. Kosarev, G. Brown, H.-C. Chen, O. Ermolaeva, W. Hlavina, Y. Kapustin, B. Kiryutin, P. Kitts, D. Maglott, K. Pruitt, V. Sapojnikov, A. Suvorov, A. J. Mackey, R. M. Waterhouse, S. Wyder, E. M. Zdobnov, E. M. Zdobnov, S. Wyder, E. V. Kriventseva, T. Kadowaki, P. Bork, M. Aranda, R. Bao, A. Beermann, N. Berns, R. Bolognesi, F. Bonneton, D. Bopp, S. J. Brown, G. Bucher, T. Butts, A. Chaumot, R. E. Denell, D. E. K. Ferrier, M. Friedrich, C. M. Gordon,

REFERENCES

- M. Jindra, M. Klingler, Q. Lan, H. M. G. Lattorff, V. Laudet, C. von Levetsow, Z. Liu, R. Lutz, J. A. Lynch, R. N. da Fonseca, N. Posnien, R. Reuter, S. Roth, J. Savard, J. B. Schinko, C. Schmitt, M. Schoppmeier, R. Schröder, T. D. Shippy, F. Simonnet, H. Marques-Souza, D. Tautz, Y. Tomoyasu, J. Trauner, M. Van der Zee, M. Vervoort, N. Wittkopp, E. A. Wimmer, X. Yang, A. K. Jones, D. B. Sattelle, P. R. Ebert, D. Nelson, J. G. Scott, R. W. Beeman, S. Muthukrishnan, K. J. Kramer, Y. Arakane, R. W. Beeman, Q. Zhu, D. Hogenkamp, R. Dixit, B. Oppert, H. Jiang, Z. Zou, J. Marshall, E. Elpidina, K. Vinokurov, C. Oppert, Z. Zou, J. Evans, Z. Lu, P. Zhao, N. Sumathipala, B. Altincicek, A. Vilcinskas, M. Williams, D. Hultmark, C. Hetru, H. Jiang, C. J. P. Grimmelikhuijzen, F. Hauser, G. Cazzamali, M. Williamson, Y. Park, B. Li, Y. Tanaka, R. Predel, S. Neupert, J. Schachtner, P. Verleyen, F. Raible, P. Bork, M. Friedrich, K. K. O. Walden, H. M. Robertson, S. Angeli, S. Fort, G. Bucher, S. Schuetz, R. Maleszka, E. A. Wimmer, R. W. Beeman, M. Lorenzen, Y. Tomoyasu, S. C. Miller, D. Grossmann, and G. Bucher. The genome of the model beetle and pest *tribolium castaneum*. *Nature*, 452(7190):949–955, Apr. 2008. ISSN 1476-4687. doi: 10.1038/nature06784. PMID: 18362917. 10
- R. I. Tuxworth, V. Vivancos, M. B. O’Hare, and G. Tear. Interactions between the juvenile batten disease gene, CLN3, and the notch and JNK signalling pathways. *Human molecular genetics*, 18(4):667–678, Feb. 2009. ISSN 1460-2083. doi: 10.1093/hmg/ddn396. PMID: 19028667. 36
- A. Untergasser, I. Cutcutache, T. Koressaar, J. Ye, B. C. Faircloth, M. Remm, and S. G. Rozen. Primer3new capabilities and interfaces. *Nucleic Acids Research*, page gks596, June 2012. ISSN 0305-1048, 1362-4962. doi: 10.1093/nar/gks596. URL <http://nar.oxfordjournals.org/content/early/2012/06/21/nar.gks596>. PMID: 22730293. 9
- R. Urbach. A procephalic territory in drosophila exhibiting similarities and dissimilarities compared to the vertebrate midbrain/hindbrain boundary region. *Neural development*, 2:23, 2007. ISSN 1749-8104. doi: 10.1186/1749-8104-2-23. PMID: 17983473. 5
- Q. T. Wang and R. A. Holmgren. Nuclear import of cubitus interruptus is regulated by hedgehog via a mechanism distinct from ci stabilization and ci activation. *Development (Cambridge, England)*, 127(14):3131–3139, July 2000. ISSN 0950-1991. PMID: 10862750. 35

REFERENCES

- D. Weigel, G. Jürgens, M. Klingler, and H. Jäckle. Two gap genes mediate maternal terminal pattern information in drosophila. *Science (New York, N.Y.)*, 248(4954): 495–498, Apr. 1990. ISSN 0036-8075. PMID: 2158673. 58
- H. Wickham. *ggplot2: elegant graphics for data analysis*. Springer New York, 2009. ISBN 978-0-387-98140-6. URL <http://had.co.nz/ggplot2/book>. 17
- B. T. Wilhelm, S. Marguerat, S. Watt, F. Schubert, V. Wood, I. Goodhead, C. J. Penkett, J. Rogers, and J. Bähler. Dynamic repertoire of a eukaryotic transcriptome surveyed at single-nucleotide resolution. *Nature*, 453(7199):1239–1243, June 2008. ISSN 1476-4687. doi: 10.1038/nature07002. PMID: 18488015. 6
- E. A. Wimmer, S. M. Cohen, H. Jäckle, and C. Desplan. buttonhead does not contribute to a combinatorial code proposed for drosophila head development. *Development*, 124(8):1509–1517, Apr 1997. 3
- W. Wurst and L. Bally-Cuif. Neural plate patterning: upstream and downstream of the isthmus organizer. *Nature reviews. Neuroscience*, 2(2):99–108, Feb. 2001. ISSN 1471-003X. doi: 10.1038/35053516. PMID: 11253000. 5
- X. Yang, M. Weber, N. Zarinkamar, N. Posnien, F. Friedrich, B. Wigand, R. Beutel, W. G. M. Damen, G. Bucher, M. Klingler, and M. Friedrich. Probing the drosophila retinal determination gene network in tribolium (II): the pax6 genes eyeless and twin of eyeless. *Developmental biology*, 333(1):215–227, Sept. 2009. ISSN 1095-564X. doi: 10.1016/j.ydbio.2009.06.013. PMID: 19527703. 36, 58

REFERENCES

Appendix A

Clones and Primer

Table A.1: Primer to clone genes and for dsRNA templates

Gene	Primer	Sequence
<i>Tc-frizzled1</i>	frz1up1	ATGAAGCCGCTGCTCCTGCTG
	frz1lo1	TTAAACGTAAGCCGCATGTCTG
	frz1up2	CTCTGCGTGGAGAAACACAAC
	frz1lo2	GCGGACAAGGCACGGCATAG
<i>Tc-frizzled2</i>	frz2up1	ATGATGGGGTACACGAGGTTATC
	frz2lo1	TCATACGTGACTCAACGGGGGC
	frz2up2	AGCGTTGCGAGGACATCACCATC
	frz2lo2	AGCATCCACTCGTTATGGAATGC
<i>Tc-patched</i>	Ptcup1	AGTCGGACCTGTACACCAGG
	Ptclo1	CTAGCTACTGGGGCACGGTTC
	Ptcup2T7	TAATACGACTCACTATAGGCAGGCGAATCTAACACCGAA
	Ptclo2T7	TAATACGACTCACTATAGGGCCAACGATCAAGTCTTCCG
	ptcup2T7	TAATACGACTCACTATAGGACTTGTTGACTGCGGAGGTGATC
	ptclo2T7	TAATACGACTCACTATAGGGCACGGCACGTCAGTCTTTTCG
<i>Tc-smoothened</i>	Smoup1	ATGTACCTCTTGTTTGTGCTAAT
	Smolo1	TCATAACAACCTCTCTCAGTTCTGG
	Smoup2T7	TAATACGACTCACTATAGGGATCGTCTTCTGCATCATCAC
	Smolo2T7	TAATACGACTCACTATAGGGGACGCAGCTCATGTGCCA
	smoup2T7	TAATACGACTCACTATAGGGCGCGAAGACATCGTTTGCA
	smolo2T7	TAATACGACTCACTATAGGGGATGAACCAACCGCTGTACG
<i>Tc-wntless</i>	wntlF1	ATGCCGGGAACAATCCTCGA
	wntlR1	TTACTCAATACTAGCTTTTGAAGC
	wntlF2	CATGAACTACTGGGTCACTCG
	wntlR2	CCGGTAGATTATACCTTCGTAG
	wntllo2T7	TAATACGACTCACTATAGGGTGCGTGACAGCAAATGCAC
	wntlup2T7	TAATACGACTCACTATAGGTGCTCTCTTTCTGGCTCGTG

A. CLONES AND PRIMER

Table A.2: Primer for clones obtained from colleagues

Gene	cloned by	Primer	Sequence
<i>Tc-hedgehog</i>	Evgenia Ntini	Hhup1T7	TAATACGACTCACTATAGGGAGATGTAAGGAGAAGTTGAAC
		Hhlo2T7	TAATACGACTCACTATAGGCTGAAGCCAGGGTTATGTGG
		Hhup2T7	TAATACGACTCACTATAGGCAGTGACCCCATCTCATTG
<i>Tc-axin</i>	Nico Posnien	Axlo2T7	TAATACGACTCACTATAGGTCGGTCTCGCATCTGAATG
		Axup2T7	TAATACGACTCACTATAGGGAGAGCAATGTTGACGGCAG
		Axilo1T7	TAATACGACTCACTATAGGCCTGGTCTGCCGTCAACATT
		Axiup1T7	TAATACGACTCACTATAGGCGTTTCATCCCACGAACCCA
<i>Tc-arrow</i>	Nico Posnien	Arrlo1T7	TAATACGACTCACTATAGGCCTTGAACCACGACTAAAACATG
		Arrup1T7	TAATACGACTCACTATAGGTGCCATCACGAAAGAAGCCGA

Table A.3: Primer for the RNAseq in situ screen candidates

Nr	au2ID	FWD	REV
1	216	GCAGGTGGTCTGAACTTCTGAGGTA	GCCGGGTCTTGCTTAATATGTCAGT
2	219	GTCCGTTCTCTCATCATCAGTCAC	ATAATAGTTGCTGCCAAGTGCTACG
3	1265	CGAAATGACCATTTACGGCAAGTTA	CTTGGTTAGCGTAGGAGTCCCAGTT
4	1272	CGAATACATCACATTAAGGCTGACA	TCCAACCTGAATATCTTCCAACCTGTG
5	1604	CTTGCTGCTACAACCACTACGAAT	GTCTACATGGACCTTGGTTGGTTTA
6	1826	CACCTACATCAGAAATCCCAACTCG	TTTAAACAAATGACTCACCCCGTTG
7	1922	ATCTATCATCGAGGCCGTAACCTGT	ATCTACATGGACCTTGGTTGGTTTA
8	2437	AACTATGTGCCACAAGCAAATGAC	TAAGTCCTCTTCAAATCATCCTTGC
9	2544	GGGCCTGAATCCTTATCTCAATTAT	TAATATCACACAGTCACGTCCACAC
10	2727	GAAACTATCCGACTGCTTGTGATTT	TTACTCTTGCCTTTAAACCAAAGTCG
11	2852	GAGCAAGACCACACATCAGTGATAC	GCTTTTGATCAGCAGTTAGGGATAA
12	3254	GGAGGTGTAATAATCTCGCAATCC	GCTTGGGAGTAAGCGATGTAGAAA
13	3393	ATCCCTGTATTACGAATCCCTTTGT	ATCATAGACCACAGTTGGAACGAAT
15	3432	TTTAACAGCACCTGGTGAACACTAC	AATCACATCACGTGCTATGGAACATA
16	4667	CTCCAGAAGAAGGGTGTGTAATGT	ATTTGCCAAGAAGTAAACAGTCTCG
18	5115	CCCCTACGAATGCATAGAAATATGA	TATTACACTTCCGCGTTATTACCTG
19	5536	AGGGGTAGCTAGTTATCGTCTTCGT	CGGGTTTTTCATCGCTATACACTTAT
20	5804	AGAAGAAGAAGAAAGAGCGGAAAGT	AACACTGGTTACATAAACTCGTCCA
21	5809	TCATCAGTTACGAGAGCAAAGAACA	CGAATTGTAAATACACTGAGCGTTG
22	6283	CACATTTCTGATTATGCACAGCAC	TGGCAAGTAGACTAGCACGTATGAG
23	6578	CGATAATTCATATGAGGGAAATCG	CTTTGATCCTTGAATCGTTCAGTTC
24	6598	AGTACGATTACGTGGAGGACAAATC	AACCACCCCTTTGTTATTATCAGGT
25	6823	AACATACGTCCGGTCAAGCCTACATC	GCGTCATCGTCTTGTGATTATAG

Continued on next page

Table A.3 – continued from previous page

Nr	au2ID	FWD	REV
26	7373	CCTTCTCTCTAGTCTACCCCAAGGA	AGTCACTCTCATGGCACTAACTGCT
28	7815	TTCGCCCAAGTTCATGTGTAT	GTCCACCCGTTGAGTGAACATA
29	7984	TCCGGTGAATATTACAACAGAAAACC	TCAGTATCAATGGTCATTCGGTCTA
30	8329	TTTCGTCTTCACCCCTTTTTGTGCGTTAC	GTGATGCTCCCCTTGTCTGGTTTAT
31	8382	GCAGGCAACGAAACACTTTTAC	TAAATGGCACTGGCTGCTATC
32	8413	TTTATTTGAGCGTAGACCCGTACAT	CTTCCCCTCTTTGATCCACTTTTTTA
33	8500	ACTTTCTGCCTCTTTCACAGTTCAGT	GACTCGCAACTTTACCAACAGAATC
34	8732	GAAAATCAACACGCCATTACG	CAATCGGTACCACGACTCAAG
35	9385	CACGACAAAATACGCAGTTATCAGAA	ATATGTCCACAGCCAAATTTCCATC
36	10180	AACTAGTCGATGGGTTCCCTCTACCT	GCACAACCTTTCCACAACCTTTACTT
37	10490	CTCTGGAATACAACACTCCAGACAA	GCATCTTAGTCTTGTCCACCAATTCC
38	10495	ACGTACTTGCTATGTGTCCAAAGTG	ATAGACATGATAATGAGGCGATGGT
39	10496	CTTACTCGACTTCTTCGTCAAGTCC	GGGTAGTTATTGCTTGATCGTTCTG
40	10497	CAATTACGACTACTCGGACTTCACC	GACTGTCTCACCTCGTCTTCTGAC
41	11365	ACTACGTTTTCCGCTCGTTTGTATTA	CCTTGAATTTGGTTAAAGAGGAGGT
43	12008	GATTATTTTTCTCCAAAATGACGCTTCC	GTGTGAAGTCCAGACCACTCAATTTCT
44	12107	GTGTCAGAAGTGAACGAGTTGAAGA	TCACTTTCTCGCTAACTTCAGGAAT
45	12145	TTACTGCTAAAATCCGAGGACAAAAG	CTTGACAAAAGCCTAACATGTCACT
47	12777	CAGTGTTTCAATAGACATGCCAAGA	CTGATTGATTACTGACTTGGTGTGG
49	1134	CGTTTTACAAGGAAGGAATCA	TTTCGACATTTTGTCCGTTTC
50	3101	TGTGCAACAGATCCGTCACCTGTAA	TGTGTCTCAGACCTTTCTTGTGCTG
53	9100	ACAAGAATTCCACGCCTTAT	ACGGTTATGTGCAAGATGTGCG
56	10282	GTATCAAGTGCTTCCCTTTCCTCGTC	AGAACGAACCGTTTTTCGTACCATTA
57	1793	AGTTTGGGATGTAACGATGCAAGAT	CACCAAAGACAGACTGGTGCATATC
58	2626	CAAATTACTCGAGTCCGACACAATG	AGCCGGTATATTCATGTTTGCTGAT
59	5750	TCGGCCAGTACTTTGAACTTTCTTC	ATAATGTTGCAACCGCTTTGTTTCT
61	604	GTGGTTTTGTCCCATGAATGTCTAC	GACTTGCGAGACTTTATCGTCAACTG
62	954	AGAGATGACCTCACTTTACGCAACTG	GAACATACAGGTTACATCGCTGATT
63	2283	CTAGCTTCTCTTACGAGTCTCATCG	GCTGTCCCTTATTCCAGACGTATTCAG
64	3946	CGTCCTACTAAAGGAAGCCTCTCAAA	ATAAGACAAAGCAGATGGAAGTGGTG
65	9509	ATGACCTCCTCAACACCTTCAGTTC	AGTCTGTGTAATGGGCACCACTCTT
66	11416	GTACCAAATTAATCCCAGATCGCTGT	TGTAGATCGAGACCAAGTCCCTTCTTC
X1	17	ATCTTCGTTTTCGTTGTGCTCTC	CAGTCTTGAGTCCATCATCCAGGTT
X2	190	TGGGTTTTACTTCTTGTGGGTGTTG	GTGTTGCAATCCTTCTTGAACGTCT
X3	908	GTGTTATCGGTGCCGTCTCATACTC	CTGCTTATCTCTTACGGACCTCA
X5	11882	ACTGCAACTCCAACATACGAAACC	GCAATTGTCCCGTAACTCTCAACAC
X6	4742	TGAGGGTGTGTACAATACGTTTCGTT	GATGTTTCATGGGATGTGCTCGTAG
X7	12667	CATGTGGGAGAAAATCGATACGAGA	TACAACGGTTTGAGGTCCAGACTTG

A. CLONES AND PRIMER

Table A.4: Primer for non overlapping fragments of RNAseq in situ screen candidates

au2ID	Nr	Sequence
4667	16_FWDT7	AATAATACGACTCACTATAGGAGGTGCGCTGTCAACTATTACGAGT
4667	16_REVT7	AATAATACGACTCACTATAGGTCGCACTTATCTCCGGTGACTCCGG
7373	26_FWDT7	AATAATACGACTCACTATAGGTTGCGGAAAGTCCTTCAAGCGCTCG
7373	26_REVT7	AATAATACGACTCACTATAGGGCACACGAACTGCTTCTCGCCGCC
8329	30_FWDT7	AATAATACGACTCACTATAGGGAGACCTGGGGAACACCACCACGGG
8329	30_REVT7	AATAATACGACTCACTATAGGCCTCTTCATGGTGGTGTTCGGGGCG
8732	34_FWDT7	AATAATACGACTCACTATAGGCAGCCCCCAGGGGCACGGAACAGCC
8732	34_REVT7	AATAATACGACTCACTATAGGTTGCTGAATTCTCGACAAGGAGGC

Appendix B

RNAseq

B.1 Candidate Genes

The following tables contain the candidate genes from the Venn diagrams (figure 4.10). “au2ID” are the au2 gene set identifiers used in the RNAseq analysis. “TcasID” are the gene identifiers from the older Tcas3.0 gene set. “FBgnID” are the flybase identifiers (including link to FB) of the corresponding ortho/homologs. “Symbol” are the gene symbols from flybase. “fC” are fold change values when comparing treatment (*arrow*^{RNAi}, *hedgehog*^{RNAi}) to wild type. “FDR” is the false discovery rate (Benjamini Hochberg adjusted p-values).

Table B.1: Posterior Wnt targets

au2ID	TcasID	FBgnID	Symbol	fC	FDR
au2.g10073.t1	TC012363	FBgn0030616	<i>RpL37a</i>	0.37	3.38E-007
au2.g10180.t1	TC012432	FBgn0040342	<i>NA</i>	0.40	9.62E-011
au2.g10495.t1	TC012620	<i>NA</i>	<i>NA</i>	0.30	5.55E-024
au2.g10592.t1	TC011826	FBgn0039844	<i>CG1607</i>	0.25	4.68E-021
au2.g10685.t1	TC011748	FBgn0011278	<i>lbe</i>	0.12	6.27E-009
au2.g10873.t1	TC012851	FBgn0001168	<i>h</i>	0.33	4.76E-041
au2.g11365.t1	TC005856	FBgn0262954	<i>Rpb12</i>	0.47	1.51E-007
au2.g11387.t1	TC005841	FBgn0000409	<i>Cyt-c-p</i>	0.46	3.16E-013

Continued on next page

B. RNASEQ

Table B.1 – continued from previous page

au2ID	TcasID	FBgnID	Symbol	fC	FDR
au2.g11461.t1	TC005792	FBgn0013325	<i>RpL11</i>	0.46	4.79E-010
au2.g11465.t1	TC005785	FBgn0004893	<i>bowl</i>	0.28	5.32E-027
au2.g11578.t1	TC006413	FBgn0031645	<i>CG3036</i>	0.23	1.71E-030
au2.g11681.t1	TC005648	FBgn0037686	<i>RpL34b</i>	0.42	1.73E-008
au2.g11821.t1	TC006567	FBgn0261608	<i>RpL37A</i>	0.48	4.91E-006
au2.g11882.t1	TC005505	NA	NA	0.47	2.44E-017
au2.g12008.t1	TC006707	FBgn0039081	<i>Irk2</i>	0.32	9.22E-014
au2.g12141.t1	TC006782	FBgn0010408	<i>RpS9</i>	0.40	5.58E-012
au2.g12331.t1	TC011204	FBgn0028697	<i>RpL15</i>	0.43	4.02E-013
au2.g12498.t1	TC011085	FBgn0004403	<i>RpS14a</i>	0.40	2.20E-011
au2.g12523.t1	TC011406	FBgn0000273	<i>Pka-C1</i>	0.48	1.46E-006
au2.g1265.t1	NA	NA	NA	0.32	2.93E-008
au2.g12777.t1	NA	NA	NA	0.41	8.79E-018
au2.g1479.t1	TC001756	FBgn0011016	<i>SsRbeta</i>	0.41	2.96E-011
au2.g1604.t1	TC004178	NA	NA	0.39	1.20E-010
au2.g1783.t1	TC002098	FBgn0037328	<i>RpL35A</i>	0.44	1.18E-008
au2.g1826.t1	TC016001	NA	NA	0.42	1.57E-026
au2.g1922.t1	NA	NA	NA	0.42	1.22E-016
au2.g1949.t1	TC001524	FBgn0086710	<i>RpL30</i>	0.38	2.77E-009
au2.g216.t1	NA	NA	NA	0.23	8.35E-019
au2.g219.t1	TC015494	FBgn0023214	<i>edl</i>	0.49	1.76E-014
au2.g2239.t1	NA	FBgn0038834	<i>RpS30</i>	0.42	4.08E-009
au2.g2250.t1	TC004892	FBgn0038834	<i>RpS30</i>	0.41	1.69E-009
au2.g2324.t1	TC004444	FBgn0063492	<i>GstE8</i>	0.38	4.12E-019
au2.g2437.t1	TC000813	NA	NA	0.38	1.90E-018
au2.g2544.t1	TC000868	FBgn0004858	<i>elB</i>	0.20	1.04E-080
au2.g2727.t1	TC000592	NA	NA	0.27	1.68E-040
au2.g279.t1	TC015179	FBgn0037723	<i>SpdS</i>	0.44	5.62E-008
au2.g3132.t1	TC000355	FBgn0029868	<i>CG3446</i>	0.48	2.97E-007

Continued on next page

B.1 Candidate Genes

Table B.1 – continued from previous page

au2ID	TcasID	FBgnID	Symbol	fC	FDR
au2.g3150.t1	TC001225	FBgn0003942	<i>RpS27A</i>	0.44	4.82E-008
au2.g3254.t1	NA	NA	NA	0.28	9.77E-035
au2.g3381.t1	TC000180	FBgn0032518	<i>RpL24</i>	0.46	8.42E-009
au2.g3484.t1	TC002331	FBgn0033961	<i>CG12859</i>	0.49	9.46E-006
au2.g3829.t1	TC003304	FBgn0031066	<i>CoVIb</i>	0.46	1.07E-010
au2.g491.t1	TC015654	FBgn0015288	<i>RpL22</i>	0.44	2.60E-011
au2.g5142.t1	TC003967	FBgn0017579	<i>RpL14</i>	0.42	3.77E-010
au2.g5337.t1	NA	NA	NA	0.49	5.54E-005
au2.g5437.t1	TC007795	FBgn0031980	<i>RpL36A</i>	0.44	7.40E-008
au2.g5472.t1	TC007682	FBgn0052238	<i>CG32238</i>	0.46	2.63E-006
au2.g5557.t1	TC007636	FBgn0031505	<i>CG12400</i>	0.46	7.73E-008
au2.g5635.t1	TC007576	FBgn0000251	<i>cad</i>	0.19	9.28E-092
au2.g5804.t1	NA	FBgn0032694	<i>MESR3</i>	0.41	5.60E-020
au2.g6369.t1	TC008413	FBgn0031645	<i>CG3036</i>	0.44	4.21E-010
au2.g6853.t1	TC013812	FBgn0035280	<i>Cpr62Bb</i>	0.39	3.75E-007
au2.g6993.t1	TC013723	FBgn0013753	<i>Bgb</i>	0.17	1.56E-106
au2.g6995.t1	TC014076	FBgn0011723	<i>byn</i>	0.07	6.16E-044
au2.g7373.t1	TC013474	FBgn0002573	<i>sens</i>	0.18	2.36E-047
au2.g7499.t1	TC014405	FBgn0010411	<i>RpS18</i>	0.43	2.56E-008
au2.g7550.t1	TC013365	FBgn0010638	<i>Sec61beta</i>	0.42	3.72E-010
au2.g7723.t1	TC014598	FBgn0003900	<i>twi</i>	0.39	4.59E-016
au2.g7751.t1	TC013195	FBgn0053511	<i>CG33511</i>	0.33	3.39E-010
au2.g7815.t1	TC013163	FBgn0000411	<i>D</i>	0.33	9.01E-043
au2.g7865.t1	TC014685	FBgn0050045	<i>Cpr49Aa</i>	0.25	6.31E-014
au2.g791.t1	TC014844	NA	NA	0.42	2.80E-005
au2.g8207.t1	NA	FBgn0052495	<i>CG32495</i>	0.34	1.15E-016
au2.g8303.t1	TC009469	FBgn0000606	<i>eve</i>	0.25	2.20E-067
au2.g8329.t1	TC009480	NA	NA	0.23	5.82E-029
au2.g8342.t1	TC009485	FBgn0010078	<i>RpL23</i>	0.46	3.99E-009

Continued on next page

B. RNASEQ

Table B.1 – continued from previous page

au2ID	TcasID	FBgnID	Symbol	fC	FDR
au2.g8382.t1	TC009307	NA	<i>NA</i>	0.41	5.37E-014
au2.g8413.t1	TC009288	NA	<i>NA</i>	0.43	1.26E-018
au2.g8461.t1	TC009260	FBgn0260441	<i>RpS12</i>	0.43	1.01E-007
au2.g8732.t1	TC015888	NA	<i>NA</i>	0.44	3.54E-006
au2.g9275.t1	NA	FBgn0086472	<i>RpS25</i>	0.50	1.04E-005
au2.g9928.t1	TC004308	FBgn0015521	<i>RpS21</i>	0.44	2.67E-008

Table B.2: Anterior Wnt targets

au2ID	TcasID	FBgnID	Symbol	fC	FDR
au2.g10282.t1	TC011993	NA	<i>NA</i>	0.43	3.89E-005
au2.g1134.t1	TC004646	NA	<i>NA</i>	0.37	2.24E-030
au2.g1793.t1	TC005250	FBgn0000052	<i>ade2</i>	0.45	1.51E-025
au2.g2626.t1	TC000937	FBgn0000078	<i>Amy-d</i>	0.33	2.79E-011
au2.g2627.t1	TC000638	FBgn0020506	<i>Amyrel</i>	0.28	3.11E-009
au2.g3101.t1	TC001186	FBgn0044028	<i>Notum</i>	0.43	3.31E-022
au2.g5750.t1	TC007996	FBgn0031514	<i>NA</i>	0.26	1.06E-032
au2.g5990.t1	TC008176	FBgn0019650	<i>toy</i>	0.39	4.91E-007

Table B.3: Posterior hedgehog targets

au2ID	TcasID	FBgnID	Symbol	fC	FDR
au2.g10304.t1	TC012497	FBgn0015032	<i>Cyp4c3</i>	0.20	0.037
au2.g10402.t1	TC012546	FBgn0032219	<i>CG4995</i>	0.20	0.001
au2.g10490.t1	TC012616	FBgn0031294	<i>IA-2</i>	0.40	0.019

Continued on next page

B.1 Candidate Genes

Table B.3 – continued from previous page

au2ID	TcasID	FBgnID	Symbol	fC	FDR
au2.g10496.t1	TC011888	NA	NA	0.37	0.016
au2.g10497.t1	NA	NA	NA	0.43	0.073
au2.g1056.t1	TC013596	FBgn0000116	<i>Argk</i>	0.43	0.001
au2.g10672.t1	TC011760	NA	NA	0.14	5.37E-005
au2.g10678.t1	TC011756	FBgn0038966	<i>pinta</i>	0.38	0.047
au2.g10709.t1	TC012758	FBgn0025697	<i>santa-maria</i>	0.33	0.003
au2.g10716.t1	NA	FBgn0025697	<i>santa-maria</i>	0.34	0.002
au2.g10739.t1	TC011714	FBgn0052473	<i>CG32473</i>	0.28	0.004
au2.g11036.t1	NA	NA	NA	0.12	3.36E-006
au2.g11038.t1	TC006091	NA	NA	0.23	0.017
au2.g11146.t1	TC005995	FBgn0025866	<i>CalpB</i>	0.43	0.044
au2.g11302.t1	TC006255	FBgn0265137	<i>Spn42Da</i>	0.42	0.012
au2.g11360.t1	TC005860	FBgn0030968	<i>CG7322</i>	0.39	0.048
au2.g11652.t1	TC005669	FBgn0036995	NA	0.36	0.002
au2.g12010.t1	TC005437	FBgn0034394	<i>CG15096</i>	0.31	0.034
au2.g12107.t1	TC005380	NA	NA	0.31	0.017
au2.g12145.t1	TC005344	FBgn0264493	<i>rdx</i>	0.39	0.023
au2.g12173.t1	TC005327	FBgn0050106	<i>CCHa1r</i>	0.30	0.019
au2.g12247.t1	TC012946	NA	NA	0.31	0.001
au2.g12667.t1	TC011481	NA	NA	0.32	0.008
au2.g1272.t1	TC010864	FBgn0031538	NA	0.38	0.015
au2.g1382.t1	TC004597	FBgn0029896	<i>CG3168</i>	0.32	0.004
au2.g17.t1	TC015373	NA	NA	0.44	0.047
au2.g190.t1	TC015478	NA	NA	0.32	0.008
au2.g1938.t1	TC005191	FBgn0036857	<i>CG9629</i>	0.34	0.001
au2.g216.t1	NA	NA	NA	0.50	0.033
au2.g257.t1	TC015522	FBgn0032287	<i>CG6415</i>	0.41	0.033

Continued on next page

B. RNASEQ

Table B.3 – continued from previous page

au2ID	TcasID	FBgnID	Symbol	fC	FDR
au2.g2727.t1	TC000592	NA	NA	0.48	0.057
au2.g279.t1	TC015179	FBgn0037723	<i>SpdS</i>	0.38	0.008
au2.g2852.t1	TC000520	FBgn0003495	<i>spz</i>	0.36	0.010
au2.g2952.t1	TC000459	FBgn0033913	<i>CG8468</i>	0.45	0.031
au2.g3393.t1	NA	FBgn0038149	NA	0.37	0.043
au2.g3395.t1	NA	FBgn0038149	NA	0.25	0.022
au2.g3396.t1	NA	FBgn0038149	NA	0.25	0.022
au2.g3415.t1	TC000174	FBgn0038149	NA	0.38	0.023
au2.g3417.t1	TC000172	FBgn0038149	NA	0.23	0.010
au2.g3418.t1	NA	FBgn0038149	NA	0.27	0.024
au2.g3432.t1	TC001375	FBgn0051974	<i>CG31974</i>	0.34	0.010
au2.g3731.t1	TC003228	FBgn0036316	<i>CG10960</i>	0.31	0.036
au2.g3759.t1	TC003203	FBgn0030574	<i>CG9413</i>	0.39	0.024
au2.g4120.t1	TC002989	FBgn0036169	<i>Fuca</i>	0.28	0.000
au2.g4122.t1	TC002988	FBgn0036169	<i>Fuca</i>	0.28	0.002
au2.g4461.t1	TC000091	FBgn0025592	<i>Gyk</i>	0.49	0.068
au2.g4667.t1	TC010540	FBgn0002528	<i>LanB2</i>	0.40	0.000
au2.g4688.t1	TC010496	FBgn0037801	<i>CG3999</i>	0.35	0.000
au2.g46.t1	TC015389	FBgn0038695	NA	0.20	0.000
au2.g4742.t1	TC003773	FBgn0030334	<i>Karl</i>	0.31	0.016
au2.g505.t1	TC015039	NA	NA	0.30	0.050
au2.g5092.t1	TC003919	NA	NA	0.29	0.020
au2.g5115.t1	TC003939	NA	NA	0.36	0.035
au2.g5129.t1	TC002464	FBgn0027611	<i>LM408</i>	0.31	0.000
au2.g5536.t1	TC007646- GA	FBgn0085424	<i>nub</i>	0.45	0.047
au2.g5809.t1	TC008043	FBgn0026403	<i>Ndg</i>	0.30	0.000
au2.g5840.t1	TC008063	FBgn0004567	<i>slp2</i>	0.38	0.050

Continued on next page

B.1 Candidate Genes

Table B.3 – continued from previous page

au2ID	TcasID	FBgnID	Symbol	fC	FDR
au2.g5953.t1	TC007351	FBgn0026721	<i>fat-spondin</i>	0.33	0.006
au2.g6037.t1	TC008202	FBgn0031381	<i>Npc2a</i>	0.34	0.011
au2.g6199.t1	TC007187	FBgn0051871	<i>CG31871</i>	0.26	0.000
au2.g6283.t1	TC007141	FBgn0000242	<i>Bx</i>	0.34	0.011
au2.g6578.t1	TC016044	FBgn0000313	<i>chp</i>	0.35	0.001
au2.g6598.t1	TC002354	FBgn0261243	<i>Psa</i>	0.49	0.040
au2.g6712.t1	TC010939	FBgn0035665	<i>Jon65Aiii</i>	0.30	0.066
au2.g6823.t1	TC013978	NA	NA	0.25	3.07E-005
au2.g6909.t1	TC014022	FBgn0035575	NA	0.33	0.004
au2.g7000.t1	TC013718	FBgn0024150	<i>Ac78C</i>	0.37	0.019
au2.g7384.t1	TC013464	FBgn0031913	<i>CG5958</i>	0.43	0.036
au2.g7869.t1	TC013128	FBgn0050045	<i>Cpr49Aa</i>	0.46	0.078
au2.g7901.t1	TC014706	FBgn0033629	<i>Tsp47F</i>	0.28	0.007
au2.g7984.t1	TC013049	FBgn0038257	<i>smp-30</i>	0.33	0.001
au2.g832.t1	TC011529	FBgn0040322	<i>GGBP2</i>	0.40	0.073
au2.g8486.t1	TC009570	FBgn0037736	NA	0.21	0.071
au2.g8500.t1	TC009233	NA	NA	0.20	3.28E-005
au2.g8529.t1	TC009593	FBgn0034999	<i>CG3394</i>	0.31	0.001
au2.g9014.t1	TC009808	FBgn0041630	<i>Hexo1</i>	0.39	0.006
au2.g908.t1	TC001613	FBgn0036756	<i>cln3</i>	0.44	0.049
au2.g9100.t1	TC009861	FBgn0003174	<i>pwn</i>	0.44	0.012
au2.g9261.t1	TC008883	FBgn0086909	<i>CG31751</i>	0.35	0.025
au2.g9385.t1	TC008806	NA	NA	0.35	0.006
au2.g9440.t1	TC008778	FBgn0041630	<i>Hexo1</i>	0.32	0.001
au2.g9492.t1	TC008734	FBgn0039527	<i>CG5639</i>	0.49	0.011
au2.g9629.t1	TC010171	FBgn0037215	<i>CG12582</i>	0.31	0.022
au2.g9865.t1	TC012282	FBgn0040251	<i>Ugt86Di</i>	0.47	0.072
au2.g9867.t1	TC012285	FBgn0040257	<i>Ugt86Dc</i>	0.36	0.001

Continued on next page

B. RNASEQ

Table B.3 – continued from previous page

au2ID	TcasID	FBgnID	Symbol	fC	FDR
au2.g9915.t1	TC012152	FBgn0032612	<i>CG13282</i>	0.35	0.070
au2.g993.t1	TC014177	FBgn0036975	<i>CG5618</i>	0.40	0.015

Table B.4: Anterior hedgehog targets

au2ID	TcasID	FBgnID	Symbol	fC	FDR
au2.g11416.t1	TC005822	NA	NA	0.38	0.044
au2.g2229.t1	TC004494	FBgn0034093	NA	0.23	0.023
au2.g2283.t1	TC004922	FBgn0043791	<i>CG8147</i>	0.48	0.070
au2.g2626.t1	TC000937	FBgn0000078	<i>Amy-d</i>	0.43	0.027
au2.g3946.t1	TC003369	FBgn0011576	<i>Cyp4d2</i>	0.37	0.026
au2.g604.t1	TC015713	FBgn0030598	<i>CG9503</i>	0.42	0.035
au2.g9509.t1	TC010105	FBgn0011296	<i>l(2)efl</i>	0.31	0.005
au2.g954.t1	TC004121	FBgn0034089	NA	0.50	0.078

B.2 Gene ontology enrichment

The following tables contain all the significantly enriched GO terms found with the AMIGO term enrichment tool [Carbon et al., 2009]. Since in *Tribolium* only a small subset of genes has GO annotations, I used the annotations of *Drosophila*. Enrichment was only found in the posterior Wnt target gene set. This set contained 72 genes, however, for only 52 a *Drosophila* ortho/homolog was found.

The tool compares the sample frequency, i.e. the frequency of a given GO term among the 52 genes of the target gene set, to the background frequency. The background frequency is the frequency of a given GO term in the whole *Drosophila*

B.2 Gene ontology enrichment

genome. The calculated p-value is adjusted for multiple testing with the Bonferroni correction.

Table B.5: Biological Process

GO term	P-value	Sample frequency	Background frequency
GO:0034645 cellular macromolecule biosynthetic process	4.67e-12	32/52 (61.5%)	1971/13796 (14.3%)
GO:0009059 macromolecule biosynthetic process	5.18e-12	32/52 (61.5%)	1978/13796 (14.3%)
GO:0000022 mitotic spindle elongation	5.83e-12	11/52 (21.2%)	80/13796 (0.6%)
GO:0051231 spindle elongation	7.74e-12	11/52 (21.2%)	82/13796 (0.6%)
GO:0044249 cellular biosynthetic process	1.35e-11	34/52 (65.4%)	2374/13796 (17.2%)
GO:1901576 organic substance biosynthetic process	1.81e-11	34/52 (65.4%)	2397/13796 (17.4%)
GO:0010467 gene expression	3.42e-11	33/52 (63.5%)	2276/13796 (16.5%)
GO:0009058 biosynthetic process	3.49e-11	34/52 (65.4%)	2449/13796 (17.8%)
GO:0006412 translation	3.02e-09	20/52 (38.5%)	800/13796 (5.8%)
GO:0044237 cellular metabolic process	1.66e-08	41/52 (78.8%)	4580/13796 (33.2%)
GO:0007052 mitotic spindle organization	2.62e-07	11/52 (21.2%)	210/13796 (1.5%)
GO:0009987 cellular process	9.21e-07	49/52 (94.2%)	7741/13796 (56.1%)
GO:0007051 spindle organization	1.60e-06	11/52 (21.2%)	249/13796 (1.8%)

Continued on next page

B. RNASEQ

Table B.5 – continued from previous page

GO term	P-value	Sample frequency	Background frequency
GO:0044260 cellular macromolecule metabolic process	7.45e-06	33/52 (63.5%)	3507/13796 (25.4%)
GO:0008152 metabolic process	2.29e-05	42/52 (80.8%)	5916/13796 (42.9%)
GO:0000226 microtubule cytoskeleton organization	2.58e-05	12/52 (23.1%)	408/13796 (3.0%)
GO:0043170 macromolecule metabolic process	2.51e-04	34/52 (65.4%)	4238/13796 (30.7%)
GO:0044267 cellular protein metabolic process	3.23e-04	22/52 (42.3%)	1875/13796 (13.6%)
GO:0007017 microtubule-based process	3.46e-04	12/52 (23.1%)	518/13796 (3.8%)
GO:0007010 cytoskeleton organization	4.41e-04	13/52 (25.0%)	637/13796 (4.6%)
GO:0071704 organic substance metabolic process	1.31e-03	37/52 (71.2%)	5264/13796 (38.2%)
GO:0044238 primary metabolic process	3.25e-03	35/52 (67.3%)	4924/13796 (35.7%)
GO:0007442 hindgut morphogenesis	3.56e-03	5/52 (9.6%)	63/13796 (0.5%)
GO:0061525 hindgut development	3.56e-03	5/52 (9.6%)	63/13796 (0.5%)
GO:0000278 mitotic cell cycle	4.53e-03	11/52 (21.2%)	547/13796 (4.0%)
GO:0048546 digestive tract morphogenesis	7.39e-03	5/52 (9.6%)	73/13796 (0.5%)
GO:0006366 transcription from RNA polymerase II promoter	8.00e-03	10/52 (19.2%)	470/13796 (3.4%)
GO:0007369 gastrulation	1.85e-02	5/52 (9.6%)	88/13796 (0.6%)

Continued on next page

B.2 Gene ontology enrichment

Table B.5 – continued from previous page

GO term	P- value	Sample frequency	Background frequency
GO:0071822 protein complex subunit organization	2.47e-02	11/52 (21.2%)	655/13796 (4.7%)
GO:0019538 protein metabolic process	2.56e-02	22/52 (42.3%)	2427/13796 (17.6%)
GO:0006357 regulation of transcription from RNA polymerase II promoter	2.83e-02	9/52 (17.3%)	432/13796 (3.1%)
GO:0048619 embryonic hindgut morphogenesis	4.72e-02	4/52 (7.7%)	54/13796 (0.4%)
GO:0055123 digestive system development	4.75e-02	5/52 (9.6%)	107/13796 (0.8%)
GO:0048565 digestive tract development	4.75e-02	5/52 (9.6%)	107/13796 (0.8%)
GO:0009880 embryonic pattern specification	5.99e-02	7/52 (13.5%)	269/13796 (1.9%)
GO:0043933 macromolecular complex subunit organization	6.17e-02	11/52 (21.2%)	724/13796 (5.2%)
GO:0045944 positive regulation of transcription from RNA polymerase II promoter	7.68e-02	6/52 (11.5%)	192/13796 (1.4%)
GO:0044271 cellular nitrogen compound biosynthetic process	9.95e-02	14/52 (26.9%)	1205/13796 (8.7%)

B. RNASEQ

Table B.6: Cellular Component

GO term	P-value	Sample frequency	Background frequency
GO:0044391 ribosomal subunit	3.66e-22	20/52 (38.5%)	176/13796 (1.3%)
GO:0022626 cytosolic ribosome	3.40e-21	20/52 (38.5%)	196/13796 (1.4%)
GO:0044445 cytosolic part	7.52e-20	20/52 (38.5%)	228/13796 (1.7%)
GO:0005840 ribosome	5.94e-18	20/52 (38.5%)	283/13796 (2.1%)
GO:0022625 cytosolic large ribosomal subunit	1.97e-15	12/52 (23.1%)	59/13796 (0.4%)
GO:0030529 ribonucleoprotein complex	1.80e-12	21/52 (40.4%)	620/13796 (4.5%)
GO:0015934 large ribosomal subunit	4.30e-12	12/52 (23.1%)	108/13796 (0.8%)
GO:0005829 cytosol	1.40e-10	20/52 (38.5%)	678/13796 (4.9%)
GO:0022627 cytosolic small ribosomal subunit	2.91e-09	8/52 (15.4%)	43/13796 (0.3%)
GO:0043229 intracellular organelle	4.03e-09	40/52 (76.9%)	4158/13796 (30.1%)
GO:0043226 organelle	4.90e-09	40/52 (76.9%)	4181/13796 (30.3%)
GO:0015935 small ribosomal subunit	2.77e-07	8/52 (15.4%)	74/13796 (0.5%)
GO:0044424 intracellular part	2.78e-07	42/52 (80.8%)	5228/13796 (37.9%)
GO:0005622 intracellular	5.34e-07	42/52 (80.8%)	5323/13796 (38.6%)

Continued on next page

B.2 Gene ontology enrichment

Table B.6 – continued from previous page

GO term	P-value	Sample frequency	Background frequency
GO:0044446 intracellular organelle part	5.61e-07	29/52 (55.8%)	2428/13796 (17.6%)
GO:0044422 organelle part	7.27e-07	29/52 (55.8%)	2454/13796 (17.8%)
GO:0005737 cytoplasm	3.50e-06	31/52 (59.6%)	3002/13796 (21.8%)
GO:0032991 macromolecular complex	3.68e-06	29/52 (55.8%)	2624/13796 (19.0%)
GO:0043228 non-membrane-bounded organelle	5.77e-06	22/52 (42.3%)	1503/13796 (10.9%)
GO:0043232 intracellular non-membrane-bounded organelle	5.77e-06	22/52 (42.3%)	1503/13796 (10.9%)
GO:0044444 cytoplasmic part	1.08e-05	27/52 (51.9%)	2376/13796 (17.2%)
GO:0044464 cell part	2.86e-05	42/52 (80.8%)	5954/13796 (43.2%)
GO:0005623 cell	2.86e-05	42/52 (80.8%)	5954/13796 (43.2%)

Table B.7: Molecular Function

GO term	P-value	Sample frequency	Background frequency
GO:0003735 structural constituent of ribosome	2.68e-18	20/52 (38.5%)	272/13796 (2.0%)
GO:0005198 structural molecule activity	7.13e-14	22/52 (42.3%)	606/13796 (4.4%)

Continued on next page

B. RNASEQ

Table B.7 – continued from previous page

GO term	P-value	Sample frequency	Background frequency
GO:0000981 sequence-specific DNA binding RNA polymerase II transcription factor activity	3.17e-04	8/52 (15.4%)	180/13796 (1.3%)
GO:0003705 RNA polymerase II distal enhancer sequence-specific DNA binding transcription factor activity	6.44e-03	5/52 (9.6%)	71/13796 (0.5%)
GO:0003700 sequence-specific DNA binding transcription factor activity	4.18e-02	9/52 (17.3%)	454/13796 (3.3%)
GO:0001071 nucleic acid binding transcription factor activity	4.18e-02	9/52 (17.3%)	454/13796 (3.3%)

B.3 *Tc-senseless* phylogenetic tree



Figure B.1: *Tc-senseless* phylogenetic tree - Alignments of the best two hits of the gene au2.g7373 show that it is the ortholog of *Dm-senseless*. Sequences were identified using BLAST. Alignment and tree construction was done with Multalin [Corpet, 1988]

B. RNASEQ

Appendix C

Scripts

C.1 R

C.1.1 DESeq Analysis

This script contains all the relevant parameters which were used in the statistical analysis of the RNAseq data using the *Tc-arrow*^{RNAi} as example.

```
1 #!/usr/bin/Rscript
2
3 ####R packages
4 library("DESeq")
5 library("RColorBrewer")
6 library("gplots")
7
8 datafile <- ("counts_arrow.csv")
9 ## read in as table with headers and gene names in the
   first column
10 counts_arrow <- read.table( datafile , header=TRUE, row.
   names=1)
11 counts_arrow = counts_arrow[,c(order(colnames(counts_arrow
   )))]
12 ## assign conditions (treatments)
```

C. SCRIPTS

```
13 conds_arrow = as.factor(gsub('[0-9]', '', colnames(counts_
    arrow), perl=T))
14
15 ###arrow
16 cds_arrow <- newCountDataSet(counts_arrow, conds_arrow )
17 cds_arrow <- estimateSizeFactors( cds_arrow )
18 cds_arrow <- estimateDispersions( cds_arrow )
19
20 pdf(file="DispersionPlot_arrow.pdf")
21 plotDispEsts(cds_arrow)
22 dev.off()
23
24 #####PCA
25 cdsBlind_arrow = estimateDispersions( cds_arrow, method="
    blind" )
26 vsd_arrow = varianceStabilizingTransformation( cdsBlind_
    arrow )
27 dists_arrow = dist( t( exprs(vsd_arrow) ) )
28 pdf(file="PCA_plot_arrow.pdf")
29 plotPCA(vsd_arrow, intgroup="condition")
30 dev.off()
31
32 #####heatmap
33 hmcol = colorRampPalette(brewer.pal(9, "GnBu"))(100)
34 mat = as.matrix( dists_arrow )
35 rownames(mat) = colnames(mat) = with(pData(cdsBlind_arrow)
    , paste(condition))
36 pdf(file="heatmap_arrow.pdf")
37 heatmap.2(mat, trace="none", col = rev(hmcol), margin=c
    (13, 13))
38 dev.off()
39
40 ##filtering independent
41 rs = rowSums( counts( cds_arrow ))
```

```
42 theta = 0.25
43 use = (rs > quantile(rs, probs=theta))
44 table(use)
45 cdsFilt_arrow = cds_arrow[ use, ]
46
47 #####PCA
48 cdsFiltBlind_arrow = estimateDispersions( cdsFilt_arrow,
      method="blind" )
49 vsdFilt_arrow = varianceStabilizingTransformation(
      cdsFiltBlind_arrow )
50 distsFilt_arrow = dist( t( exprs(vsdFilt_arrow) ) )
51 pdf( file="PCA_plot_Filt_arrow.pdf" )
52 plotPCA( vsdFilt_arrow, intgroup="condition" )
53 dev.off()
54
55 #####heatmap
56 mat = as.matrix( distsFilt_arrow )
57 rownames(mat) = colnames(mat) = with(pData(cdsFiltBlind_
      arrow), paste(condition))
58 pdf( file="heatmapFilt_arrow.pdf" )
59 heatmap.2(mat, trace="none", col = rev(hmcol), margin=c
      (13, 13))
60 dev.off()
61
62 ##statistical test for arrow
63 resarrow <- nbinomTest( cdsFilt_arrow, "wildtype", "arrow"
      )
64
65 ##MA-plot
66 pdf("MAplot_arrow.pdf")
67 plotMA( resarrow )
68 dev.off()
69
70 ##rename headers
```

C. SCRIPTS

```
71 colnames(resarrow)= c("id", "arrowbaseMean", "
    arrowbaseMeanA", "arrowbaseMeanB", "arrowfoldChange", "
    arrowlog2FoldChange", "arrowpval", "arrowpadj")
72
73 ##significance criteria
74 resSigarrow <- resarrow[ resarrow$arrowpadj < 0.1, ]
75 ##up and down regulated
76 resSigarrowup <- resSigarrow[ resSigarrow$
    arrowlog2FoldChange > 1,]
77 resSigarrowdown <- resSigarrow[ resSigarrow$
    arrowlog2FoldChange < -1,]
78 ##output data tables
79 write.csv( resarrow , file="resarrow.csv")
80 write.csv( resSigarrow , file="resarrow_sig.csv")
81 write.csv( resSigarrowdown , file="arrow_down.csv")
82 write.csv( resSigarrowup , file="arrow_up.csv")
```

C.1.2 Miscellaneous

The following scripts contain the GO annotations, modified MA-plots from DE-Seq, Venn diagrams and a barplot example used in cuticle analysis.

```
1 #####
2 ## GO annotations ##
3 #####
4
5 ##read in association table
6 Tc_GO <- read.csv( file="TCau2association.csv", header=T,
    fill=T)
7 ##add FB and BB links
8 fb.FBlink = paste( '=HYPERLINK("http://www.flybase.org/
    reports/', Tc_GO$FBgnID, '.html")', sep=' ')
9 Tc_GO <- cbind(Tc_GO, fb.FBlink)
10
11 #####remove NA rows, merge to Dm ortho/hom GO annotations
```

```

12 resSigarrowdown_NA <- resSigarrowdown[complete.cases(
    resSigarrowdown),]
13 resSigarrowdown_GO <- merge(resSigarrowdown_NA, Tc_GO, by.
    x="id", by.y="au2ID", all=F)
14 write.csv(resSigarrowdown_GO, file="resSigarrowdown_GO.csv
    ")
15
16 resSigarrowup_NA <- resSigarrowup[complete.cases(
    resSigarrowup),]
17 resSigarrowup_GO <- merge(resSigarrowup_NA, Tc_GO, by.x="
    id", by.y="au2ID", all=F)
18 write.csv(resSigarrowup_GO, file="resSigarrowup_GO.csv")
19
20 #####
21 ## MA-plots ##
22 #####
23
24 ## rename headers for plotMA function
25 resarrow2 <- resarrow
26 colnames(resarrow2)= c("id", "baseMean", "baseMeanA", "
    baseMeanB", "foldChange", "log2FoldChange", "pval", "
    padj")
27
28 ###modified plotMA function from DESeq package
29 plotMAnew <- function (x, ylim, col = ifelse(x$padj <= 0.1
    & abs(x$log2FoldChange) >=1, "red3", "gray32"),
30     linecol = "#ff000080", xlab = NULL,
31     ylab = NULL, log = "x", cex = 0.45,
32     ...)
33 {
34     if (!(is.data.frame(x) && all(c("baseMean", "
        log2FoldChange") %in%
35         colnames(x))))

```

C. SCRIPTS

```
36     stop("'x' must be a data frame with columns named
37           'baseMean', 'log2FoldChange'.")
38   x = subset(x, baseMean != 0)
39   py = x$log2FoldChange
40   if (missing(ylim))
41     ylim = c(-4, 4)
42   plot(x$baseMean, pmax(ylim[1], pmin(ylim[2], py)), log
43         = log,
44         pch = ifelse(py < ylim[1], 6, ifelse(py > ylim[2],
45         2,
46         16)), cex = cex, col = col, xlab = NULL, ylab
47         = NULL,
48         ylim = ylim, yaxp=c(-4,4,8))
49   abline(h = -1, lwd = 1.2, col = linecol)
50   abline(h = 1, lwd = 1.2, col = linecol)
51 }
52
53 plotMAnew( resarrow2 )
54
55 #####
56 ## cuticle barplots ##
57 #####
58
59 library(ggplot2)
60
61 eRNAi <- read.csv(file="g7373_eRNAi.R.csv", header=T)
62
63 ggplot(eRNAi, aes(x = Scale, y = Percentage, fill = Type))
64   +
65   geom_bar(position = "dodge", stat="identity") +
66   facet_grid(. ~Treatment) +
67   scale_fill_brewer(type="qual", palette=3) +
68   scale_x_discrete(limits=c(1,2)) +
69   scale_y_continuous(limits=c(0,100)) +
```



```

65 xlab("injection timepoint") +
66 ylab("Percentage")

1 #####
2 ## Venn diagrams ##
3 #####
4
5 ## source("http://faculty.ucr.edu/~tgirke/Documents/R_
   BioCond/My_R_Scripts/overLapper.R")
6 source("overLapper.R")
7
8 ##Wnt targets
9 ##arrow, frizzled, orthodenticle, torso, wntless
10 candidates_afwto = list(resSigarrowdown_NA$id,
   resSigfrizzledown_NA$id, resSigorthodenticledown_NA$id
   , resSigtorsodown_NA$id, resSigwntlessdown_NA$id)
11
12 names(candidates_afwto) <- c("Arrow", "Frizzled",
   "Orthodenticle", "Torso", "Wntless")
13 setlist_afwto <- candidates_afwto
14 OLlist_afwto <- overLapper(setlist=setlist_afwto, sep="",
   type="vennsets")
15
16 counts_afwto <- list(sapply(OLlist_afwto$Venn_List, length
   ))
17 pdf(file="Venn_Diagram_New_Down_Arrow_Frizzled_
   Orthodenticle_Torso_Wntless.pdf")
18 vennPlot(counts=counts_afwto, mysub="Top: var1;", )
19 dev.off()
20
21 ## arrow frz wls torso
22 newcands_afwt <- cbind( OLlist_afwto$Venn_List$
   ArrowFrizzledTorsoWntless)
23 colnames(newcands_afwt) <- "Vennset"

```

C. SCRIPTS

```
24 newcands_afwt_a <- merge( newcands_afwt , resSigarrowdown -
    GO, by.x="Vennset" , by.y="id" , all=F)
25 write.csv(newcands_afwt_a, file="Venn_New_Down_Arrow -
    Frizzled_Wntless_Torso.csv" )
26
27 ## arrow frz wls otd
28 newcands_afwo <- cbind( OList_afwto$Venn_List$
    ArrowFrizzledOrthodenticleWntless)
29 colnames(newcands_afwo) <- "Vennset"
30 newcands_afwo_a <- merge( newcands_afwo , resSigarrowdown -
    GO, by.x="Vennset" , by.y="id" , all=F)
31 write.csv(newcands_afwo_a, file="Venn_New_Down_Arrow -
    Frizzled_Wntless_Orthodenticle.csv" )
32
33
34 #### HH targets
35 ## hedgehog , torso , orthodenticle
36 candidates_hto = list( resSighedgehogdown_NA$id ,
    resSigorthodenticledown_NA$id , resSigtorsodown_NA$id )
37
38 names(candidates_hto) <- c( "Hedgehog" , "Orthodenticle" ,
    "Torso" )
39 setlist_hto <- candidates_hto
40 OList_hto <- overLapper( setlist=setlist_hto , sep="" , type
    ="vennsets" )
41
42 counts_hto <- list( sapply( OList_hto$Venn_List , length ) )
43 pdf( file="Venn_New_Down_Hedgehog_Orthodenticle_Torso.pdf" )
44 vennPlot( counts=counts_hto , mysub="Top: var1;" )
45 dev.off()
46
47 ##hedgehog torso
48 cand_ho <- cbind( OList_hto$Venn_List$HedgehogTorso)
49 colnames(cand_ho) <- "Vennset"
```

```
50 cand_s_hto_a <- merge( cand_s_hto, resSighedgehogdown_GO, by
  .x="Vennset", by.y="id", all=F)
51 write.csv(cand_s_hto_a, file="Venn_Down_New_Hedgehog_Torso.
  csv")
52
53 ## hedgehog orthodenticle
54 cand_ho <- cbind( OList_hto$Venn_List$
  HedgehogOrthodenticle)
55 colnames(cand_ho) <- "Vennset"
56 cand_ho_a <- merge( cand_ho, resSighedgehogdown_GO, by.x
  ="Vennset", by.y="id", all=F)
57 write.csv(cand_ho_a, file="Venn_Down_New_Hedgehog_
  Orthodenticle.csv")
```

C. SCRIPTS

C.2 Console

C.2.1 Mapping and counting RNAseq reads

This script contains the mapping parameters used within bowtie2 and the steps in samtools to get the final counts and mapping statistics.

```
1 /home/ubu1204/NGS/bowtie2-2.0.6/bowtie2-build au2.mrna.tl
   Tcas.au2.tl_index
2 time(
3 for i in {1..39};do
4     /home/ubu1204/NGS/bowtie2-2.0.6/bowtie2 -p 12 -q -D
       20 -R 3 -N 1 -L 20 -i S,1,0.50 -x Tcas.au2.tl_
       index -U *.${i}.fastq -S sample${i}.sam;
5     ./samtools/samtools -n 12 view -bS sample${i}.sam >
       sample${i}.bam;
6     samtools sort -m 3000000000 sample${i}.bam sample${i}.
       sorted;
7     samtools index sample${i}.sorted.bam;
8     samtools idxstats sample${i}.sorted.bam > sample${i}.
       counts.txt;
9     samtools flagstat sample${i}.sorted.bam > sample${i}.
       flagstat;
10    rm sample${i}.sam;
11    rm sample${i}.bam;
12        done
13 )
```

C.2.2 BLAST

This is an example on how to use BLAST. First the reference database is formatted. Then the query sequences, stored in a fasta file, can be BLASTed. Blastn was used to check the sequences of clones. Blastp was used to identify homologous sequences in other species.

```
1 # protein blast , reference is a fasta file with amino acid
   sequences
2 formatdb -i reference_amino_acid.fasta -o T -p T
3 # -b, number of alignments shown -d, reference -i query
   sequences
4 blastall -p blastp -b 1 -d reference.fasta -i query.fasta
   -o output_file
5
6 #nucleotide blast , reference is a fasta file with
   nucleotide sequences
7 formatdb -i reference_nucleotide.fasta -p F
8 blastall -p blastn -b 1 -d reference.fasta -i query.fasta
   -o output_file
```

C. SCRIPTS

Curriculum Vitae

Georg Oberhofer

Address

Petrikirchstrasse 12
37077 Göttingen
Germany
Email: goberho@gwdg.de

Personal Details

Gender: Male
Date of birth: 22nd of April, 1981
Place of birth: Innichen, Italy
Present Citizenship: Italian

Education

1987 - 1992 Elementary school, Innichen
1992 - 1995 Grammar school, Innichen
1995 - 2000 Highschool, Bruneck
07/2000 Graduation from high school in “Technical Engineering”
10/2000 Studies of chemistry, University of Innsbruck

03/2004 Studies of chemistry, University of Vienna, specialisation part with focus on biochemistry and inorganic chemistry

05/2009 Diploma thesis at the department of biochemistry in Vienna

01/2010 PhD thesis at the department of developmental biology in Göttingen

Language Knowledge

German

Italian

English

List of Publications

J. Fu, N. Posnien, R. Bolognesi, T. D. Fischer, P. Rayl, **G. Oberhofer**, P. Kitze-
mann, S. J. Brown, and G. Bucher. Asymmetrically expressed axin required
for anterior development in tribolium. *Proceedings of the National Academy of
Sciences of the United States of America*, 109(20):77827786, May 2012. ISSN
1091-6490. doi:10.1073/pnas.1116641109. PMID: 22552230.

A. D. Peel, J. Schanda, D. Grossmann, F. Ruge, **G. Oberhofer**, A. F. Gilles,
J. B. Schinko, M. Klingler, and G. Bucher. Tc-knirps plays different roles in the
speci- fication of antennal and mandibular parasegment boundaries and is regu-
lated by a pair-rule gene in the beetle tribolium castaneum. *BMC developmental
biology*, 13: 25, 2013. ISSN 1471-213X. doi: 10.1186/1471-213X-13-25. PMID:
23777260.

K. A. Panfilio, **G. Oberhofer**, and S. Roth. High plasticity in epithelial morpho-
genesis during insect dorsal closure. *Biology open*, 2(11):11081118, 2013. ISSN
2046-6390. doi: 10.1242/bio.20136072. PMID: 24244847.

G.Oberhofer, D. Grossmann, T. Beissbarth and G. Bucher. RNAseq after RNAi
reveals differences in anterior and posterior target genes in *Tribolium*. (**in prepa-
ration**).